EUROPEAN ORGANISATION FOR NUCLEAR RESEARCH (CERN)

Submitted to: Phys. Rev. D

CERN-EP-2020-235
March 16, 2021

arXiv:2103.08189v1 [hep-ex] 15 Mar 2021

Search for bottom-squark pair production in pp collision events at $\sqrt{s}$ = 13 TeV with hadronically decaying τ-leptons, b-jets and missing transverse momentum using the ATLAS detector

The ATLAS Collaboration

A search for pair production of bottom squarks in events with hadronically decaying τ-leptons, b-tagged jets and large missing transverse momentum is presented. The analyzed dataset is based on proton–proton collisions at $\sqrt{s}$ = 13 TeV delivered by the Large Hadron Collider and recorded by the ATLAS detector from 2015 to 2018, and corresponds to an integrated luminosity of 139 fb^{-1}. The observed data are compatible with the expected Standard Model background. Results are interpreted in a simplified model where each bottom squark is assumed to decay into the second-lightest neutralino $\tilde{\chi}_2^0$ and a bottom quark, with $\tilde{\chi}_2^0$ decaying into a Higgs boson and the lightest neutralino $\tilde{\chi}_1^0$. The search focuses on final states where at least one Higgs boson decays into a pair of hadronically decaying τ-leptons. This allows the acceptance and thus the sensitivity to be significantly improved relative to the previous results at low masses of the $\tilde{\chi}_2^0$, where bottom-squark masses up to 850 GeV are excluded at the 95% confidence level, assuming a mass difference of 130 GeV between $\tilde{\chi}_2^0$ and $\tilde{\chi}_1^0$. Model-independent upper limits are also set on the cross section of processes beyond the Standard Model.

© 2021 CERN for the benefit of the ATLAS Collaboration.
Reproduction of this article or parts of it is allowed as specified in the CC-BY-4.0 license.

1 Introduction

Although the Standard Model (SM) of particle physics is a very successful theory, it does not provide a natural explanation for the large hierarchy between the energy scale of electroweak interactions and the Planck scale related to the gravitational interaction. Nor does it have a viable candidate particle for dark matter, and it does not include a quantum description of gravity. Supersymmetry (SUSY) [1–6] is a theoretical framework that extends the SM by introducing partner states for the known particles, where the partners have the same quantum numbers as the respective SM particles but differ in spin by half a unit. This leads to new loop corrections to the Higgs boson mass that cancel out those involving SM particles, thereby solving the hierarchy problem [7–10]. When conservation of R-parity [11] is assumed, the lightest supersymmetric particle is stable and would be a viable candidate for dark matter if it is weakly interacting [12, 13]. However, SUSY must be a broken symmetry in order to allow the supersymmetric particles to be heavier than their SM partners and evade detection so far. Naturalness arguments [14, 15] support the assumption that the partner states of the third-generation quarks, the top squarks $\tilde{t}$ and the bottom squarks $\tilde{b}$, should be light and thus have relatively large production cross sections. They might even be the only strongly produced supersymmetric states within the current mass reach of the LHC.

This paper presents a search for pair production of bottom squarks $\tilde{b}$ that decay via the second-lightest neutralino $\tilde{\chi}_2^0$ to the lightest neutralino $\tilde{\chi}_1^0$. The neutralinos $\tilde{\chi}_{1,2,3,4}^0$ together with the charginos $\tilde{\chi}_{1,2}^{\pm}$ are mixtures of the partner states of the electroweak gauge bosons (bino and winos) and Higgs bosons (higgsinos). The simplified model [16–18] of production and decay of supersymmetric particles considered in this search is shown in Figure 1. It is inspired by the Minimal Supersymmetric Standard Model [19, 20] in scenarios where the branching ratio $\mathcal{B}(\tilde{\chi}_2^0 \to h\tilde{\chi}_1^0)$ is enhanced, e.g. when the $\tilde{\chi}_1^0$ is bino-like and the $\tilde{\chi}_2^0$ a wino–higgsino mixture. The branching ratio $\mathcal{B}(\tilde{b} \to b\tilde{\chi}_2^0)$ is large compared to that of the direct decay $\mathcal{B}(\tilde{b} \to b\tilde{\chi}_1^0)$, which is studied elsewhere [21], when the mixture of the bottom squark is such that it is mostly the superpartner of the left-chiral bottom quark, the $\tilde{\chi}_1^0$ is mostly bino, and the $\tilde{\chi}_2^0$ mostly wino. A wino- or higgsino-like $\tilde{\chi}_2^0$ will be accompanied by a $\tilde{\chi}_1^{\pm}$, which allows the decay $\tilde{b} \to t\tilde{\chi}_1^-$. This decay mode is relevant if the mass difference between the bottom squark and the chargino is larger than the top-quark mass. In the simplified model, $\mathcal{B}(\tilde{b} \to b\tilde{\chi}_2^0)$ and $\mathcal{B}(\tilde{\chi}_2^0 \to h\tilde{\chi}_1^0)$ are assumed to be 100%. Moreover, the Higgs boson is assumed to have the same properties as in the SM, namely $m(h) = 125\,\text{GeV}$, $\mathcal{B}(h \to b\bar{b}) = 58\%$, and $\mathcal{B}(h \to \tau^+\tau^-) = 6.3\%$. Only decays of the Higgs bosons into $b\bar{b}$, $\tau^+\tau^-$, W^+W^- and ZZ are considered in the signal-model generation. Furthermore, the mass difference $\Delta m(\tilde{\chi}_2^0, \tilde{\chi}_1^0)$ between the $\tilde{\chi}_2^0$ and $\tilde{\chi}_1^0$ is set to 130 GeV such that the Higgs boson produced in the decay of the $\tilde{\chi}_2^0$ is on its mass shell. The free parameters of the model are chosen to be the masses $m(\tilde{b})$ and $m(\tilde{\chi}_2^0)$.

The signal model illustrated in Figure 1 yields a final state with two bottom quarks, two Higgs bosons, and missing transverse momentum from the two $\tilde{\chi}_1^0$ particles that escape the detector without interacting. This analysis selects a final state with a pair of τ-leptons arising from the decay of one of the Higgs bosons, such that it complements a previous ATLAS search [22], which focuses on final states with multiple b-jets. This particular decay mode of the Higgs boson has never been exploited by a bottom-squark search until now. The neutrinos from the τ-lepton decays provide a source of missing transverse momentum in addition to the pair of $\tilde{\chi}_1^0$. This increases the acceptance of the search in the region of parameter space where the $\tilde{\chi}_2^0$ is relatively light and the $\tilde{\chi}_1^0$ moderately boosted, where the previous ATLAS analysis has limited sensitivity. The same simplified model has been employed by the CMS Collaboration in a search targeting $h \to \gamma\gamma$ decays [23]. Using a dataset of 77.5 fb^{-1}, the CMS analysis excludes bottom-squark masses up to 530 GeV

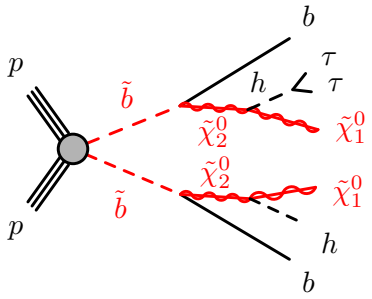


Figure 1: Simplified model of bottom-squark pair production and the decay chain targeted by this analysis.

for an almost massless $\tilde{\chi}_1^0$ at the 95% confidence level, and bottom-squark masses up to at least 400 GeV for heavier masses of the $\tilde{\chi}_1^0$.

The paper is structured as follows. After this introduction, Section 2 briefly describes the ATLAS detector, and Section 3 presents the dataset and simulated event samples. The reconstruction of physics objects is described in Section 4, and the signal selection and analysis discriminants are detailed in Section 5. The procedures to derive the background estimate are explained in Section 6, followed by a summary of the systematic uncertainties in Section 7. Section 8 presents the results from the analysis and their interpretation, and conclusions are given in Section 9.

2 ATLAS detector

The ATLAS experiment [24–27] at the LHC is a multipurpose particle detector with a forward–backward symmetric cylindrical geometry and nearly 4π coverage in solid angle.[1] It consists of an inner tracking detector surrounded by a thin superconducting solenoid providing a 2 T axial magnetic field, electromagnetic and hadronic calorimeters, and a muon spectrometer. The inner tracking detector covers the pseudorapidity range $|\eta| < 2.5$. It consists of silicon pixel, silicon microstrip, and transition radiation tracking detectors. Lead/liquid-argon (LAr) sampling calorimeters provide electromagnetic (EM) energy measurements with high granularity. A steel/scintillator-tile hadronic calorimeter covers the central pseudorapidity range ($|\eta| < 1.7$). The endcap and forward regions are instrumented with LAr calorimeters for EM and hadronic energy measurements up to $|\eta| = 4.9$. The muon spectrometer surrounds the calorimeters and is based on three large air-core toroidal superconducting magnets with eight coils each. The muon spectrometer includes a system of precision tracking chambers and fast detectors for triggering. A two-level trigger system is used to select events. The level-1 trigger is implemented in hardware and uses information from the calorimeters and the muon spectrometer to accept events at a maximum rate of 100 kHz. This is followed by a software-based high-level trigger (HLT) that reduces the event rate to 1 kHz on average depending on the data-taking conditions.

[1] ATLAS uses a right-handed coordinate system with its origin at the nominal interaction point (IP) in the center of the detector and the z-axis along the beam pipe. The x-axis points from the IP to the center of the LHC ring, and the y-axis points upwards. Cylindrical coordinates (r, ϕ) are used in the transverse plane, ϕ being the azimuthal angle around the z-axis. The pseudorapidity is defined in terms of the polar angle θ as $\eta = -\ln\tan(\theta/2)$. Angular distance is measured in units of $\Delta R \equiv \sqrt{(\Delta\eta)^2 + (\Delta\phi)^2}$.

3 Data and simulated event samples

The dataset used in this analysis consists of proton–proton collision data collected with the ATLAS detector during the second run of the LHC from 2015 to 2018 at a center-of-mass energy of $\sqrt{s} = 13$ TeV and with a minimum separation of 25 ns between consecutive crossings of proton bunches from the two beams. After applying data-quality requirements that ensure that all detector subsystems were operational, the total integrated luminosity of this data sample is 139 fb^{-1} with an uncertainty of 1.7% [28], obtained using the LUCID-2 detector [29] for the primary luminosity measurements.

The SUSY signal and SM background processes are modeled with Monte Carlo (MC) simulations, except for the multijet background, which is estimated from data. The modeling of the two dominant SM background processes, namely top-quark production and production of Z bosons with decays into τ-leptons ($Z(\tau\tau)$), was improved by normalizing their contributions to data as described in Section 6. Simulated samples were produced using the ATLAS simulation infrastructure [30] with either a full simulation of the ATLAS detector in GEANT4 [31], or a faster variant that relies on a parameterized response of the calorimeters [32]. The latter was only used for the simulation of bottom-squark signals and to evaluate systematic uncertainties associated with generator modeling. The effect of multiple interactions in the same and neighboring bunch crossings (pileup) was modeled by overlaying the hard-scattering event with simulated inelastic pp collisions generated with PYTHIA 8.186 [33] using the NNPDF2.3LO set of parton distribution functions (PDFs) [34] and the A3 set of tuned parameters (tune) [35]. Simulated event samples were weighted to reproduce the distribution of the number of pileup interactions observed in the data. For all simulated samples except those generated with SHERPA [36], the EVTGEN [37] program was used to simulate the decays of bottom and charm hadrons.

The production of $t\bar{t}$ events was modeled using the POWHEG-BOX v2 generator [38–41] at next-to-leading order (NLO) in QCD with the NNPDF3.0NLO PDF set [42] and the h_{damp} parameter[2] set to $1.5m_{\text{top}}$ [43]. Parton showering, hadronization, and the underlying event were modeled with PYTHIA 8.230 [44], using the A14 tune [45] and the NNPDF2.3LO PDF set. The $t\bar{t}$ sample was normalized to the cross-section prediction at next-to-next-to-leading order (NNLO) in QCD, including the resummation of next-to-next-to-leading logarithmic (NNLL) soft-gluon terms calculated using TOP++2.0 [46–52].

The production of a top quark in association with a W boson was modeled using the POWHEG-BOX v2 generator [39–41, 53] at NLO in QCD using the five-flavor scheme. Single-top-quark production in the t-channel was modeled using the POWHEG-BOX v2 generator [39–41, 54] at NLO in QCD using the four-flavor scheme. The s-channel production was modeled using the POWHEG-BOX v2 generator [39–41, 55] at NLO in QCD in the five-flavor scheme. For all three channels, the NNPDF3.0NLO PDF set was used for the matrix elements calculation. The events were interfaced with PYTHIA 8.230 using the A14 tune and the NNPDF2.3LO PDF set.

Production of top-quark pairs in association with a W, Z or Higgs boson (collectively denoted by $t\bar{t}X$) was modeled using the MADGRAPH5_aMC@NLO v2.3.3 generator [56] at NLO in QCD with NNPDF3.0NLO PDFs. The events were interfaced to PYTHIA 8.210 using the A14 tune and the NNPDF2.3LO PDF set.

The production of V+jets ($V = W, Z$) was simulated with the SHERPA v2.2.1 generator [36] using NLO matrix elements for up to two jets, and leading-order (LO) matrix elements for up to four jets calculated with the Comix [57] and OpenLoops libraries [58, 59]. They were matched with the SHERPA parton showers [60]

[2] The h_{damp} parameter is a resummation damping factor that controls the matching of POWHEG matrix elements to the parton shower and regulates the high-p_{T} radiation against which the $t\bar{t}$ system recoils.

using the MEPS@NLO prescription [61–64] and the tune developed by the SHERPA authors. The NNPDF3.0NNLO PDF set [42] was used and the samples were normalized to a NNLO prediction [65].

The SUSY signal samples were generated with MADGRAPH5_aMC@NLO v2.2.3 [56] using NNPDF2.3LO PDFs, and the modeling of the parton showering, hadronization and underlying event was performed with PYTHIA 8.210 with the A14 tune. The LO matrix elements include the emission of up to two additional partons. The matching between parton showers and matrix elements was done with the CKKW-L prescription [66, 67], with a matching scale set to one quarter of the mass of the bottom squark. Signal samples were generated with bottom-squark masses $m(\tilde{b})$ ranging from 250 GeV to 1000 GeV, and masses of the second-lightest neutralino $m(\tilde{\chi}_2^0)$ between 131 GeV and 380 GeV. Signal cross sections were calculated to approximate NNLO in QCD, adding the resummation of soft gluon emission at NNLL accuracy [68–75]. The nominal cross sections and their uncertainties were derived using the PDF4LHC15_mc PDF set, following the recommendations of Ref. [76], and decrease from 24.8 ± 1.6 pb at $m(\tilde{b}) = 250$ GeV to 14.5 ± 1.5 fb at $m(\tilde{b}) = 900$ GeV.

4 Event reconstruction

In this section, the reconstruction of the analysis objects from the detector data is described. The search presented in this paper is based on events which have b-jets, hadronically decaying τ-leptons and large missing transverse momentum in the final state. In addition to these, selections are used where τ-leptons are substituted with muons to improve the background model.

Inner-detector tracks with $p_{\mathrm{T}} > 500$ MeV are used to reconstruct primary vertices [77]. If several vertex candidates are found, the one with the largest sum of the squared transverse momenta of associated tracks Σp_{T}^2 is treated as the hard-scattering vertex.

An anti-k_t clustering algorithm [78, 79] with a radius parameter of $R = 0.4$ is used to reconstruct jet candidates in the calorimeter. Jets are built from massless positive-energy topological clusters [80] of calorimeter cells containing energy above a noise threshold, measured at the electromagnetic energy scale. The jet candidates are calibrated using jet energy scale (JES) corrections derived from data and simulation [81]. A global sequential calibration procedure is applied to improve the jet energy resolution (JER). Jets with $p_{\mathrm{T}} > 20$ GeV and $|\eta| < 2.8$ are selected, and a set of quality criteria are applied to reject jets not originating from pp collisions [82]. To suppress jets from pileup interactions, a jet-vertex-tagging algorithm [83] is employed for jets with $p_{\mathrm{T}} < 120$ GeV and $|\eta| < 2.5$. Jets containing b-hadrons are tagged as b-jets using a boosted decision tree (BDT) algorithm that exploits the impact parameters of tracks within the jet as well as secondary vertex information [84, 85]. The optimal working point for this analysis has an efficiency of 77%, with an approximate misidentification probability of 20% for jets arising from charm quarks, 6.7% for hadronically decaying τ-leptons, and 0.9% for light-flavor jets in simulated $t\bar{t}$ events.

The reconstruction of hadronically decaying τ-leptons [86] is seeded by anti-k_t jets ($R = 0.4$) built from topological clusters calibrated with a local hadronic weighting scheme [87]. The τ-leptons are built from clusters and tracks found within $\Delta R = 0.2$ of the seed jet axis. The tracks are selected by a set of BDTs, and only the candidates with one or three associated tracks and a charge sum of ± 1 are considered. The τ-leptons are required to have $p_{\mathrm{T}} > 20$ GeV and $|\eta| < 2.5$, and the transition region between barrel and endcap calorimeters ($1.37 < |\eta| < 1.52$) is excluded. The energy calibration is based on a boosted regression tree that exploits energy and shower-shape measurements from the calorimeter, information from particle-flow reconstruction [88] and the number of pileup interactions. A recurrent neural network

algorithm [89] is used to distinguish between jets and τ-leptons. It uses as input a set of high-level variables combining tracking and calorimeter measurements, as well as low-level variables from individual tracks and clusters. The *loose* identification working point is applied, corresponding to efficiencies of 85% and 75% for 1-prong and 3-prong τ-leptons, respectively. To reduce background from electrons that are misidentified as τ-leptons, 1-prong τ-lepton candidates are discarded if a nearby electron passes the *very loose* working point of the likelihood-based algorithm used to identify electrons. This requirement is tuned to have an efficiency of 95% for hadronically decaying τ-leptons [90].

Muon candidates are reconstructed by combining information from the muon spectrometer and the inner tracking detectors [91]. They are required to have $p_{\mathrm{T}} > 10\,\mathrm{GeV}$ and $|\eta| < 2.7$, to satisfy the *medium* identification criteria, and to pass a $|z_0 \sin\theta| < 0.5\,\mathrm{mm}$ requirement on the longitudinal impact parameter.[3] After discarding the candidates failing the *overlap-removal* procedure described below, stricter requirements are applied: muons must have $p_{\mathrm{T}} > 25\,\mathrm{GeV}$, meet the *loose* isolation criteria and satisfy the requirement $|d_0|/\sigma(d_0) < 3$ on the transverse impact parameter d_0 and its uncertainty $\sigma(d_0)$.

Electron candidates are reconstructed by matching energy clusters in the electromagnetic calorimeter to tracks from the inner tracking detector [92] and are required to have $p_{\mathrm{T}} > 10\,\mathrm{GeV}$ and $|\eta| < 2.47$. A requirement on the longitudinal impact parameter $|z_0 \sin\theta| < 0.5\,\mathrm{mm}$ discards electrons not associated with the primary vertex. Electrons are included in the computation of missing transverse momentum and in the overlap-removal procedure, but are not used otherwise.

The missing transverse momentum vector $\vec{p}_{\mathrm{T}}^{\,\mathrm{miss}}$ is defined as the negative vector sum of the transverse momenta of all reconstructed objects mentioned above, with an additional soft term including all tracks from the primary vertex that are not associated with a reconstructed object [93]. The magnitude of $\vec{p}_{\mathrm{T}}^{\,\mathrm{miss}}$ is denoted by $E_{\mathrm{T}}^{\mathrm{miss}}$.

An overlap-removal procedure is performed after event reconstruction to resolve ambiguities when a single physical object is reconstructed as multiple final-state objects. If two electrons share the same track, the electron with lower transverse momentum is discarded. Any τ-leptons overlapping with an electron or a muon within $\Delta R_y \equiv \sqrt{(\Delta y)^2 + (\Delta\phi)^2} < 0.2$ are removed. If an electron and a muon share the same inner-detector track, the muon is removed if it is tagged as a minimum-ionizing particle in the calorimeter, otherwise the electron is discarded. If a jet overlaps with an electron or a muon candidate within $\Delta R_y < 0.2$, the jet is removed. An exception is when a jet that has more than two associated tracks overlaps with a muon within $\Delta R_y < 0.2$, in which case the jet is kept and the muon is discarded. Finally, electron and muon candidates lying $0.2 < \Delta R_y < 0.4$ from a jet and jets within $\Delta R_y = 0.2$ of a τ-lepton candidate are discarded.

The same reconstruction and identification algorithms are used for both data and simulation. Dedicated correction factors are applied to jet, τ-lepton, electron and muon candidates to account for differences in efficiencies and energy calibrations between data and simulation.

5 Event selection

All selections used in this analysis require events to pass a $E_{\mathrm{T}}^{\mathrm{miss}}$ trigger [94] or a combined $E_{\mathrm{T}}^{\mathrm{miss}} + b$-jet trigger, except for specific selections used for the background estimate which rely on single-muon or

[3] The transverse impact parameter is defined as the distance of closest approach in the transverse plane between a track and the beam-line. The longitudinal impact parameter corresponds to the z-coordinate distance between the point along the track at which the transverse impact parameter is defined and the primary vertex.

Table 1: Summary of the common analysis preselection. The requirements in the upper part of the table apply to all analysis regions, those in the lower part of the table to all but the $Z(\tau\tau)$ control regions as discussed in Section 6.

$N_\tau + N_\mu$		≥ 1	
N_{jets}		≥ 3	
$p_{\text{T}}(\text{jet}_1)$		$> 140\,\text{GeV}$	
$p_{\text{T}}(\text{jet}_2)$		$> 100\,\text{GeV}$	
$\Delta\phi(\text{jet}_{1,2}, \vec{p}_{\text{T}}^{\text{miss}})$		> 0.5	
$N_{b\text{-jets}}$		≥ 2	
$p_{\text{T}}(b\text{-jet}_1)$		$> 100\,\text{GeV}$	
Trigger	$E_{\text{T}}^{\text{miss}} + b$-jet	OR	$E_{\text{T}}^{\text{miss}}$
$E_{\text{T}}^{\text{miss}}$	$> 160\,\text{GeV}$		$> 200\,\text{GeV}$

single-jet triggers as described in Section 6. The b-jet and muon objects reconstructed by the trigger algorithms are required to geometrically match the corresponding reconstructed analysis objects defined in Section 4, otherwise the event is discarded. The HLT threshold of the $E_{\text{T}}^{\text{miss}}$ trigger increased from 70 to 110 GeV over the data-taking period. The $E_{\text{T}}^{\text{miss}} + b$-jet trigger had HLT thresholds of 60 GeV on $E_{\text{T}}^{\text{miss}}$ and 80 GeV on the transverse momentum of the b-jet, and the efficiency of the online b-jet identification algorithm determined for simulated $t\bar{t}$ events was 60% in 2016 and 50% in 2017 and 2018. This trigger increases the acceptance for low-$E_{\text{T}}^{\text{miss}}$ signals expected from low-mass bottom squarks. The dataset associated with the $E_{\text{T}}^{\text{miss}} + b$-jet trigger has a reduced integrated luminosity of 127 fb^{-1} because this trigger was not active in 2015, and stricter data-quality requirements are applied to b-jet triggers in 2016 and 2017 to ensure a valid beam-spot determination.

Events are rejected if no primary vertex with at least two tracks is found or if they contain a jet failing to meet the *loose* quality criteria described in Ref. [82]. Furthermore, events are rejected if they contain muons with a large track-curvature uncertainty or muons which are likely to originate from cosmic rays as indicated by a large displacement from the primary vertex.

Events are required to have at least three jets, among which at least two must be b-tagged unless stated otherwise. The leading and subleading jets are required to have $p_{\text{T}} > 140\,\text{GeV}$ and $p_{\text{T}} > 100\,\text{GeV}$, respectively, and the leading b-jet is required to have $p_{\text{T}} > 100\,\text{GeV}$. The $E_{\text{T}}^{\text{miss}}$ requirement depends on the trigger considered: the $E_{\text{T}}^{\text{miss}} + b$-jet trigger reaches maximum efficiency for $E_{\text{T}}^{\text{miss}} > 160\,\text{GeV}$, while the $E_{\text{T}}^{\text{miss}}$ trigger requires $E_{\text{T}}^{\text{miss}} > 200\,\text{GeV}$ to be fully efficient.

To suppress the multijet background, events are vetoed if the angular separation in the transverse plane $\Delta\phi(\text{jet}_{1,2}, \vec{p}_{\text{T}}^{\text{miss}})$ between one of the two leading jets and $\vec{p}_{\text{T}}^{\text{miss}}$ is less than 0.5. All analysis selections require the presence of at least one τ-lepton or one muon in the event. This common preselection is summarized in Table 1. In the following, the number of objects in an event is generically written as N_{object}, and indices '1' and '2' refer to the leading and subleading objects, respectively, which are ordered by decreasing transverse momentum.

On top of the preselection from Table 1, a set of signal regions (SRs) are defined in order to target the bottom-squark signal processes illustrated in Figure 1. All SRs require at least two hadronically decaying τ-leptons with opposite electric charge (referred to as the OS criterion) and no muon to be present.

Additional kinematic selections are applied to suppress the SM background. These selections are described in the following and summarized in Table 2. They are optimized by maximizing the signal significance [95]

in the previously nonexcluded parameter space of the targeted signal model.

To ensure compatibility with a Higgs boson decay, the visible invariant mass of the two leading τ-leptons must satisfy $55\,\text{GeV} < m(\tau_1, \tau_2) < 120\,\text{GeV}$. The lower bound suppresses the $Z(\tau\tau)$ background, while the upper bound reduces 'nonresonant' background contributions where the τ-leptons do not originate from the same resonance. Events are required to have $H_\text{T} > 1100\,\text{GeV}$, where $H_\text{T} \equiv \sum p_\text{T}^\tau + \sum p_\text{T}^\mu + \sum p_\text{T}^\text{jet}$ is the scalar sum of the transverse momenta of all τ-leptons, muons and jets in the event. This variable exploits the fact that signals with large bottom-squark masses are expected to produce highly boosted particles in the final state.

The stransverse mass variable [96, 97], denoted m_T2, is used to discriminate between the signal process and the top-quark production background. It is designed to have an endpoint for background processes such as top-quark production where the two τ-leptons originate from separate decay branches. For the signal process, the two τ-leptons originate from a resonant Higgs boson decay, and the m_T2 spectrum has a pronounced tail towards larger values. The m_T2 variable is computed as

$$m_\text{T2} = \min_{\vec{p}_\text{T}^{\,a}+\vec{p}_\text{T}^{\,b}=\vec{p}_\text{T}^{\,\text{miss}}} \left(\max \left[m_\text{T}(\vec{p}_\text{T}^{\,\tau_1}, \vec{p}_\text{T}^{\,a}), m_\text{T}(\vec{p}_\text{T}^{\,\tau_2}, \vec{p}_\text{T}^{\,b}) \right] \right),$$

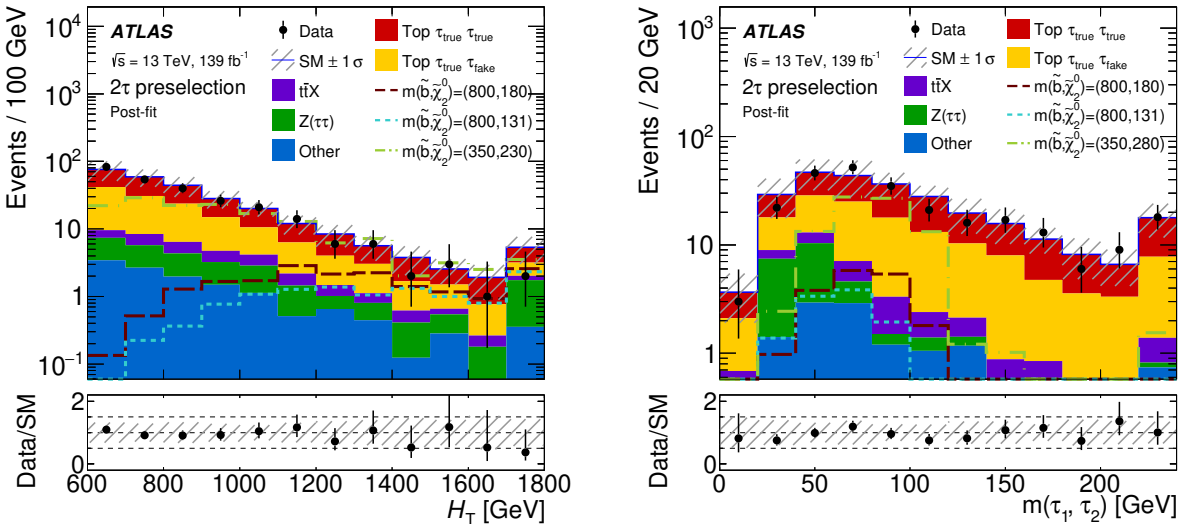
where $\vec{p}_\text{T}^{\,\tau_1,\tau_2}$ correspond to the transverse momenta of the two leading τ-leptons, and (a, b) refers to two invisible particles assumed to be produced with transverse momentum $\vec{p}_\text{T}^{\,a,b}$. The masses of the invisible particles are free parameters and set to $m_a = m_b \equiv m_\text{inv}$. The transverse mass m_T is defined as $m_\text{T}^2(\vec{p}_\text{T}^{\,\tau_1}, \vec{p}_\text{T}^{\,a}) = m_a^2 + 2\left(p_\text{T}^{\tau_1}\sqrt{m_a^2 + \left(p_\text{T}^a\right)^2} - \vec{p}_\text{T}^{\,\tau_1} \cdot \vec{p}_\text{T}^{\,a}\right)$, where the τ-lepton mass is set to 0 GeV. The m_T2 distribution peaks at 0 GeV for both the bottom-squark signal and the dominant $t\bar{t}$ background when setting m_inv to 0 GeV, providing poor discrimination. The discrimination improves as m_inv is increased, and a value of 120 GeV is found to result in an m_T2 distribution that best separates the signal from the background. All SRs require $m_\text{T2} > 140\,\text{GeV}$. Some of the CRs also make use of the transverse mass of a τ-lepton, which is computed as $\left(m_\text{T}^\tau\right)^2 = 2(p_\text{T}^\tau E_\text{T}^\text{miss} - \vec{p}_\text{T}^{\,\tau} \cdot \vec{p}_\text{T}^{\,\text{miss}})$.

The last discriminant is Θ_min, defined as the smallest three-dimensional angle of the four combinations between either of the two leading τ-leptons and either of the two leading b-jets. For the $t\bar{t}$ background, the smallest angle is expected from configurations where the b-jet and the τ-lepton originate from the same top-quark decay, resulting in relatively low values of Θ_min. For $Z(\tau\tau) + b\bar{b}$ events with a highly boosted Z boson, the pair of τ-leptons recoils against the b-jets, and large values of Θ_min are expected. For signal events where $\tilde{b} \to b\tilde{\chi}_2^0 \to bh(\tau\tau)\tilde{\chi}_1^0$, the angle between the b-jet and the τ-lepton pair increases with the $\tilde{b}$ mass, and so does Θ_min. A multi-bin SR with three Θ_min bins (< 0.5, $[0.5, 1.0]$, > 1.0) is defined in order to take advantage of these features. A single-bin SR requiring $\Theta_\text{min} > 0.6$ is used to provide cross-section limits on generic processes beyond the Standard Model (BSM). The product of kinematic acceptance and reconstruction and identification efficiencies of the single-bin SR for the signal process ranges between $6.4 \cdot 10^{-6}$ at $m(\tilde{b}) = 250\,\text{GeV}$ and $m(\tilde{\chi}_2^0) = 150\,\text{GeV}$ and $1.4 \cdot 10^{-3}$ at $m(\tilde{b}) = 900\,\text{GeV}$ and $m(\tilde{\chi}_2^0) = 150\,\text{GeV}$.

Examples of signal and background kinematic distributions are shown in Figure 2. The two plots show the H_T and $m(\tau_1, \tau_2)$ variables after the preselection. The estimated SM background is scaled by the normalization factors from the background fit described in Section 6, and the distributions for several signal models are overlaid.

Table 2: Definition of the single-bin and multi-bin signal regions. The requirements are applied in addition to the preselection from Table 1. The single-bin and multi-bin SRs only differ by the Θ_{min} requirement.

	Common SR requirements	
N_μ	0	
N_τ	≥ 2	
$\text{OS}(\tau_1, \tau_2)$	yes	
$m(\tau_1, \tau_2)$	[55, 120] GeV	
m_{T2}	> 140 GeV	
H_{T}	> 1100 GeV	
	Single-bin SR	Multi-bin SR
Θ_{min}	> 0.6	3 bins: < 0.5, $[0.5, 1.0]$, > 1.0



(a) (b)

Figure 2: Kinematic distributions of data and SM background for events that pass the preselection and have at least two hadronically decaying τ-leptons. Predictions from three signal models are also shown, where the masses $m(\tilde{b})$ and $m(\tilde{\chi}_2^0)$ are given in GeV in the legend. Distributions are displayed for the (a) H_{T} and (b) $m(\tau_1, \tau_2)$ variables. The hatched band indicates the total statistical and systematic uncertainty of the SM background. The "Other" contribution includes all the backgrounds not explicitly listed in the legend (V+jets except $Z(\tau\tau)$+jets, diboson/triboson, multijet). The top-quark and $Z(\tau\tau)$ background contributions are scaled with the normalization factors obtained from the background-only fit described in Section 6. The rightmost bin includes the overflow. The bottom panel shows the ratio of the observed data and the expected Standard Model background.

6 Background estimation

The largest backgrounds in the SRs are from $t\bar{t}$ and single-top-quark processes, referred to as top-quark background, and $Z(\tau\tau)$ produced in association with b-jets. Subdominant contributions arise from $t\bar{t}X$ processes, while other backgrounds such as multijet or diboson and triboson production are found to be negligible. The normalization of the two dominant backgrounds is fitted to the data in dedicated control regions (CRs) kinematically close to the SRs but where little signal is expected. The normalization factors are derived with a likelihood fit based on the HistFitter framework [98]. The fit uses as input the observed data yields, the expected yields predicted from simulation, as well as the statistical and systematic uncertainties described in Section 7. Two main fit setups are employed in the analysis. The background-only fit refers to the configuration that only includes the CRs, and where no signal is considered. The signal-plus-background fit includes both the CRs and the SRs, and it takes into account a possible signal contribution in the fitted regions. It is used to establish exclusion limits as discussed in Section 8. In both cases, the fit is performed simultaneously over all the relevant regions. Subdominant background contributions are normalized according to their cross sections and the integrated luminosity of the data. The multijet background is determined from data. Validation regions (VRs) are defined in phase-space regions as close as possible to that of the SRs. The VRs are not included in the fit. They are used to validate the background-model extrapolation from the CRs to the SRs by comparing the observed data with the fitted background predictions. As such, they are designed to have little signal contribution. The methods used to estimate the various backgrounds are described in the following, together with the associated CRs and VRs.

Multijet production is an important background at hadron colliders, but it is efficiently suppressed in this analysis by the requirement of two hadronically decaying τ-leptons, two b-jets, large $E_{\mathrm{T}}^{\mathrm{miss}}$, and $\Delta\phi(\mathrm{jet}_{1,2}, \vec{p}_{\mathrm{T}}^{\,\mathrm{miss}}) > 0.5$. A data-driven jet-smearing method [99] is employed to estimate this background. Events recorded by single-jet triggers are processed through an energy-smearing procedure that emulates $E_{\mathrm{T}}^{\mathrm{miss}}$ originating from resolution effects. The normalization of the smeared pseudo-data template is derived in events where one of the two leading jets is aligned with $\vec{p}_{\mathrm{T}}^{\,\mathrm{miss}}$ in the transverse plane. Except for that multijet-enriched selection, the multijet background is found to be negligible in all analysis selections. Therefore, its normalization is kept constant in the fits, for simplicity.

The design of the control regions for the top-quark and $Z(\tau\tau) + b\bar{b}$ backgrounds is driven by two main considerations. Firstly, the hadronically decaying τ-leptons selected in the analysis are either prompt τ-leptons from electroweak boson decays, or jets misidentified as τ-leptons. They are referred to as *true* τ-leptons (τ_{true}) and *fake* τ-leptons (τ_{fake}), respectively, and their contributions must be handled separately in the background model. No such distinction is made for b-jets, as the fraction of misidentified b-jets does not exceed 10% in the analysis phase space. The top-quark background in the SRs is composed of $\tau_{\mathrm{true}}\tau_{\mathrm{true}}$ and $\tau_{\mathrm{true}}\tau_{\mathrm{fake}}$ contributions of comparable magnitude, where one τ-lepton comes from a W-boson decay, and the second τ-lepton either comes from the other W-boson decay or from a jet misidentified as a τ-lepton. The $\tau_{\mathrm{fake}}\tau_{\mathrm{fake}}$ contribution is negligible due to the large jet rejection provided by the τ-lepton identification algorithm. In the case of $Z(\tau\tau) + b\bar{b}$ events, only the $\tau_{\mathrm{true}}\tau_{\mathrm{true}}$ contribution is found to be relevant. Secondly, the background normalization factors cannot be accurately determined using events containing two hadronically decaying τ-leptons (τ_{had}) and two b-jets, as the low event yields remaining after the preselection do not allow control regions with sufficient statistical power, high purity, and low signal contamination to be defined.

Because of these limitations the CRs are based on final states where either one or two τ-leptons are replaced with muons. The CR_Top_$\mu\tau_{\mathrm{true}}$ and CR_Top_$\mu\tau_{\mathrm{fake}}$ selections are defined to respectively target top-quark

Table 3: Definition of the control regions used for the top-quark background. The requirements are applied in addition to the preselection. A dash means that no requirement on this variable is applied.

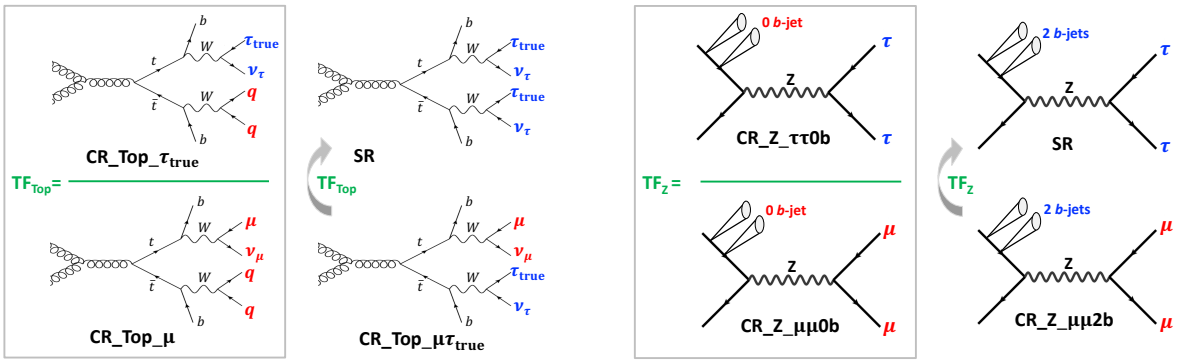
	CR_Top_μ	CR_Top_τ_{true}	CR_Top_μτ_{true}	CR_Top_μτ_{fake}
N_μ	1	0	1	1
N_τ	0	1	1	1
OS(μ, τ)	–	–	yes	yes
H_{T}	[600, 1000] GeV			
m_{T}^{τ}	–	< 80 GeV	< 80 GeV	> 100 GeV

events with one muon plus either one τ_{true} or one τ_{fake} in the final state, where the muon replaces a τ_{true} from one of the W-boson decays. The CR_Z_μμ2b region is defined to select $Z(\mu\mu) + b\bar{b}$ events. By trading $W(\tau\nu)$ for $W(\mu\nu)$ and $Z(\tau\tau)$ for $Z(\mu\mu)$, the CRs target the desired background processes but benefit from larger yields due to the branching ratio $\mathcal{B}(\tau \to \tau_{\text{had}}\nu_\tau)$ of 65% that does not apply to muons, and the reconstruction and identification efficiencies that are higher for muons. In the top-quark CRs, event yields are further increased by a combinatorial factor of two.

The normalization factors derived for background events with muons are not directly applicable to background events in the SRs that contain two hadronically decaying τ-leptons. The replacement of τ-leptons with muons has an impact on the reconstructed event kinematics and the selection efficiency of background processes, which needs to be accounted for. This is done by introducing additional CRs and normalization factors, two for the top-quark background and two for the $Z(\tau\tau) + b\bar{b}$ background, that allow an extrapolation from muon to τ-lepton selections. As mentioned in Section 4, corrections are already applied to muons and τ-leptons in the simulation to match the efficiencies and energy calibration measured in data. The background normalization factors from the additional CRs thus mostly account for acceptance effects.

The definitions of the four control regions used to normalize the top-quark background are summarized in Table 3. The CR_Top_μτ_{true} and CR_Top_μτ_{fake} regions select events that contain exactly one muon and one τ-lepton of opposite electric charge. Like all control regions defined in this analysis, they use the H_{T} range from 600 to 1000 GeV. For CR_Top_μτ_{true}, the τ-lepton transverse mass m_{T}^{τ} must be lower than 80 GeV, which results in a high purity of true τ-leptons. For CR_Top_μτ_{fake}, m_{T}^{τ} has to be larger than 100 GeV, which gives a roughly equal mix of true and fake τ-leptons. The CR_Top_τ_{true} selection is identical to that of CR_Top_μτ_{true} except that events must not contain a muon. This region has a high purity in top-quark background events decaying semileptonically with a true τ-lepton in the final state. The CR_Top_μ selection is defined in a similar way, with one muon and no τ-lepton, selecting high-purity semileptonic top-quark processes with a muon in the final state.

The way the four CRs from Table 3 are used to derive normalization factors for the top-quark background processes is illustrated in Figure 3(a). The expected yields for top-quark production with true and fake τ-leptons from Monte Carlo simulation are respectively multiplied by normalization factors $\omega_{\tau_{\text{true}}}$ and $\omega_{\tau_{\text{fake}}}$, that float freely in the fit and are constrained by data mainly through CR_Top_μτ_{true} and CR_Top_μτ_{fake}. To account for the different lepton flavors in the signal region (with two τ-leptons) and the control region (one τ-lepton and one muon), the top-quark production yields are further multiplied by additional freely floating normalization factors $\omega_{1\tau}$ and $\omega_{1\mu}$, which are constrained mainly through the regions CR_Top_τ_{true} and CR_Top_μ. A transfer factor $\text{TF}_{\text{Top}} \equiv \omega_{1\tau}/\omega_{1\mu}$ is used to correct for the difference between requiring a muon and a true τ-lepton. This means that a simulated top-quark event with one true and one fake τ-lepton



(a) (b)

Figure 3: Schematic representation of the control region setup that is used to constrain the normalization of the (a) top-quark and (b) $Z(\tau\tau)$+jets backgrounds in the signal regions. The arrows represent the transfer factors associated with the replacement of muons with true τ-leptons, which correct for acceptance. For the top-quark background, the sketch illustrates the normalization strategy for the τ_{true} τ_{true} contribution. A similar strategy is employed for the τ_{true} τ_{fake} contribution, where the τ_{fake} can originate from a jet from a hadronically decaying W boson, a b-jet, or a jet from initial-state radiation.

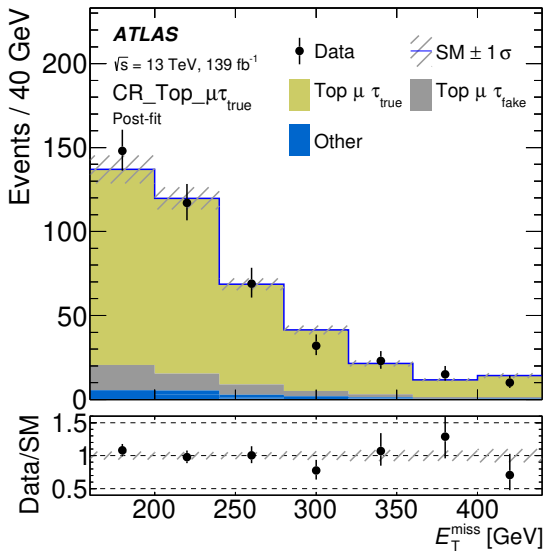
Table 4: Definition of the control regions used for the Z+jets background. The requirements are applied in addition to the set of preselection criteria reported in the upper part of Table 1. A dash means that no requirement on this variable is applied.

	CR_Z_μμ2b	CR_Z_μμ0b	CR_Z_$\tau\tau$0b
Trigger	single-muon		$E_{\text{T}}^{\text{miss}}$
N_μ	2		0
N_τ	0		2
$N_{b\text{-jets}}$	2	0	0
$p_{\text{T}}(\mu_1)$	> 30 GeV		–
$E_{\text{T}}^{\text{miss}}$	< 100 GeV		> 200 GeV
$p_{\text{T}}(\mu_1, \mu_2)$	> 200 GeV		–
$m(\mu_1, \mu_2)$	[81, 101] GeV		–
$m_{\text{T}}^{\tau_1} + m_{\text{T}}^{\tau_2}$	–		< 100 GeV
H_{T}	[600, 1000] GeV		

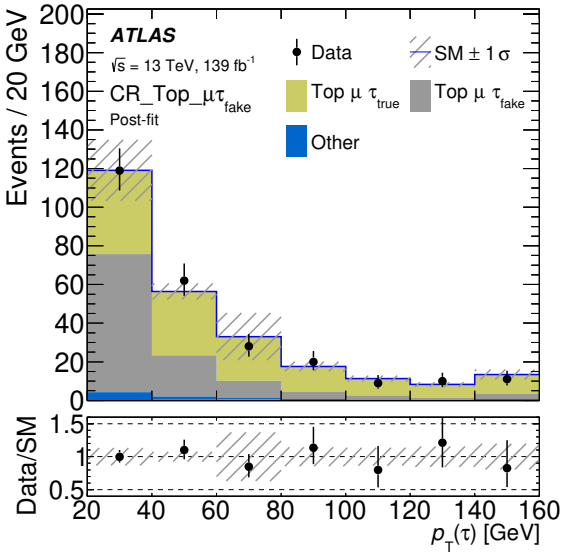
in one of the signal regions receives a normalization factor $\omega_{\tau_{\text{fake}}} \times \text{TF}_{\text{Top}}$, and a simulated top-quark event with two true τ-leptons a normalization factor $\omega_{\tau_{\text{true}}} \times \text{TF}_{\text{Top}}$.

Figure 4 shows several examples of distributions from the four control regions associated with the top-quark background. In these plots, the predicted background contributions from simulation are scaled with the normalization factors obtained from the background-only fit. All of the CRs show good agreement between the SM prediction and the data. They also have high purity in the respective top-quark background processes except for CR_Top_μτ_{fake}, where the purity is only 43% because it is difficult to isolate the contribution of the top-quark background with fake τ-leptons.

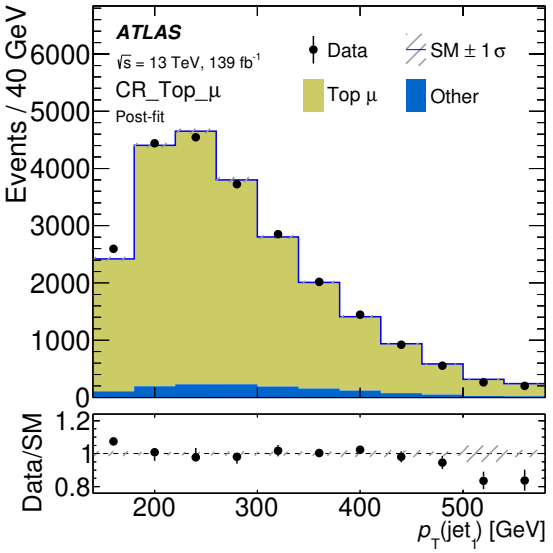
The three control regions that target the $Z(\tau\tau)$ background are summarized in Table 4. The CR_Z_μμ2b selection is defined using events with two muons of opposite electric charge, taken as proxies for two true



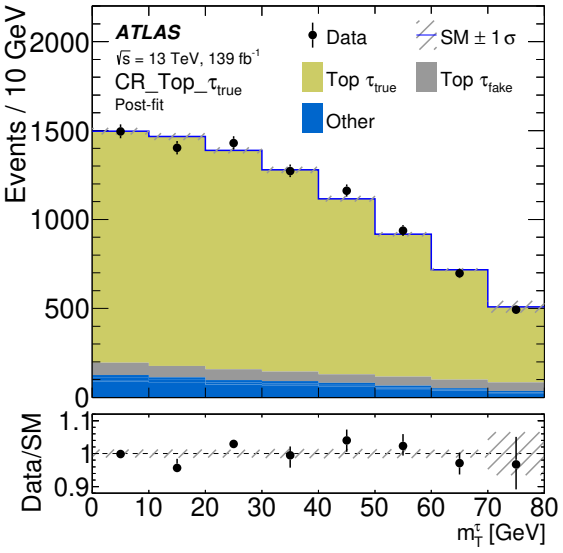
(a) $E_{\mathrm{T}}^{\mathrm{miss}}$ in CR_Top_μτ_{true}



(b) $p_{\mathrm{T}}(\tau)$ in CR_Top_μτ_{fake}



(c) $p_{\mathrm{T}}(\mathrm{jet}_1)$ in CR_Top_μ



(d) m_{T}^{τ} in CR_Top_τ_{true}

Figure 4: Kinematic distributions from the four control regions associated with the top-quark background, showing (a) $E_{\mathrm{T}}^{\mathrm{miss}}$ in CR_Top_μτ_{true}, (b) $p_{\mathrm{T}}(\tau)$ in CR_Top_μτ_{fake}, (c) $p_{\mathrm{T}}(\mathrm{jet}_1)$ in CR_Top_μ, and (d) m_{T}^{τ} in CR_Top_τ_{true}. The hatched band indicates the total statistical and systematic uncertainty of the SM background. The top-quark and $Z(\tau\tau)$ background contributions are scaled with the normalization factors obtained from the background-only fit. The "Other" contribution includes all the backgrounds not explicitly listed in the legend (V+jets, $t\bar{t}X$, diboson/triboson, multijet). The rightmost bin includes the overflow. The bottom panel shows the ratio of the observed data and the expected Standard Model background.

τ-leptons, and two b-jets. Since $Z(\mu\mu)$+jets processes do not have large $E_{\mathrm{T}}^{\mathrm{miss}}$ in the final state, the events are selected using a single-muon trigger, which has its efficiency plateau at $p_{\mathrm{T}}(\mu) > 30\,\mathrm{GeV}$. The invariant mass of the dimuon system is required to be within 10 GeV of the Z-boson mass, and $E_{\mathrm{T}}^{\mathrm{miss}}$ to be lower than 100 GeV to increase the purity of the selection. To move the CR closer to the relevant phase space, H_{T}

Table 5: Values of normalization and transfer factors with their statistical and systematic uncertainties as obtained from the background-only fit, in the top part of the table for top-quark background processes, and in the bottom part for Z+jets. The control regions that primarily affect the normalization factors are listed, together with the purity of the CR in the relevant background process. As $\mathrm{TF}_{\mathrm{Top}}$ and TF_Z are ratios of two normalization factors, one of which (the denominator) is listed in the row directly above, the table lists the respective second control region (the numerator of the ratio) and its purity in top-quark or $Z(\tau\tau) + b\bar{b}$ events.

Normalization / transfer factor	Fitted value	Control region	Purity
$\omega_{\tau_{\mathrm{true}}}$	0.88 ± 0.16	CR_Top_μτ_{true}	86%
		CR_Top_μτ_{fake}	53%
$\omega_{\tau_{\mathrm{fake}}}$	0.79 ± 0.30	CR_Top_μτ_{fake}	43%
		CR_Top_μτ_{true}	9%
$\omega_{1\mu}$	0.91 ± 0.10	CR_Top_μ	94%
$\mathrm{TF}_{\mathrm{Top}} \equiv \omega_{1\tau}/\omega_{1\mu}$	0.98 ± 0.04	CR_Top_τ_{true}	88%
$\omega_{\mathrm{Z\mu\mu2b}}$	1.28 ± 0.12	CR_Z_μμ2b	89%
$\omega_{\mathrm{Z\mu\mu0b}}$	1.00 ± 0.05	CR_Z_μμ0b	96%
$\mathrm{TF}_Z \equiv \omega_{\mathrm{Z}\tau\tau\mathrm{0b}}/\omega_{\mathrm{Z\mu\mu0b}}$	0.99 ± 0.17	CR_Z_$\tau\tau$0b	79%

must be in the range [600, 1000] GeV, and the transverse momentum of the muon pair $p_{\mathrm{T}}(\mu_1, \mu_2)$ must be larger than 200 GeV, which is a typical value found in simulation for the p_{T} of the Z boson in $Z(\tau\tau)$ events after the preselection. The $Z(\mu\mu)$ background is multiplied by the freely floating normalization factor $\omega_{\mathrm{Z\mu\mu2b}}$, which is constrained through CR_Z_μμ2b.

The two additional control regions CR_Z_μμ0b and CR_Z_$\tau\tau$0b are used to correct for the difference in acceptance and efficiency when replacing the τ-leptons with muons to estimate the Z+jets background. The interplay of these CRs is illustrated in Figure 3(b). The CR_Z_μμ0b selection is the same as for CR_Z_μμ2b but with a b-jet veto, whereas CR_Z_$\tau\tau$0b requires the presence of two τ-leptons with opposite electric charge and no b-jet. The CR_Z_$\tau\tau$0b events are selected with an $E_{\mathrm{T}}^{\mathrm{miss}}$ trigger and $E_{\mathrm{T}}^{\mathrm{miss}} > 200$ GeV as is done for the SRs, and muons are vetoed in this region. Additionally, the sum of τ-lepton transverse masses $m_{\mathrm{T}}^{\tau_1} + m_{\mathrm{T}}^{\tau_2}$ has to be lower than 100 GeV to increase the purity in $Z(\tau\tau)$ events. In all of these three CRs, H_{T} is again required to be within [600, 1000] GeV.

From these two auxiliary control regions, the freely floating normalization factor $\omega_{\mathrm{Z\mu\mu0b}}$ and transfer factor $\mathrm{TF}_Z \equiv \omega_{\mathrm{Z}\tau\tau\mathrm{0b}}/\omega_{\mathrm{Z\mu\mu0b}}$ are derived in the background fit. The background normalization in CR_Z_μμ0b is absorbed into $\omega_{\mathrm{Z\mu\mu0b}}$. The transfer factor TF_Z transfers the normalization from CR_Z_μμ0b to CR_Z_$\tau\tau$0b, and from CR_Z_μμ2b to the SRs, i.e. $Z(\tau\tau) + b\bar{b}$ events in the SRs are scaled by $\omega_{\mathrm{Z\mu\mu2b}} \cdot \mathrm{TF}_Z$.

All normalization and transfer factors are obtained from a simultaneous fit of the seven CRs for the top-quark and $Z(\tau\tau)$ backgrounds. Table 5 lists the values of the normalization factors and transfer factors and their uncertainties, the names of the control regions that determine the normalization factors and the respective purities of the control regions in top-quark or Z+jets events. The transfer factors $\mathrm{TF}_{\mathrm{Top}}$ and TF_Z are computed from ratios of two normalization factors as explained above. For these, one row in the table ($\omega_{1\mu}$ and $\omega_{\mathrm{Z\mu\mu0b}}$) gives the values forming the respective denominators of the ratios, showing how well the data and simulated events agree in these regions. The row below gives the transfer factor ($\mathrm{TF}_{\mathrm{Top}}$ and TF_Z, respectively). In these rows, the table lists the second control region (the numerator of the ratio) and its purity.

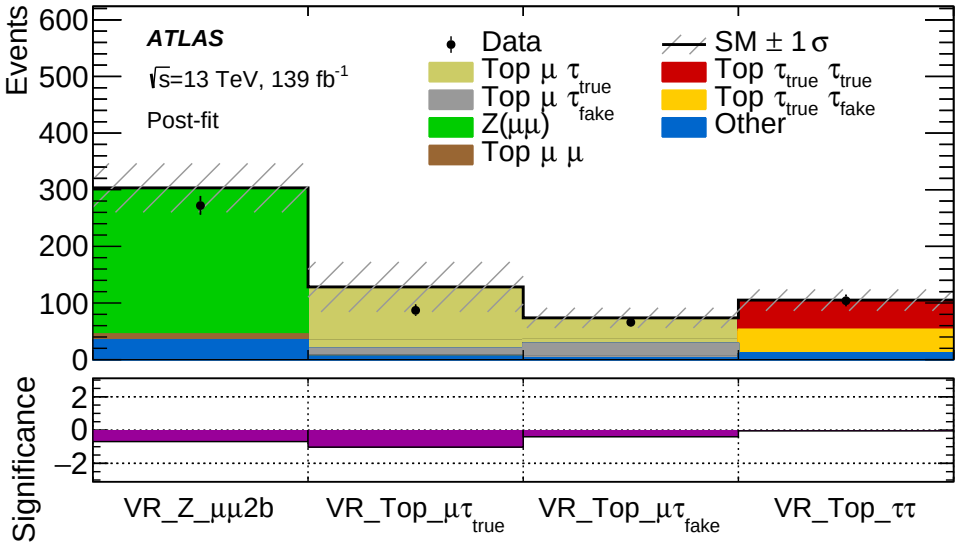


Figure 5: The upper panel shows the expected number of SM background events and the number of events observed in data for each of the four validation regions. In the lower panel, the significance of the deviation of the observed yield from the expected yield is shown. The top-quark, $Z(\tau\tau)$ and $Z(\mu\mu)$ background contributions are scaled with the normalization factors obtained from the background-only fit described in Section 6. The hatched band indicates the total statistical and systematic uncertainty of the SM background. The "Other" contribution includes all the backgrounds not explicitly listed in the legend (V+jets except $Z(\mu\mu)$+jets, $t\bar{t}X$, diboson/triboson, multijet).

Three validation regions are defined to check the extrapolation from CR_Top_μτ_{true}, CR_Top_μτ_{fake}, and CR_Z_μμ2b in the H_{T} variable. This is done by changing the requirement on H_{T} that is applied in the CRs from 600 GeV $< H_{\text{T}} <$ 1000 GeV to 1000 GeV $< H_{\text{T}} <$ 1500 GeV in the VRs, while keeping all other requirements the same as for the respective CRs. Shifting the H_{T} range moves the validation regions closer to the signal regions, which require $H_{\text{T}} >$ 1100 GeV. The VRs and the SRs are mutually exclusive due to the muon veto that is part of the signal-region selections. The names of the three VRs match those of the corresponding CRs. A fourth validation region, VR_Top_$\tau\tau$, is defined to validate the extrapolation from muons to τ-leptons in events with two b-jets and two hadronically decaying τ-leptons which pass the $E_{\text{T}}^{\text{miss}}$ trigger or the $E_{\text{T}}^{\text{miss}}$ + b-jet trigger and the corresponding trigger-plateau requirements. To avoid overlap of this VR with the SRs, H_{T} is required to be within [600, 1000] GeV. In addition, the visible di-τ mass $m(\tau_1, \tau_2)$ is required to be either lower than 40 GeV or larger than 90 GeV to reduce the contribution from a possible bottom-squark signal.

Figure 5 shows that the expected background yields after the fit and the observed yields agree within one standard deviation for all four validation regions, demonstrating good modeling of the SM background. Figure 6 shows the Θ_{min} distribution in VR_Top_$\tau\tau$. Good agreement between the background model and the data is observed. The contribution of a potential signal from the model in Figure 1 to the control regions does not exceed 7% at the low end of the range of bottom-squark masses covered by the signal models and quickly falls to below a percent at the high end. For the validation regions it is around 15% for low $m(\tilde{b})$ and again falls to a percent or less for larger $m(\tilde{b})$.

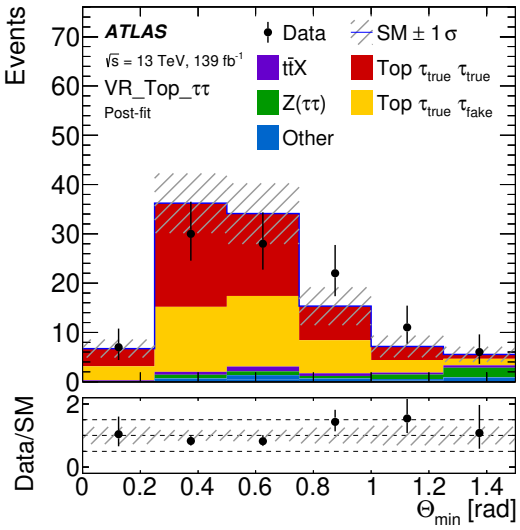


Figure 6: Kinematic distribution of the Θ_{min} variable in the VR_Top_$\tau\tau$ region. The hatched band indicates the total statistical and systematic uncertainty of the SM background. The "Other" contribution includes all the backgrounds not explicitly listed in the legend (V+jets except $Z(\tau\tau)$+jets, diboson/triboson, multijet). The top-quark and $Z(\tau\tau)$ background contributions are scaled with the normalization factors obtained from the background-only fit. The rightmost bin includes the overflow. The bottom panel shows the ratio of the observed data and the expected Standard Model background.

7 Systematic uncertainties

The experimental uncertainties considered in this analysis comprise systematic uncertainties in the reconstruction, identification, calibration and corrections applied to the physical objects used in the analysis. They are assumed to be correlated across analysis regions and between the background processes and the signal. Theoretical uncertainties include contributions from generator modeling as well as cross-section uncertainties. They are assumed to be correlated across analysis regions but uncorrelated between different background processes. When assuming no correlation between analysis regions, the total background uncertainty increases by about 5 percentage points for the single-bin SR, and the exclusion contour does not change significantly.

The experimental uncertainties related to jets include uncertainties in the energy scale [81] and resolution [100], jet-vertex-tagging uncertainties [83] and flavor-tagging uncertainties [84, 101, 102]. Flavor-related uncertainties come from the uncertainties in data-to-simulation correction factors for efficiencies and fake rates and from the extrapolation over jet p_{T}. The τ-lepton uncertainties arise from the energy calibration, and reconstruction and identification efficiencies [86, 90]. The energy scale uncertainties include the nonclosure of the calibration and uncertainties in the detector response estimated from simulation, as well as uncertainties in the relative calibration of data and simulation measured in $Z(\tau_\mu\tau_{\text{had}})$ events. An uncertainty at high-p_{T}, based on single-particle response uncertainties, is taken into account. Muon-related uncertainties [91] are not relevant in the signal regions, as events with muons do not enter these, but they can be important in control regions with muons. Uncertainties related to electrons have a negligible impact on this analysis. The systematic uncertainties affecting the energy or momentum of calibrated objects are propagated to the $E_{\text{T}}^{\text{miss}}$ calculation. Specific uncertainties in the soft-term contribution to the $E_{\text{T}}^{\text{miss}}$ [93] are also considered.

Table 6: Dominant systematic uncertainties in the background prediction for the signal regions after the fit to the control regions. "Other" includes the uncertainties arising from muons, jet-vertex tagging, modeling of pileup, the $E_{\mathrm{T}}^{\mathrm{miss}}$ computation, multijet background, and luminosity. The individual uncertainties can be correlated and do not necessarily add in quadrature to equal the total uncertainty.

Uncertainty	Single-bin SR	Multi-bin SR		
		$\Theta_{\mathrm{min}} < 0.5$	$0.5 < \Theta_{\mathrm{min}} < 1.0$	$\Theta_{\mathrm{min}} > 1.0$
Generator modeling	37%	42%	44%	27%
Normalization / transfer factors	15%	11%	12%	18%
JER and JES	12%	5.1%	9.8%	22%
τ-leptons	8.3%	3.5%	2.3%	15%
MC statistical uncertainty	6.9%	6.8%	7.2%	11%
Flavor tagging	3.8%	1.0%	1.8%	5.4%
Other	2.9%	1.3%	1.8%	6.6%
Total	40%	43%	46%	41%

The theoretical uncertainties related to variations of the PDFs [76], strong coupling constant α_{s} and renormalization and factorization scales μ_{r} and μ_{f} [103] are evaluated from generator weights for all background samples. The sets include the nominal PDF as well as 100 variations. The PDF uncertainty is obtained as the envelope of all the variations. The uncertainty related to α_{s} is evaluated by computing $\alpha_{\mathrm{s}} = 0.119$ and $\alpha_{\mathrm{s}} = 0.117$ parameterizations and averaging the difference between them. The PDF and α_{s} uncertainties are then added in quadrature. In order to derive the scale uncertainties, μ_{r} and μ_{f} are varied up and down by a factor of two. Three independent nuisance parameters are used, two resulting from keeping one of the scales constant while varying the other one, and the third being the coherent variation of both scales. The variations are normalized to the nominal sum of weights so that the effect on the normalization included in the cross-section uncertainty is not double-counted. For all simulated processes that are not normalized to the data, uncertainties in the cross section and in the integrated luminosity of the data are applied.

For $t\bar{t}$ and single-top-quark production, generator uncertainties related to hard scattering and matching are evaluated by comparing Powheg-Box+Pythia with MadGraph5_aMC@NLO+Pythia. Parton-showering uncertainties are estimated by comparison with Powheg-Box+Herwig7. Uncertainties in the initial-state and final-state radiation are evaluated by simultaneously testing the impact of scale variations and eigenvariations of the A14 tune [45]. For $t\bar{t}$ production, an additional comparison with the h_{damp} parameter set to $3m_{\mathrm{top}}$ is included. For single-top-quark production, an uncertainty in the treatment of the $Wt/t\bar{t}$ interference is considered by comparing samples produced with the nominal diagram-removal scheme [104] with alternative samples generated with a diagram-subtraction scheme [43, 104].

For the V+jets processes, additional uncertainties related to the resummation and CKKW matching scales [63, 64] are considered. For the $Z(\mu\mu)$+jets and $Z(\tau\tau)$+jets backgrounds, the nominal Sherpa samples are compared with alternative samples produced with MadGraph5_aMC@NLO+Pythia. For diboson and $t\bar{t}X$ samples, the PDF, scale and cross-section uncertainties are used.

For the bottom-squark signal samples, uncertainties in the acceptance related to the factorization and renormalization scales, merging scales, parton shower tuning and radiation uncertainties are considered. An additional uncertainty accounts for differences between samples produced with the full detector simulation and the parameterized calorimeter response.

Table 7: The observed event yields in data, the total expected yields from SM processes obtained from the background-only fit and breakdown of individual contributions, and the expected signal contributions for three benchmark models are shown for the single-bin signal region and the three bins of the multi-bin signal region. Total uncertainties combining the statistical and systematic uncertainties are quoted for the background processes. For the signal, the quoted uncertainties are only statistical. "Other" combines all SM background contributions that are not listed explicitly, covering V+jets except for $Z(\tau\tau)$+jets, multijet, diboson and triboson contributions. The dash means that no events pass the selection.

	Single-bin SR	Multi-bin SR		
		$\Theta_{\text{min}} < 0.5$	$0.5 < \Theta_{\text{min}} < 1.0$	$\Theta_{\text{min}} > 1.0$
Observed events	4	3	1	3
Total SM background	3.8 ± 1.5	2.7 ± 1.1	3.5 ± 1.6	1.5 ± 0.6
Top quark τ_{true} τ_{true}	1.4 ± 0.9	1.6 ± 0.7	1.9 ± 1.0	$0.30^{+0.41}_{-0.30}$
Top quark τ_{true} τ_{fake}	0.92 ± 0.62	0.76 ± 0.43	0.96 ± 0.69	0.22 ± 0.17
Top quark τ_{fake} τ_{fake}	$0.11^{+0.26}_{-0.11}$	0.06 ± 0.06	$0.12^{+0.23}_{-0.12}$	$0.04^{+0.05}_{-0.04}$
$t\bar{t}X$	0.52 ± 0.42	0.18 ± 0.10	$0.26^{+0.31}_{-0.26}$	0.31 ± 0.22
$Z(\tau\tau)$+jets	0.73 ± 0.25	0.05 ± 0.05	0.17 ± 0.16	0.59 ± 0.22
Other	0.07 ± 0.04	—	0.04 ± 0.01	0.06 ± 0.03
$m(\tilde{b}, \tilde{\chi}_2^0) = (800, 131)$ GeV	5.6 ± 1.4	0.14 ± 0.06	1.5 ± 0.4	4.3 ± 1.1
$m(\tilde{b}, \tilde{\chi}_2^0) = (800, 180)$ GeV	9.3 ± 2.2	$0.08^{+0.14}_{-0.08}$	2.4 ± 0.6	7.1 ± 1.7
$m(\tilde{b}, \tilde{\chi}_2^0) = (350, 280)$ GeV	6.4 ± 2.1	2.7 ± 0.9	4.1 ± 1.3	4.8 ± 1.8

A summary of the dominant systematic uncertainties in the background prediction for the signal regions is given in Table 6. The largest source of uncertainty is the generator modeling, and here in particular the modeling of the top-quark background, mainly the modeling of the hard-scatter process and ISR uncertainties. Second-leading in size is the total uncertainty in the normalization and transfer factors, which is obtained from the fit. As the transfer factors are ratios of normalization factors, and a large part of the uncertainties cancel out in the ratio, the uncertainties in the transfer factors are comparatively small.

8 Results

The event yields for all signal regions are reported in Table 7. The SM background prediction is based on the background-only fit described in Section 6. To illustrate the order of magnitude of the contribution of signal events, the expected yields for three benchmark signal models are included in the table. The single-bin SR and the first two bins of the multi-bin SR are dominated by top-quark production, whereas for $\Theta_{\text{min}} > 1.0$ the $Z(\tau\tau)$ background is the largest contribution. Other SM processes contribute very little to the signal regions. Figure 7 shows a comparison of data and background yields in the SRs together with the corresponding significances quantifying the deviation of the observed yields from the SM expectation in the bottom panel. No significant excess of data above the expected yields from the SM background processes is observed in any of the signal regions. The p-value for the event yield in the single-bin signal region to fluctuate to at least the observed value under the background-only hypothesis is $p(s = 0) = 0.44$.

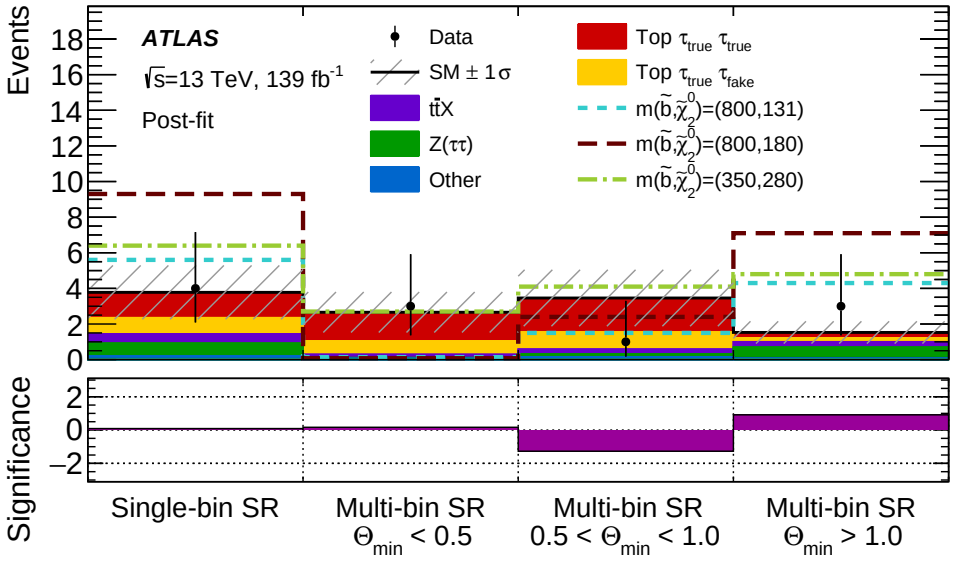


Figure 7: Comparison of the expected and observed event yields in the signal regions defined in Table 2. The top-quark and $Z(\tau\tau)$ background contributions are scaled with the normalization factors obtained from the background-only fit. The "Other" contribution includes all the backgrounds not explicitly listed in the legend (V+jets except $Z(\tau\tau)$+jets, diboson/triboson, multijet). The hatched band indicates the total statistical and systematic uncertainty of the SM background. The contributions from three signal models to the signal regions are also displayed, where the masses $m(\tilde{b})$ and $m(\tilde{\chi}_2^0)$ are given in GeV in the legend. The lower panel shows the significance of the deviation of the observed yield from the expected background yield.

Exclusion contours at the 95% confidence level (CL) are derived from the yields in the multi-bin signal region for the two-dimensional parameter space of $m(\tilde{b})$ and $m(\tilde{\chi}_2^0)$ in the simplified model from Figure 1. A fixed mass difference of 130 GeV between the second-lightest neutralino $\tilde{\chi}_2^0$ and lightest neutralino $\tilde{\chi}_1^0$ is assumed for all signal models. The probabilities that the data are compatible with the background-only and signal-plus-background hypotheses are evaluated using a one-sided profile-likelihood-ratio test statistic and the CL_s prescription [105]. The computations rely on asymptotic properties of the profile-likelihood ratio [95]. Systematic uncertainties are treated as nuisance parameters with Gaussian probability densities in the likelihood function. The resulting observed and expected exclusion contours are shown in Figure 8. The uncertainties in the cross section of the supersymmetric signal are not included in the fit but shown as an uncertainty band around the observed limit contour. Since the observed data yield is larger than the expected total background in the highest Θ_{min} bin, which is most sensitive to models with large $m(\tilde{b})$, the observed exclusion contour deviates inwards from the expected contour with increasing $m(\tilde{b})$, but it stays within the uncertainty band of the expected limit. The search is optimized for the low-$m(\tilde{\chi}_2^0)$ region and has sensitivity to models with $m(\tilde{\chi}_2^0)$ up to 300 GeV. Bottom squarks with masses up to 850 GeV are excluded in this region. For $m(\tilde{\chi}_2^0)$ below about 200 GeV, the softer $E_{\text{T}}^{\text{miss}}$ spectrum of the signal results in a lower acceptance, leading to a slightly reduced exclusion reach in bottom-squark mass. The parameter-space region where $\Delta m(\tilde{b}, \tilde{\chi}_2^0) \lesssim 20$ GeV cannot be excluded as the bottom-squark decay products are not boosted enough, and the stringent kinematic requirements in the SRs result in low signal acceptance. These results are overlaid on the observed exclusion contour from a previous ATLAS search [22] to demonstrate the complementarity of the two approaches. The new results have unique sensitivity to a previously uncovered

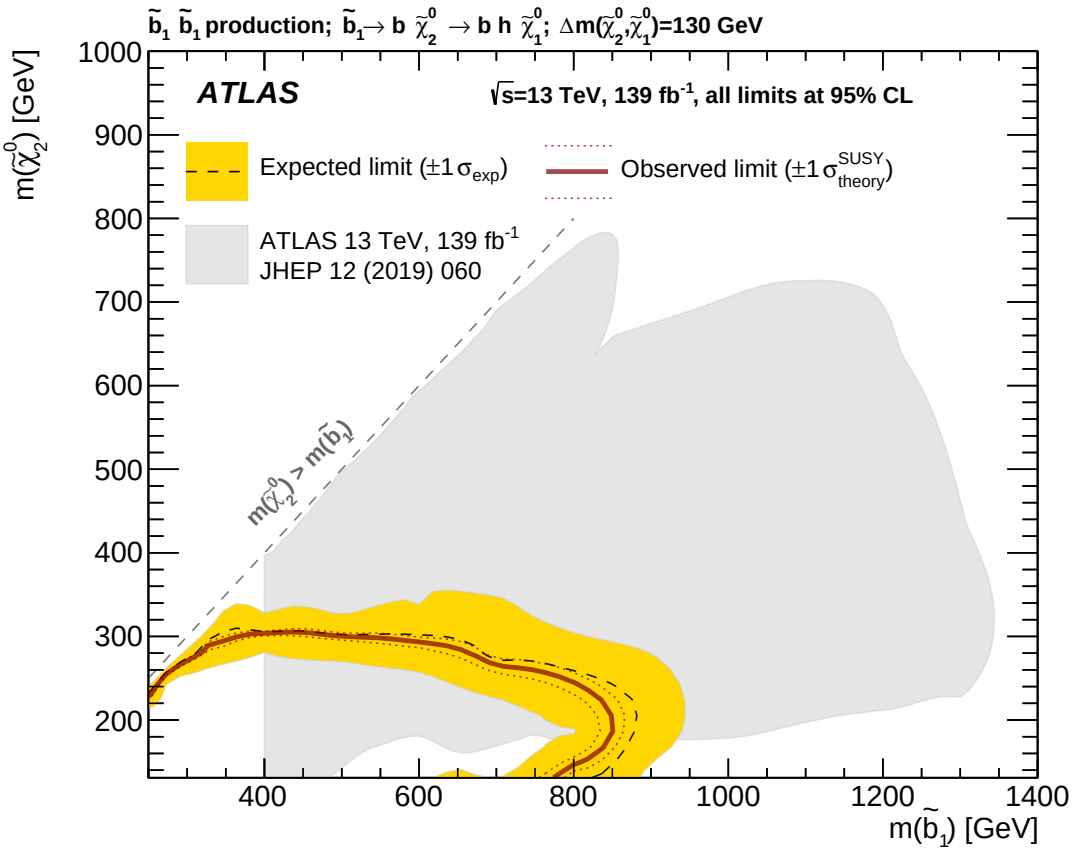


Figure 8: Exclusion contours at the 95% CL as a function of $m(\tilde{b})$ and $m(\tilde{\chi}_2^0)$, assuming $\Delta m(\tilde{\chi}_2^0, \tilde{\chi}_1^0) = 130\,\text{GeV}$. Observed and expected limits are shown for the present search that requires hadronically decaying τ-leptons, b-jets and $E_{\text{T}}^{\text{miss}}$ in the final state. The observed exclusion limit from a previous ATLAS search [22] that requires b-jets and $E_{\text{T}}^{\text{miss}}$ in the final state is also displayed. The region $m(\tilde{b}) < 400\,\text{GeV}$ is excluded by a previous search from CMS [23].

region of parameter space at low $\tilde{\chi}_2^0$ masses, where the previous search quickly loses sensitivity.

The results from the single-bin signal region can be interpreted in terms of model-independent upper limits on the event yields from potential BSM processes. The fit is performed simultaneously over the CRs and the single-bin SR, assuming no signal contribution in the CRs. The profile-likelihood-ratio test statistic is evaluated using pseudo-experiments. An upper limit of 0.05 fb is derived for the visible cross section σ_{vis}, defined as the product of the cross section, acceptance and selection efficiency of such processes. In addition, Table 8 summarizes the expected and observed 95% CL upper limits on the number of BSM events, as well as the confidence level of the background-only hypothesis CL_{b}. The p-value and the corresponding significance for the background-only hypothesis to fluctuate to at least the observed values are also included.

Table 8: Upper limits at 95% CL on the visible cross section σ_{vis}, on the number of signal events (S^{95}_{obs}), and on number of signal events given the expected number (and $\pm 1\sigma$ excursions of the expectation) of background events (S^{95}_{exp}). The last two columns indicate the CL_b value, i.e. the confidence level observed for the background-only hypothesis, the discovery p-value ($p(s = 0)$), and its associated significance Z.

Signal region	σ_{vis} [fb]	S^{95}_{obs}	S^{95}_{exp}	CL_b	$p(s = 0)$ (Z)
Single-bin SR	0.05	6.6	$6.0^{+2.3}_{-1.6}$	0.62	0.34 (0.41)

9 Conclusion

A search for bottom-squark pairs in events with b-jets, hadronically decaying τ-leptons and large missing transverse momentum is presented. A simplified SUSY model assuming $\tilde{b} \to b\tilde{\chi}^0_2 \to bh\tilde{\chi}^0_1$ is considered, where at least one Higgs boson decays into a pair of τ-leptons. This analysis has unique sensitivity at low $\tilde{\chi}^0_2$ masses due to the presence of hadronically decaying τ-leptons, which mitigates the Standard Model background, and to the associated ν_τ-neutrinos that add to the $E^{\text{miss}}_{\text{T}}$ originating from the $\tilde{\chi}^0_1$. A multi-bin signal region exploiting angular correlations between the b-jets and the hadronically decaying τ-leptons is used to search for a $\tilde{b}$ signal, and a single-bin signal region is employed for a model-independent statistical interpretation. The data observed in the signal regions are compatible with the expected Standard Model background. Exclusion limits are placed on the bottom-squark mass at the 95% confidence level. For $m(\tilde{\chi}^0_2)$ ranging from 130 GeV to 180 GeV, bottom-squark masses below 775 GeV to 850 GeV are excluded. This extends significantly beyond the reach of a previous ATLAS search [22], which was performed in final states with b-jets and large $E^{\text{miss}}_{\text{T}}$, in this challenging region of parameter space.

Acknowledgments

We thank CERN for the very successful operation of the LHC, as well as the support staff from our institutions without whom ATLAS could not be operated efficiently.

We acknowledge the support of ANPCyT, Argentina; YerPhI, Armenia; ARC, Australia; BMWFW and FWF, Austria; ANAS, Azerbaijan; SSTC, Belarus; CNPq and FAPESP, Brazil; NSERC, NRC and CFI, Canada; CERN; ANID, Chile; CAS, MOST and NSFC, China; COLCIENCIAS, Colombia; MSMT CR, MPO CR and VSC CR, Czech Republic; DNRF and DNSRC, Denmark; IN2P3-CNRS and CEA-DRF/IRFU, France; SRNSFG, Georgia; BMBF, HGF and MPG, Germany; GSRT, Greece; RGC and Hong Kong SAR, China; ISF and Benoziyo Center, Israel; INFN, Italy; MEXT and JSPS, Japan; CNRST, Morocco; NWO, Netherlands; RCN, Norway; MNiSW and NCN, Poland; FCT, Portugal; MNE/IFA, Romania; JINR; MES of Russia and NRC KI, Russian Federation; MESTD, Serbia; MSSR, Slovakia; ARRS and MIZŠ, Slovenia; DST/NRF, South Africa; MICINN, Spain; SRC and Wallenberg Foundation, Sweden; SERI, SNSF and Cantons of Bern and Geneva, Switzerland; MOST, Taiwan; TAEK, Turkey; STFC, United Kingdom; DOE and NSF, United States of America. In addition, individual groups and members have received support from BCKDF, CANARIE, Compute Canada, CRC and IVADO, Canada; Beijing Municipal Science & Technology Commission, China; COST, ERC, ERDF, Horizon 2020 and Marie Skłodowska-Curie Actions, European Union; Investissements d'Avenir Labex, Investissements d'Avenir Idex and ANR, France; DFG and AvH Foundation, Germany; Herakleitos, Thales and Aristeia programmes co-financed by EU-ESF and the Greek NSRF, Greece; BSF-NSF and GIF, Israel; La Caixa Banking Foundation, CERCA Programme

Generalitat de Catalunya and PROMETEO and GenT Programmes Generalitat Valenciana, Spain; Göran Gustafssons Stiftelse, Sweden; The Royal Society and Leverhulme Trust, United Kingdom.

The crucial computing support from all WLCG partners is acknowledged gratefully, in particular from CERN, the ATLAS Tier-1 facilities at TRIUMF (Canada), NDGF (Denmark, Norway, Sweden), CC-IN2P3 (France), KIT/GridKA (Germany), INFN-CNAF (Italy), NL-T1 (Netherlands), PIC (Spain), ASGC (Taiwan), RAL (UK) and BNL (USA), the Tier-2 facilities worldwide and large non-WLCG resource providers. Major contributors of computing resources are listed in Ref. [106].

References

[1] Y. Golfand and E. Likhtman, *Extension of the Algebra of Poincare Group Generators and Violation of P Invariance*, JETP Lett. **13** (1971) 323, [Pisma Zh. Eksp. Teor. Fiz. **13** (1971) 452].

[2] D. Volkov and V. Akulov, *Is the neutrino a goldstone particle?* Phys. Lett. B **46** (1973) 109.

[3] J. Wess and B. Zumino, *Supergauge transformations in four dimensions*, Nucl. Phys. B **70** (1974) 39.

[4] J. Wess and B. Zumino, *Supergauge invariant extension of quantum electrodynamics*, Nucl. Phys. B **78** (1974) 1.

[5] S. Ferrara and B. Zumino, *Supergauge invariant Yang-Mills theories*, Nucl. Phys. B **79** (1974) 413.

[6] A. Salam and J. Strathdee, *Super-symmetry and non-Abelian gauges*, Phys. Lett. B **51** (1974) 353.

[7] N. Sakai, *Naturalnes in Supersymmetric Guts*, Z. Phys. C **11** (1981) 153.

[8] S. Dimopoulos, S. Raby, and F. Wilczek, *Supersymmetry and the scale of unification*, Phys. Rev. D **24** (1981) 1681.

[9] L. E. Ibáñez and G. G. Ross, *Low-energy predictions in supersymmetric grand unified theories*, Phys. Lett. B **105** (1981) 439.

[10] S. Dimopoulos and H. Georgi, *Softly broken supersymmetry and SU(5)*, Nucl. Phys. B **193** (1981) 150.

[11] G. R. Farrar and P. Fayet, *Phenomenology of the production, decay, and detection of new hadronic states associated with supersymmetry*, Phys. Lett. B **76** (1978) 575.

[12] H. Goldberg, *Constraint on the Photino Mass from Cosmology*, Phys. Rev. Lett. **50** (1983) 1419, Erratum: Phys. Rev. Lett. **103** (2009) 099905.

[13] J. Ellis, J. Hagelin, D. V. Nanopoulos, K. A. Olive, and M. Srednicki, *Supersymmetric relics from the big bang*, Nucl. Phys. B **238** (1984) 453.

[14] R. Barbieri and G. Giudice, *Upper bounds on supersymmetric particle masses*, Nucl. Phys. B **306** (1988) 63.

[15] B. de Carlos and J. Casas, *One-loop analysis of the electroweak breaking in supersymmetric models and the fine-tuning problem*, Phys. Lett. B **309** (1993) 320, arXiv: hep-ph/9303291.

[16] J. Alwall, M.-P. Le, M. Lisanti, and J. G. Wacker, *Searching for directly decaying gluinos at the Tevatron*, Phys. Lett. B **666** (2008) 34, arXiv: 0803.0019 [hep-ph].

[17] J. Alwall, P. Schuster, and N. Toro, *Simplified models for a first characterization of new physics at the LHC*, Phys. Rev. D **79** (2009) 075020, arXiv: 0810.3921 [hep-ph].

[18] D. Alves et al., *Simplified models for LHC new physics searches*, J. Phys. G **39** (2012) 105005, arXiv: 1105.2838 [hep-ph].

[19] P. Fayet, *Supersymmetry and weak, electromagnetic and strong interactions*, Phys. Lett. B **64** (1976) 159.

[20] P. Fayet, *Spontaneously broken supersymmetric theories of weak, electromagnetic and strong interactions*, Phys. Lett. B **69** (1977) 489.

[21] ATLAS Collaboration, *Search for supersymmetry in events with b-tagged jets and missing transverse momentum in pp collisions at* $\sqrt{s} = 13$ *TeV with the ATLAS detector*, JHEP **11** (2017) 195, arXiv: 1708.09266 [hep-ex].

[22] ATLAS Collaboration, *Search for bottom-squark pair production with the ATLAS detector in final states containing Higgs bosons, b-jets and missing transverse momentum*, JHEP **12** (2019) 060, arXiv: 1908.03122 [hep-ex].

[23] CMS Collaboration, *Search for supersymmetry using Higgs boson to diphoton decays at* $\sqrt{s}$ = 13 *TeV*, JHEP **11** (2019) 109, arXiv: 1908.08500 [hep-ex].

[24] ATLAS Collaboration, *The ATLAS Experiment at the CERN Large Hadron Collider*, JINST **3** (2008) S08003.

[25] ATLAS Collaboration, *ATLAS Insertable B-Layer Technical Design Report*, ATLAS-TDR-19; CERN-LHCC-2010-013, 2010, URL: https://cds.cern.ch/record/1291633.

[26] ATLAS Collaboration, *ATLAS Insertable B-Layer: Technical Design Report Addendum*, ATLAS-TDR-19-ADD-1; CERN-LHCC-2012-009, 2012, URL: https://cds.cern.ch/record/1451888.

[27] B. Abbott et al., *Production and integration of the ATLAS Insertable B-Layer*, JINST **13** (2018) T05008, arXiv: 1803.00844 [physics.ins-det].

[28] ATLAS Collaboration, *Luminosity determination in pp collisions at* $\sqrt{s}$ = 13 *TeV using the ATLAS detector at the LHC*, ATLAS-CONF-2019-021, 2019, URL: https://cds.cern.ch/record/2677054.

[29] G. Avoni et al., *The new LUCID-2 detector for luminosity measurement and monitoring in ATLAS*, JINST **13** (2018) P07017.

[30] ATLAS Collaboration, *The ATLAS Simulation Infrastructure*, Eur. Phys. J. C **70** (2010) 823, arXiv: 1005.4568 [physics.ins-det].

[31] S. Agostinelli et al., *GEANT4 – a simulation toolkit*, Nucl. Instrum. Meth. A **506** (2003) 250.

[32] ATLAS Collaboration, *The simulation principle and performance of the ATLAS fast calorimeter simulation FastCaloSim*, ATL-PHYS-PUB-2010-013, 2010, URL: https://cds.cern.ch/record/1300517.

[33] T. Sjöstrand, S. Mrenna, and P. Skands, *A brief introduction to PYTHIA 8.1*, Comput. Phys. Commun. **178** (2008) 852, arXiv: 0710.3820 [hep-ph].

[34] R. D. Ball et al., *Parton distributions with LHC data*, Nucl. Phys. B **867** (2013) 244, arXiv: 1207.1303 [hep-ph].

[35] ATLAS Collaboration, *The Pythia 8 A3 tune description of ATLAS minimum bias and inelastic measurements incorporating the Donnachie–Landshoff diffractive model*, ATL-PHYS-PUB-2016-017, 2016, URL: https://cds.cern.ch/record/2206965.

[36] E. Bothmann et al., *Event Generation with Sherpa 2.2*, SciPost Phys. **7** (2019) 034, arXiv: 1905.09127 [hep-ph].

[37] D. J. Lange, *The EvtGen particle decay simulation package*, Nucl. Instrum. Meth. A **462** (2001) 152.

[38] S. Frixione, P. Nason, and G. Ridolfi, *A positive-weight next-to-leading-order Monte Carlo for heavy flavour hadroproduction*, JHEP **09** (2007) 126, arXiv: 0707.3088 [hep-ph].

[39] P. Nason, *A new method for combining NLO QCD with shower Monte Carlo algorithms*, JHEP **11** (2004) 040, arXiv: hep-ph/0409146.

[40] S. Frixione, P. Nason, and C. Oleari, *Matching NLO QCD computations with parton shower simulations: the POWHEG method*, JHEP **11** (2007) 070, arXiv: 0709.2092 [hep-ph].

[41] S. Alioli, P. Nason, C. Oleari, and E. Re, *A general framework for implementing NLO calculations in shower Monte Carlo programs: the POWHEG BOX*, JHEP **06** (2010) 043, arXiv: 1002.2581 [hep-ph].

[42] R. D. Ball et al., *Parton distributions for the LHC run II*, JHEP **04** (2015) 040, arXiv: 1410.8849 [hep-ph].

[43] ATLAS Collaboration, *Studies on top-quark Monte Carlo modelling for Top2016*, ATL-PHYS-PUB-2016-020, 2016, URL: https://cds.cern.ch/record/2216168.

[44] T. Sjöstrand et al., *An introduction to PYTHIA 8.2*, Comput. Phys. Commun. **191** (2015) 159, arXiv: 1410.3012 [hep-ph].

[45] ATLAS Collaboration, *ATLAS Pythia 8 tunes to 7 TeV data*, ATL-PHYS-PUB-2014-021, 2014, URL: https://cds.cern.ch/record/1966419.

[46] M. Beneke, P. Falgari, S. Klein, and C. Schwinn, *Hadronic top-quark pair production with NNLL threshold resummation*, Nucl. Phys. B **855** (2012) 695, arXiv: 1109.1536 [hep-ph].

[47] M. Cacciari, M. Czakon, M. Mangano, A. Mitov, and P. Nason, *Top-pair production at hadron colliders with next-to-next-to-leading logarithmic soft-gluon resummation*, Phys. Lett. B **710** (2012) 612, arXiv: 1111.5869 [hep-ph].

[48] P. Bärnreuther, M. Czakon, and A. Mitov, *Percent-Level-Precision Physics at the Tevatron: Next-to-Next-to-Leading Order QCD Corrections to $q\bar{q} \to t\bar{t} + X$*, Phys. Rev. Lett. **109** (2012) 132001, arXiv: 1204.5201 [hep-ph].

[49] M. Czakon and A. Mitov, *NNLO corrections to top-pair production at hadron colliders: the all-fermionic scattering channels*, JHEP **12** (2012) 054, arXiv: 1207.0236 [hep-ph].

[50] M. Czakon and A. Mitov, *NNLO corrections to top pair production at hadron colliders: the quark-gluon reaction*, JHEP **01** (2013) 080, arXiv: 1210.6832 [hep-ph].

[51] M. Czakon, P. Fiedler, and A. Mitov, *Total Top-Quark Pair-Production Cross Section at Hadron Colliders Through $O(\alpha_S^4)$*, Phys. Rev. Lett. **110** (2013) 252004, arXiv: 1303.6254 [hep-ph].

[52] M. Czakon and A. Mitov, *Top++: A program for the calculation of the top-pair cross-section at hadron colliders*, Comput. Phys. Commun. **185** (2014) 2930, arXiv: 1112.5675 [hep-ph].

[53] E. Re, *Single-top Wt-channel production matched with parton showers using the POWHEG method*, Eur. Phys. J. C **71** (2011) 1547, arXiv: 1009.2450 [hep-ph].

[54] R. Frederix, E. Re, and P. Torrielli, *Single-top t-channel hadroproduction in the four-flavour scheme with POWHEG and aMC@NLO*, JHEP **09** (2012) 130, arXiv: 1207.5391 [hep-ph].

[55] S. Alioli, P. Nason, C. Oleari, and E. Re, *NLO single-top production matched with shower in POWHEG: s- and t-channel contributions*, JHEP **09** (2009) 111, arXiv: 0907.4076 [hep-ph], Erratum: JHEP **02** (2010) 011.

[56] J. Alwall et al., *The automated computation of tree-level and next-to-leading order differential cross sections, and their matching to parton shower simulations*, JHEP **07** (2014) 079, arXiv: 1405.0301 [hep-ph].

[57] T. Gleisberg and S. Höche, *Comix, a new matrix element generator*, JHEP **12** (2008) 039, arXiv: 0808.3674 [hep-ph].

[58] F. Cascioli, P. Maierhöfer, and S. Pozzorini, *Scattering Amplitudes with Open Loops*, Phys. Rev. Lett. **108** (2012) 111601, arXiv: 1111.5206 [hep-ph].

[59] A. Denner, S. Dittmaier, and L. Hofer, *COLLIER: A fortran-based complex one-loop library in extended regularizations*, Comput. Phys. Commun. **212** (2017) 220, arXiv: 1604.06792 [hep-ph].

[60] S. Schumann and F. Krauss, *A parton shower algorithm based on Catani–Seymour dipole factorisation*, JHEP **03** (2008) 038, arXiv: 0709.1027 [hep-ph].

[61] S. Höche, F. Krauss, M. Schönherr, and F. Siegert, *A critical appraisal of NLO+PS matching methods*, JHEP **09** (2012) 049, arXiv: 1111.1220 [hep-ph].

[62] S. Höche, F. Krauss, M. Schönherr, and F. Siegert, *QCD matrix elements + parton showers. The NLO case*, JHEP **04** (2013) 027, arXiv: 1207.5030 [hep-ph].

[63] S. Catani, F. Krauss, R. Kuhn, and B. R. Webber, *QCD Matrix Elements + Parton Showers*, JHEP **11** (2001) 063, arXiv: hep-ph/0109231.

[64] S. Höche, F. Krauss, S. Schumann, and F. Siegert, *QCD matrix elements and truncated showers*, JHEP **05** (2009) 053, arXiv: 0903.1219 [hep-ph].

[65] C. Anastasiou, L. J. Dixon, K. Melnikov, and F. Petriello, *High precision QCD at hadron colliders: Electroweak gauge boson rapidity distributions at next-to-next-to leading order*, Phys. Rev. D **69** (2004) 094008, arXiv: hep-ph/0312266.

[66] L. Lönnblad, *Correcting the Colour-Dipole Cascade Model with Fixed Order Matrix Elements*, JHEP **05** (2002) 046, arXiv: hep-ph/0112284.

[67] L. Lönnblad and S. Prestel, *Matching tree-level matrix elements with interleaved showers*, JHEP **03** (2012) 019, arXiv: 1109.4829 [hep-ph].

[68] W. Beenakker, C. Borschensky, M. Krämer, A. Kulesza, and E. Laenen, *NNLL-fast: predictions for coloured supersymmetric particle production at the LHC with threshold and Coulomb resummation*, JHEP **12** (2016) 133, arXiv: 1607.07741 [hep-ph].

[69] W. Beenakker et al., *NNLL resummation for squark and gluino production at the LHC*, JHEP **12** (2014) 023, arXiv: 1404.3134 [hep-ph].

[70] W. Beenakker et al., *Towards NNLL resummation: hard matching coefficients for squark and gluino hadroproduction*, JHEP **10** (2013) 120, arXiv: 1304.6354 [hep-ph].

[71] W. Beenakker et al., *NNLL resummation for squark-antisquark pair production at the LHC*, JHEP **01** (2012) 076, arXiv: 1110.2446 [hep-ph].

[72] W. Beenakker et al., *Soft-gluon resummation for squark and gluino hadroproduction*, JHEP **12** (2009) 041, arXiv: 0909.4418 [hep-ph].

[73] A. Kulesza and L. Motyka, *Soft gluon resummation for the production of gluino-gluino and squark-antisquark pairs at the LHC*, Phys. Rev. D **80** (2009) 095004, arXiv: 0905.4749 [hep-ph].

[74] A. Kulesza and L. Motyka, *Threshold Resummation for Squark-Antisquark and Gluino-Pair Production at the LHC*, Phys. Rev. Lett. **102** (2009) 111802, arXiv: 0807.2405 [hep-ph].

[75] W. Beenakker, R. Höpker, M. Spira, and P. Zerwas, *Squark and gluino production at hadron colliders*, Nucl. Phys. B **492** (1997) 51, arXiv: hep-ph/9610490.

[76] J. Butterworth et al., *PDF4LHC recommendations for LHC Run II*, J. Phys. G **43** (2016) 023001, arXiv: 1510.03865 [hep-ph].

[77] ATLAS Collaboration, *Vertex Reconstruction Performance of the ATLAS Detector at* $\sqrt{s}$ = 13 *TeV*, ATL-PHYS-PUB-2015-026, 2015, URL: https://cds.cern.ch/record/2037717.

[78] M. Cacciari, G. P. Salam, and G. Soyez, *The anti-*k_t *jet clustering algorithm*, JHEP **04** (2008) 063, arXiv: 0802.1189 [hep-ph].

[79] M. Cacciari, G. P. Salam, and G. Soyez, *FastJet user manual*, Eur. Phys. J. C **72** (2012) 1896, arXiv: 1111.6097 [hep-ph].

[80] ATLAS Collaboration, *Topological cell clustering in the ATLAS calorimeters and its performance in LHC Run 1*, Eur. Phys. J. C **77** (2017) 490, arXiv: 1603.02934 [hep-ex].

[81] ATLAS Collaboration, *Jet energy scale measurements and their systematic uncertainties in proton–proton collisions at* $\sqrt{s}$ = 13 *TeV with the ATLAS detector*, Phys. Rev. D **96** (2017) 072002, arXiv: 1703.09665 [hep-ex].

[82] ATLAS Collaboration, *Selection of jets produced in* 13 *TeV proton–proton collisions with the ATLAS detector*, ATLAS-CONF-2015-029, 2015, URL: https://cds.cern.ch/record/2037702.

[83] ATLAS Collaboration, *Tagging and suppression of pileup jets with the ATLAS detector*, ATLAS-CONF-2014-018, 2014, URL: https://cds.cern.ch/record/1700870.

[84] ATLAS Collaboration, *ATLAS b-jet identification performance and efficiency measurement with* $t\bar{t}$ *events in pp collisions at* $\sqrt{s}$ = 13 *TeV*, Eur. Phys. J. C **79** (2019) 970, arXiv: 1907.05120 [hep-ex].

[85] ATLAS Collaboration, *Expected performance of the ATLAS b-tagging algorithms in Run-2*, ATL-PHYS-PUB-2015-022, 2015, URL: https://cds.cern.ch/record/2037697.

[86] ATLAS Collaboration, *Reconstruction, Energy Calibration, and Identification of Hadronically Decaying Tau Leptons in the ATLAS Experiment for Run-2 of the LHC*, ATL-PHYS-PUB-2015-045, 2015, URL: https://cds.cern.ch/record/2064383.

[87] T. Barillari et al., *Local Hadronic Calibration*, ATL-LARG-PUB-2009-001-2, 2008, URL: https://cds.cern.ch/record/1112035.

[88] ATLAS Collaboration, *Reconstruction of hadronic decay products of tau leptons with the ATLAS experiment*, Eur. Phys. J. C **76** (2016) 295, arXiv: 1512.05955 [hep-ex].

[89] ATLAS Collaboration, *Identification of hadronic tau lepton decays using neural networks in the ATLAS experiment*, ATL-PHYS-PUB-2019-033, 2019, URL: https://cds.cern.ch/record/2688062.

[90] ATLAS Collaboration, *Measurement of the tau lepton reconstruction and identification performance in the ATLAS experiment using pp collisions at* $\sqrt{s}$ = 13 *TeV*, ATLAS-CONF-2017-029, 2017, URL: https://cds.cern.ch/record/2261772.

[91] ATLAS Collaboration, *Muon reconstruction performance of the ATLAS detector in proton–proton collision data at* $\sqrt{s}$ = 13 *TeV*, Eur. Phys. J. C **76** (2016) 292, arXiv: 1603.05598 [hep-ex].

[92] ATLAS Collaboration, *Electron reconstruction and identification in the ATLAS experiment using the 2015 and 2016 LHC proton–proton collision data at* $\sqrt{s}$ = 13 *TeV*, Eur. Phys. J. C **79** (2019) 639, arXiv: 1902.04655 [hep-ex].

[93] ATLAS Collaboration, E_T^{miss} *performance in the ATLAS detector using 2015–2016 LHC pp collisions*, ATLAS-CONF-2018-023, 2018, URL: https://cds.cern.ch/record/2625233.

[94] ATLAS Collaboration, *Performance of the missing transverse momentum triggers for the ATLAS detector during Run-2 data taking*, JHEP **08** (2020) 080, arXiv: 2005.09554 [hep-ex].

[95] G. Cowan, K. Cranmer, E. Gross, and O. Vitells, *Asymptotic formulae for likelihood-based tests of new physics*, Eur. Phys. J. C **71** (2011) 1554, arXiv: 1007.1727 [physics.data-an], Erratum: Eur. Phys. J. C **73** (2013) 2501.

[96] C. G. Lester and D. J. Summers, *Measuring masses of semi-invisibly decaying particles pair produced at hadron colliders*, Phys. Lett. B **463** (1999) 99, arXiv: hep-ph/9906349 [hep-ph].

[97] C. G. Lester and B. Nachman, *Bisection-based asymmetric M_{T2} computation: a higher precision calculator than existing symmetric methods*, JHEP **03** (2015) 100, arXiv: 1411.4312 [hep-ph].

[98] M. Baak et al., *HistFitter software framework for statistical data analysis*, Eur. Phys. J. C **75** (2015) 153, arXiv: 1410.1280 [hep-ex].

[99] ATLAS Collaboration, *Search for squarks and gluinos with the ATLAS detector in final states with jets and missing transverse momentum using 4.7 fb^{-1} of $\sqrt{s}$ = 7 TeV proton–proton collision data*, Phys. Rev. D **87** (2013) 012008, arXiv: 1208.0949 [hep-ex].

[100] ATLAS Collaboration, *Jet energy resolution in proton–proton collisions at $\sqrt{s}$ = 7 TeV recorded in 2010 with the ATLAS detector*, Eur. Phys. J. C **73** (2013) 2306, arXiv: 1210.6210 [hep-ex].

[101] ATLAS Collaboration, *Measurement of b-tagging efficiency of c-jets in $t\bar{t}$ events using a likelihood approach with the ATLAS detector*, ATLAS-CONF-2018-001, 2018, URL: https://cds.cern.ch/record/2306649.

[102] ATLAS Collaboration, *Calibration of light-flavour b-jet mistagging rates using ATLAS proton–proton collision data at $\sqrt{s}$ = 13 TeV*, ATLAS-CONF-2018-006, 2018, URL: https://cds.cern.ch/record/2314418.

[103] ATLAS Collaboration, *Improvements in $t\bar{t}$ modelling using NLO+PS Monte Carlo generators for Run 2*, ATL-PHYS-PUB-2018-009, 2018, URL: https://cds.cern.ch/record/2630327.

[104] S. Frixione, E. Laenen, P. Motylinski, C. White, and B. R. Webber, *Single-top hadroproduction in association with a W boson*, JHEP **07** (2008) 029, arXiv: 0805.3067 [hep-ph].

[105] A. L. Read, *Presentation of search results: the CL_S technique*, J. Phys. G **28** (2002) 2693.

[106] ATLAS Collaboration, *ATLAS Computing Acknowledgements*, ATL-SOFT-PUB-2020-001, URL: https://cds.cern.ch/record/2717821.

The ATLAS Collaboration

G. Aad[102], B. Abbott[128], D.C. Abbott[103], A. Abed Abud[36], K. Abeling[53], D.K. Abhayasinghe[94], S.H. Abidi[167], O.S. AbouZeid[40], N.L. Abraham[156], H. Abramowicz[161], H. Abreu[160], Y. Abulaiti[6], B.S. Acharya[67a,67b,o], B. Achkar[53], L. Adam[100], C. Adam Bourdarios[5], L. Adamczyk[84a], L. Adamek[167], J. Adelman[121], A. Adiguzel[12c,ad], S. Adorni[54], T. Adye[143], A.A. Affolder[145], Y. Afik[160], C. Agapopoulou[65], M.N. Agaras[38], A. Aggarwal[119], C. Agheorghiesei[27c], J.A. Aguilar-Saavedra[139f,139a,ac], A. Ahmad[36], F. Ahmadov[80], W.S. Ahmed[104], X. Ai[18], G. Aielli[74a,74b], S. Akatsuka[86], M. Akbiyik[100], T.P.A. Åkesson[97], E. Akilli[54], A.V. Akimov[111], K. Al Khoury[65], G.L. Alberghi[23b,23a], J. Albert[176], M.J. Alconada Verzini[161], S. Alderweireldt[36], M. Aleksa[36], I.N. Aleksandrov[80], C. Alexa[27b], T. Alexopoulos[10], A. Alfonsi[120], F. Alfonsi[23b,23a], M. Alhroob[128], B. Ali[141], S. Ali[158], M. Aliev[166], G. Alimonti[69a], C. Allaire[36], B.M.M. Allbrooke[156], B.W. Allen[131], P.P. Allport[21], A. Aloisio[70a,70b], F. Alonso[89], C. Alpigiani[148], E. Alunno Camelia[74a,74b], M. Alvarez Estevez[99], M.G. Alviggi[70a,70b], Y. Amaral Coutinho[81b], A. Ambler[104], L. Ambroz[134], C. Amelung[36], D. Amidei[106], S.P. Amor Dos Santos[139a], S. Amoroso[46], C.S. Amrouche[54], F. An[79], C. Anastopoulos[149], N. Andari[144], T. Andeen[11], J.K. Anders[20], S.Y. Andrean[45a,45b], A. Andreazza[69a,69b], V. Andrei[61a], C.R. Anelli[176], S. Angelidakis[9], A. Angerami[39], A.V. Anisenkov[122b,122a], A. Annovi[72a], C. Antel[54], M.T. Anthony[149], E. Antipov[129], M. Antonelli[51], D.J.A. Antrim[18], F. Anulli[73a], M. Aoki[82], J.A. Aparisi Pozo[174], M.A. Aparo[156], L. Aperio Bella[46], N. Aranzabal[36], V. Araujo Ferraz[81a], R. Araujo Pereira[81b], C. Arcangeletti[51], A.T.H. Arce[49], J-F. Arguin[110], S. Argyropoulos[52], J.-H. Arling[46], A.J. Armbruster[36], A. Armstrong[171], O. Arnaez[167], H. Arnold[120], Z.P. Arrubarrena Tame[114], G. Artoni[134], H. Asada[117], K. Asai[126], S. Asai[163], T. Asawatavonvanich[165], N. Asbah[59], E.M. Asimakopoulou[172], L. Asquith[156], J. Assahsah[35e], K. Assamagan[29], R. Astalos[28a], R.J. Atkin[33a], M. Atkinson[173], N.B. Atlay[19], H. Atmani[65], P.A. Atmasiddha[106], K. Augsten[141], V.A. Austrup[182], G. Avolio[36], M.K. Ayoub[15a], G. Azuelos[110,ak], D. Babal[28a], H. Bachacou[144], K. Bachas[162], F. Backman[45a,45b], P. Bagnaia[73a,73b], M. Bahmani[85], H. Bahrasemani[152], A.J. Bailey[174], V.R. Bailey[173], J.T. Baines[143], C. Bakalis[10], O.K. Baker[183], P.J. Bakker[120], E. Bakos[16], D. Bakshi Gupta[8], S. Balaji[157], R. Balasubramanian[120], E.M. Baldin[122b,122a], P. Balek[180], F. Balli[144], W.K. Balunas[134], J. Balz[100], E. Banas[85], M. Bandieramonte[138], A. Bandyopadhyay[19], Sw. Banerjee[181,j], L. Barak[161], W.M. Barbe[38], E.L. Barberio[105], D. Barberis[55b,55a], M. Barbero[102], G. Barbour[95], T. Barillari[115], M-S. Barisits[36], J. Barkeloo[131], T. Barklow[153], R. Barnea[160], B.M. Barnett[143], R.M. Barnett[18], Z. Barnovska-Blenessy[60a], A. Baroncelli[60a], G. Barone[29], A.J. Barr[134], L. Barranco Navarro[45a,45b], F. Barreiro[99], J. Barreiro Guimarães da Costa[15a], U. Barron[161], S. Barsov[137], F. Bartels[61a], R. Bartoldus[153], G. Bartolini[102], A.E. Barton[90], P. Bartos[28a], A. Basalaev[46], A. Basan[100], A. Bassalat[65,ah], M.J. Basso[167], R.L. Bates[57], S. Batlamous[35f], J.R. Batley[32], B. Batool[151], M. Battaglia[145], M. Bauce[73a,73b], F. Bauer[144,*], P. Bauer[24], H.S. Bawa[31], A. Bayirli[12c], J.B. Beacham[49], T. Beau[135], P.H. Beauchemin[170], F. Becherer[52], P. Bechtle[24], H.C. Beck[53], H.P. Beck[20,q], K. Becker[178], C. Becot[46], A. Beddall[12d], A.J. Beddall[12a], V.A. Bednyakov[80], M. Bedognetti[120], C.P. Bee[155], T.A. Beermann[182], M. Begalli[81b], M. Begel[29], A. Behera[155], J.K. Behr[46], F. Beisiegel[24], M. Belfkir[5], A.S. Bell[95], G. Bella[161], L. Bellagamba[23b], A. Bellerive[34], P. Bellos[9], K. Beloborodov[122b,122a], K. Belotskiy[112], N.L. Belyaev[112], D. Benchekroun[35a], N. Benekos[10], Y. Benhammou[161], D.P. Benjamin[6], M. Benoit[29], J.R. Bensinger[26], S. Bentvelsen[120], L. Beresford[134], M. Beretta[51], D. Berge[19], E. Bergeaas Kuutmann[172], N. Berger[5], B. Bergmann[141], L.J. Bergsten[26], J. Beringer[18], S. Berlendis[7], G. Bernardi[135], C. Bernius[153], F.U. Bernlochner[24], T. Berry[94], P. Berta[100], A. Berthold[48], I.A. Bertram[90], O. Bessidskaia Bylund[182], N. Besson[144], S. Bethke[115], A. Betti[42], A.J. Bevan[93], J. Beyer[115], S. Bhatta[155], D.S. Bhattacharya[177], P. Bhattarai[26], V.S. Bhopatkar[6], R. Bi[138], R.M. Bianchi[138], O. Biebel[114], D. Biedermann[19], R. Bielski[36], K. Bierwagen[100], N.V. Biesuz[72a,72b], M. Biglietti[75a], T.R.V. Billoud[141], M. Bindi[53], A. Bingul[12d],

C. Bini[73a,73b], S. Biondi[23b,23a], C.J. Birch-sykes[101], M. Birman[180], T. Bisanz[36], J.P. Biswal[3], D. Biswas[181,j], A. Bitadze[101], C. Bittrich[48], K. Bjørke[133], T. Blazek[28a], I. Bloch[46], C. Blocker[26], A. Blue[57], U. Blumenschein[93], G.J. Bobbink[120], V.S. Bobrovnikov[122b,122a], S.S. Bocchetta[97], D. Bogavac[14], A.G. Bogdanchikov[122b,122a], C. Bohm[45a], V. Boisvert[94], P. Bokan[172,53], T. Bold[84a], A.E. Bolz[61b], M. Bomben[135], M. Bona[93], J.S. Bonilla[131], M. Boonekamp[144], C.D. Booth[94], A.G. Borbély[57], H.M. Borecka-Bielska[91], L.S. Borgna[95], A. Borisov[123], G. Borissov[90], D. Bortoletto[134], D. Boscherini[23b], M. Bosman[14], J.D. Bossio Sola[104], K. Bouaouda[35a], J. Boudreau[138], E.V. Bouhova-Thacker[90], D. Boumediene[38], A. Boveia[127], J. Boyd[36], D. Boye[33c], I.R. Boyko[80], A.J. Bozson[94], J. Bracinik[21], N. Brahimi[60d,60c], G. Brandt[182], O. Brandt[32], F. Braren[46], B. Brau[103], J.E. Brau[131], W.D. Breaden Madden[57], K. Brendlinger[46], R. Brener[160], L. Brenner[36], R. Brenner[172], S. Bressler[180], B. Brickwedde[100], D.L. Briglin[21], D. Britton[57], D. Britzger[115], I. Brock[24], R. Brock[107], G. Brooijmans[39], W.K. Brooks[146d], E. Brost[29], P.A. Bruckman de Renstrom[85], B. Brüers[46], D. Bruncko[28b], A. Bruni[23b], G. Bruni[23b], M. Bruschi[23b], N. Bruscino[73a,73b], L. Bryngemark[153], T. Buanes[17], Q. Buat[155], P. Buchholz[151], A.G. Buckley[57], I.A. Budagov[80], M.K. Bugge[133], O. Bulekov[112], B.A. Bullard[59], T.J. Burch[121], S. Burdin[91], C.D. Burgard[120], A.M. Burger[129], B. Burghgrave[8], J.T.P. Burr[46], C.D. Burton[11], J.C. Burzynski[103], V. Büscher[100], E. Buschmann[53], P.J. Bussey[57], J.M. Butler[25], C.M. Buttar[57], J.M. Butterworth[95], P. Butti[36], W. Buttinger[143], C.J. Buxo Vazquez[107], A. Buzatu[158], A.R. Buzykaev[122b,122a], G. Cabras[23b,23a], S. Cabrera Urbán[174], D. Caforio[56], H. Cai[138], V.M.M. Cairo[153], O. Cakir[4a], N. Calace[36], P. Calafiura[18], G. Calderini[135], P. Calfayan[66], G. Callea[57], L.P. Caloba[81b], A. Caltabiano[74a,74b], S. Calvente Lopez[99], D. Calvet[38], S. Calvet[38], T.P. Calvet[102], M. Calvetti[72a,72b], R. Camacho Toro[135], S. Camarda[36], D. Camarero Munoz[99], P. Camarri[74a,74b], M.T. Camerlingo[75a,75b], D. Cameron[133], C. Camincher[36], S. Campana[36], M. Campanelli[95], A. Camplani[40], V. Canale[70a,70b], A. Canesse[104], M. Cano Bret[78], J. Cantero[129], T. Cao[161], Y. Cao[173], M. Capua[41b,41a], R. Cardarelli[74a], F. Cardillo[174], G. Carducci[41b,41a], I. Carli[142], T. Carli[36], G. Carlino[70a], B.T. Carlson[138], E.M. Carlson[176,168a], L. Carminati[69a,69b], R.M.D. Carney[153], S. Caron[119], E. Carquin[146d], S. Carrá[46], G. Carratta[23b,23a], J.W.S. Carter[167], T.M. Carter[50], M.P. Casado[14,g], A.F. Casha[167], E.G. Castiglia[183], F.L. Castillo[174], L. Castillo Garcia[14], V. Castillo Gimenez[174], N.F. Castro[139a,139e], A. Catinaccio[36], J.R. Catmore[133], A. Cattai[36], V. Cavaliere[29], V. Cavasinni[72a,72b], E. Celebi[12b], F. Celli[134], K. Cerny[130], A.S. Cerqueira[81a], A. Cerri[156], L. Cerrito[74a,74b], F. Cerutti[18], A. Cervelli[23b,23a], S.A. Cetin[12b], Z. Chadi[35a], D. Chakraborty[121], J. Chan[181], W.S. Chan[120], W.Y. Chan[91], J.D. Chapman[32], B. Chargeishvili[159b], D.G. Charlton[21], T.P. Charman[93], M. Chatterjee[20], C.C. Chau[34], S. Che[127], S. Chekanov[6], S.V. Chekulaev[168a], G.A. Chelkov[80,af], B. Chen[79], C. Chen[60a], C.H. Chen[79], H. Chen[15c], H. Chen[29], J. Chen[60a], J. Chen[39], J. Chen[26], S. Chen[136], S.J. Chen[15c], X. Chen[15b], Y. Chen[60a], Y-H. Chen[46], H.C. Cheng[63a], H.J. Cheng[15a], A. Cheplakov[80], E. Cheremushkina[123], R. Cherkaoui El Moursli[35f], E. Cheu[7], K. Cheung[64], T.J.A. Chevalérias[144], L. Chevalier[144], V. Chiarella[51], G. Chiarelli[72a], G. Chiodini[68a], A.S. Chisholm[21], A. Chitan[27b], I. Chiu[163], Y.H. Chiu[176], M.V. Chizhov[80], K. Choi[11], A.R. Chomont[73a,73b], Y. Chou[103], Y.S. Chow[120], L.D. Christopher[33f], M.C. Chu[63a], X. Chu[15a,15d], J. Chudoba[140], J.J. Chwastowski[85], L. Chytka[130], D. Cieri[115], K.M. Ciesla[85], V. Cindro[92], I.A. Cioară[27b], A. Ciocio[18], F. Cirotto[70a,70b], Z.H. Citron[180,k], M. Citterio[69a], D.A. Ciubotaru[27b], B.M. Ciungu[167], A. Clark[54], P.J. Clark[50], S.E. Clawson[101], C. Clement[45a,45b], L. Clissa[23b,23a], Y. Coadou[102], M. Cobal[67a,67c], A. Coccaro[55b], J. Cochran[79], R. Coelho Lopes De Sa[103], H. Cohen[161], A.E.C. Coimbra[36], B. Cole[39], A.P. Colijn[120], J. Collot[58], P. Conde Muiño[139a,139h], S.H. Connell[33c], I.A. Connelly[57], S. Constantinescu[27b], F. Conventi[70a,al], A.M. Cooper-Sarkar[134], F. Cormier[175], K.J.R. Cormier[167], L.D. Corpe[95], M. Corradi[73a,73b], E.E. Corrigan[97], F. Corriveau[104,aa], M.J. Costa[174], F. Costanza[5], D. Costanzo[149], G. Cowan[94], J.W. Cowley[32], J. Crane[101], K. Cranmer[125], R.A. Creager[136], S. Crépé-Renaudin[58], F. Crescioli[135], M. Cristinziani[24], V. Croft[170], G. Crosetti[41b,41a], A. Cueto[5], T. Cuhadar Donszelmann[171], H. Cui[15a,15d], A.R. Cukierman[153], W.R. Cunningham[57], S. Czekierda[85],

P. Czodrowski[36], M.M. Czurylo[61b], M.J. Da Cunha Sargedas De Sousa[60b], J.V. Da Fonseca Pinto[81b], C. Da Via[101], W. Dabrowski[84a], F. Dachs[36], T. Dado[47], S. Dahbi[33f], T. Dai[106], C. Dallapiccola[103], M. Dam[40], G. D'amen[29], V. D'Amico[75a,75b], J. Damp[100], J.R. Dandoy[136], M.F. Daneri[30], M. Danninger[152], V. Dao[36], G. Darbo[55b], O. Dartsi[5], A. Dattagupta[131], T. Daubney[46], S. D'Auria[69a,69b], C. David[168b], T. Davidek[142], D.R. Davis[49], I. Dawson[149], K. De[8], R. De Asmundis[70a], M. De Beurs[120], S. De Castro[23b,23a], N. De Groot[119], P. de Jong[120], H. De la Torre[107], A. De Maria[15c], D. De Pedis[73a], A. De Salvo[73a], U. De Sanctis[74a,74b], M. De Santis[74a,74b], A. De Santo[156], J.B. De Vivie De Regie[65], D.V. Dedovich[80], A.M. Deiana[42], J. Del Peso[99], Y. Delabat Diaz[46], D. Delgove[65], F. Deliot[144], C.M. Delitzsch[7], M. Della Pietra[70a,70b], D. Della Volpe[54], A. Dell'Acqua[36], L. Dell'Asta[74a,74b], M. Delmastro[5], C. Delporte[65], P.A. Delsart[58], S. Demers[183], M. Demichev[80], G. Demontigny[110], S.P. Denisov[123], L. D'Eramo[121], D. Derendarz[85], J.E. Derkaoui[35e], F. Derue[135], P. Dervan[91], K. Desch[24], K. Dette[167], C. Deutsch[24], M.R. Devesa[30], P.O. Deviveiros[36], F.A. Di Bello[73a,73b], A. Di Ciaccio[74a,74b], L. Di Ciaccio[5], C. Di Donato[70a,70b], A. Di Girolamo[36], G. Di Gregorio[72a,72b], A. Di Luca[76a,76b], B. Di Micco[75a,75b], R. Di Nardo[75a,75b], K.F. Di Petrillo[59], R. Di Sipio[167], C. Diaconu[102], F.A. Dias[120], T. Dias Do Vale[139a], M.A. Diaz[146a], F.G. Diaz Capriles[24], J. Dickinson[18], M. Didenko[166], E.B. Diehl[106], J. Dietrich[19], S. Díez Cornell[46], C. Diez Pardos[151], A. Dimitrievska[18], W. Ding[15b], J. Dingfelder[24], S.J. Dittmeier[61b], F. Dittus[36], F. Djama[102], T. Djobava[159b], J.I. Djuvsland[17], M.A.B. Do Vale[147], M. Dobre[27b], D. Dodsworth[26], C. Doglioni[97], J. Dolejsi[142], Z. Dolezal[142], M. Donadelli[81c], B. Dong[60c], J. Donini[38], A. D'onofrio[15c], M. D'Onofrio[91], J. Dopke[143], A. Doria[70a], M.T. Dova[89], A.T. Doyle[57], E. Drechsler[152], E. Dreyer[152], T. Dreyer[53], A.S. Drobac[170], D. Du[60b], T.A. du Pree[120], Y. Duan[60d], F. Dubinin[111], M. Dubovsky[28a], A. Dubreuil[54], E. Duchovni[180], G. Duckeck[114], O.A. Ducu[36,27b], D. Duda[115], A. Dudarev[36], A.C. Dudder[100], E.M. Duffield[18], M. D'uffizi[101], L. Duflot[65], M. Dührssen[36], C. Dülsen[182], M. Dumancic[180], A.E. Dumitriu[27b], M. Dunford[61a], S. Dungs[47], A. Duperrin[102], H. Duran Yildiz[4a], M. Düren[56], A. Durglishvili[159b], D. Duschinger[48], B. Dutta[46], D. Duvnjak[1], G.I. Dyckes[136], M. Dyndal[36], S. Dysch[101], B.S. Dziedzic[85], M.G. Eggleston[49], T. Eifert[8], G. Eigen[17], K. Einsweiler[18], T. Ekelof[172], H. El Jarrari[35f], V. Ellajosyula[172], M. Ellert[172], F. Ellinghaus[182], A.A. Elliot[93], N. Ellis[36], J. Elmsheuser[29], M. Elsing[36], D. Emeliyanov[143], A. Emerman[39], Y. Enari[163], M.B. Epland[49], J. Erdmann[47], A. Ereditato[20], P.A. Erland[85], M. Errenst[182], M. Escalier[65], C. Escobar[174], O. Estrada Pastor[174], E. Etzion[161], G. Evans[139a], H. Evans[66], M.O. Evans[156], A. Ezhilov[137], F. Fabbri[57], L. Fabbri[23b,23a], V. Fabiani[119], G. Facini[178], R.M. Fakhrutdinov[123], S. Falciano[73a], P.J. Falke[24], S. Falke[36], J. Faltova[142], Y. Fang[15a], Y. Fang[15a], G. Fanourakis[44], M. Fanti[69a,69b], M. Faraj[67a,67c], A. Farbin[8], A. Farilla[75a], E.M. Farina[71a,71b], T. Farooque[107], S.M. Farrington[50], P. Farthouat[36], F. Fassi[35f], P. Fassnacht[36], D. Fassouliotis[9], M. Faucci Giannelli[50], W.J. Fawcett[32], L. Fayard[65], O.L. Fedin[137,p], W. Fedorko[175], A. Fehr[20], M. Feickert[173], L. Feligioni[102], A. Fell[149], C. Feng[60b], M. Feng[49], M.J. Fenton[171], A.B. Fenyuk[123], S.W. Ferguson[43], J. Ferrando[46], A. Ferrari[172], P. Ferrari[120], R. Ferrari[71a], D.E. Ferreira de Lima[61b], A. Ferrer[174], D. Ferrere[54], C. Ferretti[106], F. Fiedler[100], A. Filipčič[92], F. Filthaut[119], K.D. Finelli[25], M.C.N. Fiolhais[139a,139c,a], L. Fiorini[174], F. Fischer[114], J. Fischer[100], W.C. Fisher[107], T. Fitschen[21], I. Fleck[151], P. Fleischmann[106], T. Flick[182], B.M. Flierl[114], L. Flores[136], L.R. Flores Castillo[63a], F.M. Follega[76a,76b], N. Fomin[17], J.H. Foo[167], G.T. Forcolin[76a,76b], B.C. Forland[66], A. Formica[144], F.A. Förster[14], A.C. Forti[101], E. Fortin[102], M.G. Foti[134], D. Fournier[65], H. Fox[90], P. Francavilla[72a,72b], S. Francescato[73a,73b], M. Franchini[23b,23a], S. Franchino[61a], D. Francis[36], L. Franco[5], L. Franconi[20], M. Franklin[59], G. Frattari[73a,73b], A.N. Fray[93], P.M. Freeman[21], B. Freund[110], W.S. Freund[81b], E.M. Freundlich[47], D.C. Frizzell[128], D. Froidevaux[36], J.A. Frost[134], M. Fujimoto[126], C. Fukunaga[164], E. Fullana Torregrosa[174], T. Fusayasu[116], J. Fuster[174], A. Gabrielli[23b,23a], A. Gabrielli[36], S. Gadatsch[54], P. Gadow[115], G. Gagliardi[55b,55a], L.G. Gagnon[110], G.E. Gallardo[134], E.J. Gallas[134], B.J. Gallop[143], R. Gamboa Goni[93], K.K. Gan[127], S. Ganguly[180], J. Gao[60a], Y. Gao[50], Y.S. Gao[31,m], F.M. Garay Walls[146a], C. García[174], J.E. García Navarro[174], J.A. García Pascual[15a], C. Garcia-Argos[52],

M. Garcia-Sciveres[18], R.W. Gardner[37], N. Garelli[153], S. Gargiulo[52], C.A. Garner[167], V. Garonne[133], S.J. Gasiorowski[148], P. Gaspar[81b], A. Gaudiello[55b,55a], G. Gaudio[71a], P. Gauzzi[73a,73b], I.L. Gavrilenko[111], A. Gavrilyuk[124], C. Gay[175], G. Gaycken[46], E.N. Gazis[10], A.A. Geanta[27b], C.M. Gee[145], C.N.P. Gee[143], J. Geisen[97], M. Geisen[100], C. Gemme[55b], M.H. Genest[58], C. Geng[106], S. Gentile[73a,73b], S. George[94], T. Geralis[44], L.O. Gerlach[53], P. Gessinger-Befurt[100], G. Gessner[47], M. Ghasemi Bostanabad[176], M. Ghneimat[151], A. Ghosh[65], A. Ghosh[78], B. Giacobbe[23b], S. Giagu[73a,73b], N. Giangiacomi[167], P. Giannetti[72a], A. Giannini[70a,70b], G. Giannini[14], S.M. Gibson[94], M. Gignac[145], D.T. Gil[84b], B.J. Gilbert[39], D. Gillberg[34], G. Gilles[182], N.E.K. Gillwald[46], D.M. Gingrich[3,ak], M.P. Giordani[67a,67c], P.F. Giraud[144], G. Giugliarelli[67a,67c], D. Giugni[69a], F. Giuli[74a,74b], S. Gkaitatzis[162], I. Gkialas[9,h], E.L. Gkougkousis[14], P. Gkountoumis[10], L.K. Gladilin[113], C. Glasman[99], J. Glatzer[14], P.C.F. Glaysher[46], A. Glazov[46], G.R. Gledhill[131], I. Gnesi[41b,c], M. Goblirsch-Kolb[26], D. Godin[110], S. Goldfarb[105], T. Golling[54], D. Golubkov[123], A. Gomes[139a,139b], R. Goncalves Gama[53], R. Gonçalo[139a,139c], G. Gonella[131], L. Gonella[21], A. Gongadze[80], F. Gonnella[21], J.L. Gonski[39], S. González de la Hoz[174], S. Gonzalez Fernandez[14], R. Gonzalez Lopez[91], C. Gonzalez Renteria[18], R. Gonzalez Suarez[172], S. Gonzalez-Sevilla[54], G.R. Gonzalvo Rodriguez[174], L. Goossens[36], N.A. Gorasia[21], P.A. Gorbounov[124], H.A. Gordon[29], B. Gorini[36], E. Gorini[68a,68b], A. Gorišek[92], A.T. Goshaw[49], M.I. Gostkin[80], C.A. Gottardo[119], M. Gouighri[35b], A.G. Goussiou[148], N. Govender[33c], C. Goy[5], I. Grabowska-Bold[84a], E.C. Graham[91], J. Gramling[171], E. Gramstad[133], S. Grancagnolo[19], M. Grandi[156], V. Gratchev[137], P.M. Gravila[27f], F.G. Gravili[68a,68b], C. Gray[57], H.M. Gray[18], C. Grefe[24], K. Gregersen[97], I.M. Gregor[46], P. Grenier[153], K. Grevtsov[46], C. Grieco[14], N.A. Grieser[128], A.A. Grillo[145], K. Grimm[31,l], S. Grinstein[14,w], J.-F. Grivaz[65], S. Groh[100], E. Gross[180], J. Grosse-Knetter[53], Z.J. Grout[95], C. Grud[106], A. Grummer[118], J.C. Grundy[134], L. Guan[106], W. Guan[181], C. Gubbels[175], J. Guenther[77], A. Guerguichon[65], J.G.R. Guerrero Rojas[174], F. Guescini[115], D. Guest[77], R. Gugel[100], A. Guida[46], T. Guillemin[5], S. Guindon[36], J. Guo[60c], W. Guo[106], Y. Guo[60a], Z. Guo[102], R. Gupta[46], S. Gurbuz[12c], G. Gustavino[128], M. Guth[52], P. Gutierrez[128], C. Gutschow[95], C. Guyot[144], C. Gwenlan[134], C.B. Gwilliam[91], E.S. Haaland[133], A. Haas[125], C. Haber[18], H.K. Hadavand[8], A. Hadef[100], M. Haleem[177], J. Haley[129], J.J. Hall[149], G. Halladjian[107], G.D. Hallewell[102], K. Hamano[176], H. Hamdaoui[35f], M. Hamer[24], G.N. Hamity[50], K. Han[60a], L. Han[15c], L. Han[60a], S. Han[18], Y.F. Han[167], K. Hanagaki[82,u], M. Hance[145], D.M. Handl[114], M.D. Hank[37], R. Hankache[135], E. Hansen[97], J.B. Hansen[40], J.D. Hansen[40], M.C. Hansen[24], P.H. Hansen[40], E.C. Hanson[101], K. Hara[169], T. Harenberg[182], S. Harkusha[108], P.F. Harrison[178], N.M. Hartman[153], N.M. Hartmann[114], Y. Hasegawa[150], A. Hasib[50], S. Hassani[144], S. Haug[20], R. Hauser[107], M. Havranek[141], C.M. Hawkes[21], R.J. Hawkings[36], S. Hayashida[117], D. Hayden[107], C. Hayes[106], R.L. Hayes[175], C.P. Hays[134], J.M. Hays[93], H.S. Hayward[91], S.J. Haywood[143], F. He[60a], Y. He[165], M.P. Heath[50], V. Hedberg[97], A.L. Heggelund[133], N.D. Hehir[93], C. Heidegger[52], K.K. Heidegger[52], W.D. Heidorn[79], J. Heilman[34], S. Heim[46], T. Heim[18], B. Heinemann[46,ai], J.G. Heinlein[136], J.J. Heinrich[131], L. Heinrich[36], J. Hejbal[140], L. Helary[46], A. Held[125], S. Hellesund[133], C.M. Helling[145], S. Hellman[45a,45b], C. Helsens[36], R.C.W. Henderson[90], L. Henkelmann[32], A.M. Henriques Correia[36], H. Herde[26], Y. Hernández Jiménez[33f], H. Herr[100], M.G. Herrmann[114], T. Herrmann[48], G. Herten[52], R. Hertenberger[114], L. Hervas[36], G.G. Hesketh[95], N.P. Hessey[168a], H. Hibi[83], S. Higashino[82], E. Higón-Rodriguez[174], K. Hildebrand[37], J.C. Hill[32], K.K. Hill[29], K.H. Hiller[46], S.J. Hillier[21], M. Hils[48], I. Hinchliffe[18], F. Hinterkeuser[24], M. Hirose[132], S. Hirose[169], D. Hirschbuehl[182], B. Hiti[92], O. Hladik[140], J. Hobbs[155], R. Hobincu[27e], N. Hod[180], M.C. Hodgkinson[149], A. Hoecker[36], D. Hohn[52], D. Hohov[65], T. Holm[24], T.R. Holmes[37], M. Holzbock[115], L.B.A.H. Hommels[32], T.M. Hong[138], J.C. Honig[52], A. Hönle[115], B.H. Hooberman[173], W.H. Hopkins[6], Y. Horii[117], P. Horn[48], L.A. Horyn[37], S. Hou[158], A. Hoummada[35a], J. Howarth[57], J. Hoya[89], M. Hrabovsky[130], J. Hrivnac[65], A. Hrynevich[109], T. Hryn'ova[5], P.J. Hsu[64], S.-C. Hsu[148], Q. Hu[39], S. Hu[60c], Y.F. Hu[15a,15d,am], D.P. Huang[95], X. Huang[15c], Y. Huang[60a], Y. Huang[15a], Z. Hubacek[141], F. Hubaut[102], M. Huebner[24], F. Huegging[24], T.B. Huffman[134],

M. Huhtinen[36], R. Hulsken[58], R.F.H. Hunter[34], N. Huseynov[80,ab], J. Huston[107], J. Huth[59], R. Hyneman[153], S. Hyrych[28a], G. Iacobucci[54], G. Iakovidis[29], I. Ibragimov[151], L. Iconomidou-Fayard[65], P. Iengo[36], R. Ignazzi[40], R. Iguchi[163], T. Iizawa[54], Y. Ikegami[82], M. Ikeno[82], N. Ilic[119,167,aa], F. Iltzsche[48], H. Imam[35a], G. Introzzi[71a,71b], M. Iodice[75a], K. Iordanidou[168a], V. Ippolito[73a,73b], M.F. Isacson[172], M. Ishino[163], W. Islam[129], C. Issever[19,46], S. Istin[160], J.M. Iturbe Ponce[63a], R. Iuppa[76a,76b], A. Ivina[180], J.M. Izen[43], V. Izzo[70a], P. Jacka[140], P. Jackson[1], R.M. Jacobs[46], B.P. Jaeger[152], V. Jain[2], G. Jäkel[182], K.B. Jakobi[100], K. Jakobs[52], T. Jakoubek[180], J. Jamieson[57], K.W. Janas[84a], R. Jansky[54], M. Janus[53], P.A. Janus[84a], G. Jarlskog[97], A.E. Jaspan[91], N. Javadov[80,ab], T. Javůrek[36], M. Javurkova[103], F. Jeanneau[144], L. Jeanty[131], J. Jejelava[159a], P. Jenni[52,d], N. Jeong[46], S. Jézéquel[5], J. Jia[155], Z. Jia[15c], H. Jiang[79], Y. Jiang[60a], Z. Jiang[153], S. Jiggins[52], F.A. Jimenez Morales[38], J. Jimenez Pena[115], S. Jin[15c], A. Jinaru[27b], O. Jinnouchi[165], H. Jivan[33f], P. Johansson[149], K.A. Johns[7], C.A. Johnson[66], E. Jones[178], R.W.L. Jones[90], S.D. Jones[156], T.J. Jones[91], J. Jovicevic[36], X. Ju[18], J.J. Junggeburth[115], A. Juste Rozas[14,w], A. Kaczmarska[85], M. Kado[73a,73b], H. Kagan[127], M. Kagan[153], A. Kahn[39], C. Kahra[100], T. Kaji[179], E. Kajomovitz[160], C.W. Kalderon[29], A. Kaluza[100], A. Kamenshchikov[123], M. Kaneda[163], N.J. Kang[145], S. Kang[79], Y. Kano[117], J. Kanzaki[82], L.S. Kaplan[181], D. Kar[33f], K. Karava[134], M.J. Kareem[168b], I. Karkanias[162], S.N. Karpov[80], Z.M. Karpova[80], V. Kartvelishvili[90], A.N. Karyukhin[123], E. Kasimi[162], A. Kastanas[45a,45b], C. Kato[60d], J. Katzy[46], K. Kawade[150], K. Kawagoe[88], T. Kawaguchi[117], T. Kawamoto[144], G. Kawamura[53], E.F. Kay[176], F.I. Kaya[170], S. Kazakos[14], V.F. Kazanin[122b,122a], J.M. Keaveney[33a], R. Keeler[176], J.S. Keller[34], E. Kellermann[97], D. Kelsey[156], J.J. Kempster[21], J. Kendrick[21], K.E. Kennedy[39], O. Kepka[140], S. Kersten[182], B.P. Kerševan[92], S. Ketabchi Haghighat[167], F. Khalil-Zada[13], M. Khandoga[144], A. Khanov[129], A.G. Kharlamov[122b,122a], T. Kharlamova[122b,122a], E.E. Khoda[175], T.J. Khoo[77], G. Khoriauli[177], E. Khramov[80], J. Khubua[159b], S. Kido[83], M. Kiehn[36], E. Kim[165], Y.K. Kim[37], N. Kimura[95], A. Kirchhoff[53], D. Kirchmeier[48], J. Kirk[143], A.E. Kiryunin[115], T. Kishimoto[163], D.P. Kisliuk[167], V. Kitali[46], C. Kitsaki[10], O. Kivernyk[24], T. Klapdor-Kleingrothaus[52], M. Klassen[61a], C. Klein[34], M.H. Klein[106], M. Klein[91], U. Klein[91], K. Kleinknecht[100], P. Klimek[36], A. Klimentov[29], F. Klimpel[36], T. Klingl[24], T. Klioutchnikova[36], F.F. Klitzner[114], P. Kluit[120], S. Kluth[115], E. Kneringer[77], E.B.F.G. Knoops[102], A. Knue[52], D. Kobayashi[88], M. Kobel[48], M. Kocian[153], T. Kodama[163], P. Kodys[142], D.M. Koeck[156], P.T. Koenig[24], T. Koffas[34], N.M. Köhler[36], M. Kolb[144], I. Koletsou[5], T. Komarek[130], T. Kondo[82], K. Köneke[52], A.X.Y. Kong[1], A.C. König[119], T. Kono[126], V. Konstantinides[95], N. Konstantinidis[95], B. Konya[97], R. Kopeliansky[66], S. Koperny[84a], K. Korcyl[85], K. Kordas[162], G. Koren[161], A. Korn[95], I. Korolkov[14], E.V. Korolkova[149], N. Korotkova[113], O. Kortner[115], S. Kortner[115], V.V. Kostyukhin[149,166], A. Kotsokechagia[65], A. Kotwal[49], A. Koulouris[10], A. Kourkoumeli-Charalampidi[71a,71b], C. Kourkoumelis[9], E. Kourlitis[6], V. Kouskoura[29], R. Kowalewski[176], W. Kozanecki[101], A.S. Kozhin[123], V.A. Kramarenko[113], G. Kramberger[92], D. Krasnopevtsev[60a], M.W. Krasny[135], A. Krasznahorkay[36], D. Krauss[115], J.A. Kremer[100], J. Kretzschmar[91], K. Kreul[19], P. Krieger[167], F. Krieter[114], S. Krishnamurthy[103], A. Krishnan[61b], M. Krivos[142], K. Krizka[18], K. Kroeninger[47], H. Kroha[115], J. Kroll[140], J. Kroll[136], K.S. Krowpman[107], U. Kruchonak[80], H. Krüger[24], N. Krumnack[79], M.C. Kruse[49], J.A. Krzysiak[85], A. Kubota[165], O. Kuchinskaia[166], S. Kuday[4b], D. Kuechler[46], J.T. Kuechler[46], S. Kuehn[36], T. Kuhl[46], V. Kukhtin[80], Y. Kulchitsky[108,ae], S. Kuleshov[146b], Y.P. Kulinich[173], M. Kuna[58], A. Kupco[140], T. Kupfer[47], O. Kuprash[52], H. Kurashige[83], L.L. Kurchaninov[168a], Y.A. Kurochkin[108], A. Kurova[112], M.G. Kurth[15a,15d], E.S. Kuwertz[36], M. Kuze[165], A.K. Kvam[148], J. Kvita[130], T. Kwan[104], C. Lacasta[174], F. Lacava[73a,73b], D.P.J. Lack[101], H. Lacker[19], D. Lacour[135], E. Ladygin[80], R. Lafaye[5], B. Laforge[135], T. Lagouri[146c], S. Lai[53], I.K. Lakomiec[84a], J.E. Lambert[128], S. Lammers[66], W. Lampl[7], C. Lampoudis[162], E. Lançon[29], U. Landgraf[52], M.P.J. Landon[93], V.S. Lang[52], J.C. Lange[53], R.J. Langenberg[103], A.J. Lankford[171], F. Lanni[29], K. Lantzsch[24], A. Lanza[71a], A. Lapertosa[55b,55a], J.F. Laporte[144], T. Lari[69a], F. Lasagni Manghi[23b,23a], M. Lassnig[36], V. Latonova[140], T.S. Lau[63a], A. Laudrain[100], A. Laurier[34], M. Lavorgna[70a,70b],

S.D. Lawlor[94], M. Lazzaroni[69a,69b], B. Le[101], E. Le Guirriec[102], A. Lebedev[79], M. LeBlanc[7], T. LeCompte[6], F. Ledroit-Guillon[58], A.C.A. Lee[95], C.A. Lee[29], G.R. Lee[17], L. Lee[59], S.C. Lee[158], S. Lee[79], B. Lefebvre[168a], H.P. Lefebvre[94], M. Lefebvre[176], C. Leggett[18], K. Lehmann[152], N. Lehmann[20], G. Lehmann Miotto[36], W.A. Leight[46], A. Leisos[162,v], M.A.L. Leite[81c], C.E. Leitgeb[114], R. Leitner[142], K.J.C. Leney[42], T. Lenz[24], S. Leone[72a], C. Leonidopoulos[50], A. Leopold[135], C. Leroy[110], R. Les[107], C.G. Lester[32], M. Levchenko[137], J. Levêque[5], D. Levin[106], L.J. Levinson[180], D.J. Lewis[21], B. Li[15b], B. Li[106], C-Q. Li[60c,60d], F. Li[60c], H. Li[60a], H. Li[60b], J. Li[60c], K. Li[148], L. Li[60c], M. Li[15a,15d], Q.Y. Li[60a], S. Li[60d,60c,b], X. Li[46], Y. Li[46], Z. Li[60b], Z. Li[134], Z. Li[104], Z. Li[91], Z. Liang[15a], M. Liberatore[46], B. Liberti[74a], K. Lie[63c], S. Lim[29], C.Y. Lin[32], K. Lin[107], R.A. Linck[66], R.E. Lindley[7], J.H. Lindon[21], A. Linss[46], A.L. Lionti[54], E. Lipeles[136], A. Lipniacka[17], T.M. Liss[173,aj], A. Lister[175], J.D. Little[8], B. Liu[79], B.X. Liu[152], H.B. Liu[29], J.B. Liu[60a], J.K.K. Liu[37], K. Liu[60d,60c], M. Liu[60a], M.Y. Liu[60a], P. Liu[15a], X. Liu[60a], Y. Liu[46], Y. Liu[15a,15d], Y.L. Liu[106], Y.W. Liu[60a], M. Livan[71a,71b], A. Lleres[58], J. Llorente Merino[152], S.L. Lloyd[93], C.Y. Lo[63b], E.M. Lobodzinska[46], P. Loch[7], S. Loffredo[74a,74b], T. Lohse[19], K. Lohwasser[149], M. Lokajicek[140], J.D. Long[173], R.E. Long[90], I. Longarini[73a,73b], L. Longo[36], I. Lopez Paz[101], A. Lopez Solis[149], J. Lorenz[114], N. Lorenzo Martinez[5], A.M. Lory[114], A. Lösle[52], X. Lou[45a,45b], X. Lou[15a], A. Lounis[65], J. Love[6], P.A. Love[90], J.J. Lozano Bahilo[174], M. Lu[60a], Y.J. Lu[64], H.J. Lubatti[148], C. Luci[73a,73b], F.L. Lucio Alves[15c], A. Lucotte[58], F. Luehring[66], I. Luise[155], L. Luminari[73a], B. Lund-Jensen[154], N.A. Luongo[131], M.S. Lutz[161], D. Lynn[29], H. Lyons[91], R. Lysak[140], E. Lytken[97], F. Lyu[15a], V. Lyubushkin[80], T. Lyubushkina[80], H. Ma[29], L.L. Ma[60b], Y. Ma[95], D.M. Mac Donell[176], G. Maccarrone[51], C.M. Macdonald[149], J.C. MacDonald[149], J. Machado Miguens[136], R. Madar[38], W.F. Mader[48], M. Madugoda Ralalage Don[129], N. Madysa[48], J. Maeda[83], T. Maeno[29], M. Maerker[48], V. Magerl[52], N. Magini[79], J. Magro[67a,67c,r], D.J. Mahon[39], C. Maidantchik[81b], A. Maio[139a,139b,139d], K. Maj[84a], O. Majersky[28a], S. Majewski[131], Y. Makida[82], N. Makovec[65], B. Malaescu[135], Pa. Malecki[85], V.P. Maleev[137], F. Malek[58], D. Malito[41b,41a], U. Mallik[78], C. Malone[32], S. Maltezos[10], S. Malyukov[80], J. Mamuzic[174], G. Mancini[51], J.P. Mandalia[93], I. Mandić[92], L. Manhaes de Andrade Filho[81a], I.M. Maniatis[162], J. Manjarres Ramos[48], K.H. Mankinen[97], A. Mann[114], A. Manousos[77], B. Mansoulie[144], I. Manthos[162], S. Manzoni[120], A. Marantis[162], G. Marceca[30], L. Marchese[134], G. Marchiori[135], M. Marcisovsky[140], L. Marcoccia[74a,74b], C. Marcon[97], M. Marjanovic[128], Z. Marshall[18], M.U.F. Martensson[172], S. Marti-Garcia[174], C.B. Martin[127], T.A. Martin[178], V.J. Martin[50], B. Martin dit Latour[17], L. Martinelli[75a,75b], M. Martinez[14,w], P. Martinez Agullo[174], V.I. Martinez Outschoorn[103], S. Martin-Haugh[143], V.S. Martoiu[27b], A.C. Martyniuk[95], A. Marzin[36], S.R. Maschek[115], L. Masetti[100], T. Mashimo[163], R. Mashinistov[111], J. Masik[101], A.L. Maslennikov[122b,122a], L. Massa[23b,23a], P. Massarotti[70a,70b], P. Mastrandrea[72a,72b], A. Mastroberardino[41b,41a], T. Masubuchi[163], D. Matakias[29], A. Matic[114], N. Matsuzawa[163], P. Mättig[24], J. Maurer[27b], B. Maček[92], D.A. Maximov[122b,122a], R. Mazini[158], I. Maznas[162], S.M. Mazza[145], J.P. Mc Gowan[104], S.P. Mc Kee[106], T.G. McCarthy[115], W.P. McCormack[18], E.F. McDonald[105], A.E. McDougall[120], J.A. Mcfayden[18], G. Mchedlidze[159b], M.A. McKay[42], K.D. McLean[176], S.J. McMahon[143], P.C. McNamara[105], C.J. McNicol[178], R.A. McPherson[176,aa], J.E. Mdhluli[33f], Z.A. Meadows[103], S. Meehan[36], T. Megy[38], S. Mehlhase[114], A. Mehta[91], B. Meirose[43], D. Melini[160], B.R. Mellado Garcia[33f], J.D. Mellenthin[53], M. Melo[28a], F. Meloni[46], A. Melzer[24], E.D. Mendes Gouveia[139a,139e], A.M. Mendes Jacques Da Costa[21], H.Y. Meng[167], L. Meng[36], X.T. Meng[106], S. Menke[115], E. Meoni[41b,41a], S. Mergelmeyer[19], S.A.M. Merkt[138], C. Merlassino[134], P. Mermod[54], L. Merola[70a,70b], C. Meroni[69a], G. Merz[106], O. Meshkov[113,111], J.K.R. Meshreki[151], J. Metcalfe[6], A.S. Mete[6], C. Meyer[66], J-P. Meyer[144], M. Michetti[19], R.P. Middleton[143], L. Mijović[50], G. Mikenberg[180], M. Mikestikova[140], M. Mikuž[92], H. Mildner[149], A. Milic[167], C.D. Milke[42], D.W. Miller[37], L.S. Miller[34], A. Milov[180], D.A. Milstead[45a,45b], A.A. Minaenko[123], I.A. Minashvili[159b], L. Mince[57], A.I. Mincer[125], B. Mindur[84a], M. Mineev[80], Y. Minegishi[163], Y. Mino[86], L.M. Mir[14], M. Mironova[134], T. Mitani[179], J. Mitrevski[114], V.A. Mitsou[174],

M. Mittal[60c], O. Miu[167], A. Miucci[20], P.S. Miyagawa[93], A. Mizukami[82], J.U. Mjörnmark[97], T. Mkrtchyan[61a], M. Mlynarikova[121], T. Moa[45a,45b], S. Mobius[53], K. Mochizuki[110], P. Moder[46], P. Mogg[114], S. Mohapatra[39], R. Moles-Valls[24], K. Mönig[46], E. Monnier[102], A. Montalbano[152], J. Montejo Berlingen[36], M. Montella[95], F. Monticelli[89], S. Monzani[69a], N. Morange[65], A.L. Moreira De Carvalho[139a], D. Moreno[22a], M. Moreno Llácer[174], C. Moreno Martinez[14], P. Morettini[55b], M. Morgenstern[160], S. Morgenstern[48], D. Mori[152], M. Morii[59], M. Morinaga[179], V. Morisbak[133], A.K. Morley[36], G. Mornacchi[36], A.P. Morris[95], L. Morvaj[36], P. Moschovakos[36], B. Moser[120], M. Mosidze[159b], T. Moskalets[144], P. Moskvitina[119], J. Moss[31,n], E.J.W. Moyse[103], S. Muanza[102], J. Mueller[138], R.S.P. Mueller[114], D. Muenstermann[90], G.A. Mullier[97], D.P. Mungo[69a,69b], J.L. Munoz Martinez[14], F.J. Munoz Sanchez[101], P. Murin[28b], W.J. Murray[178,143], A. Murrone[69a,69b], J.M. Muse[128], M. Muškinja[18], C. Mwewa[33a], A.G. Myagkov[123,af], A.A. Myers[138], G. Myers[66], J. Myers[131], M. Myska[141], B.P. Nachman[18], O. Nackenhorst[47], A.Nag Nag[48], K. Nagai[134], K. Nagano[82], Y. Nagasaka[62], J.L. Nagle[29], E. Nagy[102], A.M. Nairz[36], Y. Nakahama[117], K. Nakamura[82], T. Nakamura[163], H. Nanjo[132], F. Napolitano[61a], R.F. Naranjo Garcia[46], R. Narayan[42], I. Naryshkin[137], M. Naseri[34], T. Naumann[46], G. Navarro[22a], P.Y. Nechaeva[111], F. Nechansky[46], T.J. Neep[21], A. Negri[71a,71b], M. Negrini[23b], C. Nellist[119], C. Nelson[104], M.E. Nelson[45a,45b], S. Nemecek[140], M. Nessi[36,f], M.S. Neubauer[173], F. Neuhaus[100], M. Neumann[182], R. Newhouse[175], P.R. Newman[21], C.W. Ng[138], Y.S. Ng[19], Y.W.Y. Ng[171], B. Ngair[35f], H.D.N. Nguyen[102], T. Nguyen Manh[110], E. Nibigira[38], R.B. Nickerson[134], R. Nicolaidou[144], D.S. Nielsen[40], J. Nielsen[145], M. Niemeyer[53], N. Nikiforou[11], V. Nikolaenko[123,af], I. Nikolic-Audit[135], K. Nikolopoulos[21], P. Nilsson[29], H.R. Nindhito[54], A. Nisati[73a], N. Nishu[60c], R. Nisius[115], I. Nitsche[47], T. Nitta[179], T. Nobe[163], D.L. Noel[32], Y. Noguchi[86], I. Nomidis[135], M.A. Nomura[29], M. Nordberg[36], J. Novak[92], T. Novak[92], O. Novgorodova[48], R. Novotny[118], L. Nozka[130], K. Ntekas[171], E. Nurse[95], F.G. Oakham[34,ak], J. Ocariz[135], A. Ochi[83], I. Ochoa[139a], J.P. Ochoa-Ricoux[146a], K. O'Connor[26], S. Oda[88], S. Odaka[82], S. Oerdek[53], A. Ogrodnik[84a], A. Oh[101], C.C. Ohm[154], H. Oide[165], R. Oishi[163], M.L. Ojeda[167], H. Okawa[169], Y. Okazaki[86], M.W. O'Keefe[91], Y. Okumura[163], A. Olariu[27b], L.F. Oleiro Seabra[139a], S.A. Olivares Pino[146a], D. Oliveira Damazio[29], J.L. Oliver[1], M.J.R. Olsson[171], A. Olszewski[85], J. Olszowska[85], Ö.O. Öncel[24], D.C. O'Neil[152], A.P. O'neill[134], A. Onofre[139a,139e], P.U.E. Onyisi[11], H. Oppen[133], R.G. Oreamuno Madriz[121], M.J. Oreglia[37], G.E. Orellana[89], D. Orestano[75a,75b], N. Orlando[14], R.S. Orr[167], V. O'Shea[57], R. Ospanov[60a], G. Otero y Garzon[30], H. Otono[88], P.S. Ott[61a], G.J. Ottino[18], M. Ouchrif[35e], J. Ouellette[29], F. Ould-Saada[133], A. Ouraou[144,*], Q. Ouyang[15a], M. Owen[57], R.E. Owen[143], V.E. Ozcan[12c], N. Ozturk[8], J. Pacalt[130], H.A. Pacey[32], K. Pachal[49], A. Pacheco Pages[14], C. Padilla Aranda[14], S. Pagan Griso[18], G. Palacino[66], S. Palazzo[50], S. Palestini[36], M. Palka[84b], P. Palni[84a], C.E. Pandini[54], J.G. Panduro Vazquez[94], P. Pani[46], G. Panizzo[67a,67c], L. Paolozzi[54], C. Papadatos[110], K. Papageorgiou[9,h], S. Parajuli[42], A. Paramonov[6], C. Paraskevopoulos[10], D. Paredes Hernandez[63b], S.R. Paredes Saenz[134], B. Parida[180], T.H. Park[167], A.J. Parker[31], M.A. Parker[32], F. Parodi[55b,55a], E.W. Parrish[121], J.A. Parsons[39], U. Parzefall[52], L. Pascual Dominguez[135], V.R. Pascuzzi[18], J.M.P. Pasner[145], F. Pasquali[120], E. Pasqualucci[73a], S. Passaggio[55b], F. Pastore[94], P. Pasuwan[45a,45b], S. Pataraia[100], J.R. Pater[101], A. Pathak[181,j], J. Patton[91], T. Pauly[36], J. Pearkes[153], M. Pedersen[133], L. Pedraza Diaz[119], R. Pedro[139a], T. Peiffer[53], S.V. Peleganchuk[122b,122a], O. Penc[140], C. Peng[63b], H. Peng[60a], B.S. Peralva[81a], M.M. Perego[65], A.P. Pereira Peixoto[139a], L. Pereira Sanchez[45a,45b], D.V. Perepelitsa[29], E. Perez Codina[168a], L. Perini[69a,69b], H. Pernegger[36], S. Perrella[36], A. Perrevoort[120], K. Peters[46], R.F.Y. Peters[101], B.A. Petersen[36], T.C. Petersen[40], E. Petit[102], V. Petousis[141], C. Petridou[162], F. Petrucci[75a,75b], M. Pettee[183], N.E. Pettersson[103], K. Petukhova[142], A. Peyaud[144], R. Pezoa[146d], L. Pezzotti[71a,71b], T. Pham[105], P.W. Phillips[143], M.W. Phipps[173], G. Piacquadio[155], E. Pianori[18], A. Picazio[103], R.H. Pickles[101], R. Piegaia[30], D. Pietreanu[27b], J.E. Pilcher[37], A.D. Pilkington[101], M. Pinamonti[67a,67c], J.L. Pinfold[3], C. Pitman Donaldson[95], M. Pitt[161], L. Pizzimento[74a,74b], A. Pizzini[120], M.-A. Pleier[29], V. Plesanovs[52], V. Pleskot[142], E. Plotnikova[80], P. Podberezko[122b,122a], R. Poettgen[97],

R. Poggi[54], L. Poggioli[135], I. Pogrebnyak[107], D. Pohl[24], I. Pokharel[53], G. Polesello[71a], A. Poley[152,168a], A. Policicchio[73a,73b], R. Polifka[142], A. Polini[23b], C.S. Pollard[46], V. Polychronakos[29], D. Ponomarenko[112], L. Pontecorvo[36], S. Popa[27a], G.A. Popeneciu[27d], L. Portales[5], D.M. Portillo Quintero[58], S. Pospisil[141], K. Potamianos[46], I.N. Potrap[80], C.J. Potter[32], H. Potti[11], T. Poulsen[97], J. Poveda[174], T.D. Powell[149], G. Pownall[46], M.E. Pozo Astigarraga[36], A. Prades Ibanez[174], P. Pralavorio[102], M.M. Prapa[44], S. Prell[79], D. Price[101], M. Primavera[68a], M.L. Proffitt[148], N. Proklova[112], K. Prokofiev[63c], F. Prokoshin[80], S. Protopopescu[29], J. Proudfoot[6], M. Przybycien[84a], D. Pudzha[137], A. Puri[173], P. Puzo[65], D. Pyatiizbyantseva[112], J. Qian[106], Y. Qin[101], A. Quadt[53], M. Queitsch-Maitland[36], G. Rabanal Bolanos[59], M. Racko[28a], F. Ragusa[69a,69b], G. Rahal[98], J.A. Raine[54], S. Rajagopalan[29], A. Ramirez Morales[93], K. Ran[15a,15d], D.F. Rassloff[61a], D.M. Rauch[46], F. Rauscher[114], S. Rave[100], B. Ravina[57], I. Ravinovich[180], J.H. Rawling[101], M. Raymond[36], A.L. Read[133], N.P. Readioff[149], M. Reale[68a,68b], D.M. Rebuzzi[71a,71b], G. Redlinger[29], K. Reeves[43], D. Reikher[161], A. Reiss[100], A. Rej[151], C. Rembser[36], A. Renardi[46], M. Renda[27b], M.B. Rendel[115], A.G. Rennie[57], S. Resconi[69a], E.D. Resseguie[18], S. Rettie[95], B. Reynolds[127], E. Reynolds[21], O.L. Rezanova[122b,122a], P. Reznicek[142], E. Ricci[76a,76b], R. Richter[115], S. Richter[46], E. Richter-Was[84b], M. Ridel[135], P. Rieck[115], O. Rifki[46], M. Rijssenbeek[155], A. Rimoldi[71a,71b], M. Rimoldi[46], L. Rinaldi[23b], T.T. Rinn[173], G. Ripellino[154], I. Riu[14], P. Rivadeneira[46], J.C. Rivera Vergara[176], F. Rizatdinova[129], E. Rizvi[93], C. Rizzi[36], S.H. Robertson[104,aa], M. Robin[46], D. Robinson[32], C.M. Robles Gajardo[146d], M. Robles Manzano[100], A. Robson[57], A. Rocchi[74a,74b], C. Roda[72a,72b], S. Rodriguez Bosca[174], A. Rodriguez Rodriguez[52], A.M. Rodríguez Vera[168b], S. Roe[36], J. Roggel[182], O. Røhne[133], R. Röhrig[115], R.A. Rojas[146d], B. Roland[52], C.P.A. Roland[66], J. Roloff[29], A. Romaniouk[112], M. Romano[23b,23a], N. Rompotis[91], M. Ronzani[125], L. Roos[135], S. Rosati[73a], G. Rosin[103], B.J. Rosser[136], E. Rossi[46], E. Rossi[75a,75b], E. Rossi[70a,70b], L.P. Rossi[55b], L. Rossini[46], R. Rosten[14], M. Rotaru[27b], B. Rottler[52], D. Rousseau[65], G. Rovelli[71a,71b], A. Roy[11], D. Roy[33f], A. Rozanov[102], Y. Rozen[160], X. Ruan[33f], T.A. Ruggeri[1], F. Rühr[52], A. Ruiz-Martinez[174], A. Rummler[36], Z. Rurikova[52], N.A. Rusakovich[80], H.L. Russell[104], L. Rustige[38,47], J.P. Rutherfoord[7], E.M. Rüttinger[149], M. Rybar[142], G. Rybkin[65], E.B. Rye[133], A. Ryzhov[123], J.A. Sabater Iglesias[46], P. Sabatini[174], L. Sabetta[73a,73b], S. Sacerdoti[65], H.F-W. Sadrozinski[145], R. Sadykov[80], F. Safai Tehrani[73a], B. Safarzadeh Samani[156], M. Safdari[153], P. Saha[121], S. Saha[104], M. Sahinsoy[115], A. Sahu[182], M. Saimpert[36], M. Saito[163], T. Saito[163], H. Sakamoto[163], D. Salamani[54], G. Salamanna[75a,75b], A. Salnikov[153], J. Salt[174], A. Salvador Salas[14], D. Salvatore[41b,41a], F. Salvatore[156], A. Salvucci[63a], A. Salzburger[36], J. Samarati[36], D. Sammel[52], D. Sampsonidis[162], D. Sampsonidou[60d,60c], J. Sánchez[174], A. Sanchez Pineda[67a,36,67c], H. Sandaker[133], C.O. Sander[46], I.G. Sanderswood[90], M. Sandhoff[182], C. Sandoval[22b], D.P.C. Sankey[143], M. Sannino[55b,55a], Y. Sano[117], A. Sansoni[51], C. Santoni[38], H. Santos[139a,139b], S.N. Santpur[18], A. Santra[174], K.A. Saoucha[149], A. Sapronov[80], J.G. Saraiva[139a,139d], O. Sasaki[82], K. Sato[169], F. Sauerburger[52], E. Sauvan[5], P. Savard[167,ak], R. Sawada[163], C. Sawyer[143], L. Sawyer[96], I. Sayago Galvan[174], C. Sbarra[23b], A. Sbrizzi[67a,67c], T. Scanlon[95], J. Schaarschmidt[148], P. Schacht[115], D. Schaefer[37], L. Schaefer[136], U. Schäfer[100], A.C. Schaffer[65], D. Schaile[114], R.D. Schamberger[155], E. Schanet[114], C. Scharf[19], N. Scharmberg[101], V.A. Schegelsky[137], D. Scheirich[142], F. Schenck[19], M. Schernau[171], C. Schiavi[55b,55a], L.K. Schildgen[24], Z.M. Schillaci[26], E.J. Schioppa[68a,68b], M. Schioppa[41b,41a], K.E. Schleicher[52], S. Schlenker[36], K.R. Schmidt-Sommerfeld[115], K. Schmieden[100], C. Schmitt[100], S. Schmitt[46], L. Schoeffel[144], A. Schoening[61b], P.G. Scholer[52], E. Schopf[134], M. Schott[100], J.F.P. Schouwenberg[119], J. Schovancova[36], S. Schramm[54], F. Schroeder[182], A. Schulte[100], H-C. Schultz-Coulon[61a], M. Schumacher[52], B.A. Schumm[145], Ph. Schune[144], A. Schwartzman[153], T.A. Schwarz[106], Ph. Schwemling[144], R. Schwienhorst[107], A. Sciandra[145], G. Sciolla[26], F. Scuri[72a], F. Scutti[105], L.M. Scyboz[115], C.D. Sebastiani[91], K. Sedlaczek[47], P. Seema[19], S.C. Seidel[118], A. Seiden[145], B.D. Seidlitz[29], T. Seiss[37], C. Seitz[46], J.M. Seixas[81b], G. Sekhniaidze[70a], S.J. Sekula[42], N. Semprini-Cesari[23b,23a], S. Sen[49], C. Serfon[29], L. Serin[65], L. Serkin[67a,67b], M. Sessa[60a], H. Severini[128], S. Sevova[153], F. Sforza[55b,55a],

A. Sfyrla[54], E. Shabalina[53], J.D. Shahinian[136], N.W. Shaikh[45a,45b], D. Shaked Renous[180], L.Y. Shan[15a], M. Shapiro[18], A. Sharma[36], A.S. Sharma[1], P.B. Shatalov[124], K. Shaw[156], S.M. Shaw[101], M. Shehade[180], Y. Shen[128], A.D. Sherman[25], P. Sherwood[95], L. Shi[95], C.O. Shimmin[183], Y. Shimogama[179], M. Shimojima[116], J.D. Shinner[94], I.P.J. Shipsey[134], S. Shirabe[165], M. Shiyakova[80,y], J. Shlomi[180], A. Shmeleva[111], M.J. Shochet[37], J. Shojaii[105], D.R. Shope[154], S. Shrestha[127], E.M. Shrif[33f], M.J. Shroff[176], E. Shulga[180], P. Sicho[140], A.M. Sickles[173], E. Sideras Haddad[33f], O. Sidiropoulou[36], A. Sidoti[23b,23a], F. Siegert[48], Dj. Sijacki[16], M.Jr. Silva[181], M.V. Silva Oliveira[36], S.B. Silverstein[45a], S. Simion[65], R. Simoniello[100], C.J. Simpson-allsop[21], S. Simsek[12b], P. Sinervo[167], V. Sinetckii[113], S. Singh[152], S. Sinha[33f], M. Sioli[23b,23a], I. Siral[131], S.Yu. Sivoklokov[113], J. Sjölin[45a,45b], A. Skaf[53], E. Skorda[97], P. Skubic[128], M. Slawinska[85], K. Sliwa[170], V. Smakhtin[180], B.H. Smart[143], J. Smiesko[28b], N. Smirnov[112], S.Yu. Smirnov[112], Y. Smirnov[112], L.N. Smirnova[113,s], O. Smirnova[97], E.A. Smith[37], H.A. Smith[134], M. Smizanska[90], K. Smolek[141], A. Smykiewicz[85], A.A. Snesarev[111], H.L. Snoek[120], I.M. Snyder[131], S. Snyder[29], R. Sobie[176,aa], A. Soffer[161], A. Søgaard[50], F. Sohns[53], C.A. Solans Sanchez[36], E.Yu. Soldatov[112], U. Soldevila[174], A.A. Solodkov[123], A. Soloshenko[80], O.V. Solovyanov[123], V. Solovyev[137], P. Sommer[149], H. Son[170], A. Sonay[14], W. Song[143], W.Y. Song[168b], A. Sopczak[141], A.L. Sopio[95], F. Sopkova[28b], S. Sottocornola[71a,71b], R. Soualah[67a,67c], A.M. Soukharev[122b,122a], D. South[46], S. Spagnolo[68a,68b], M. Spalla[115], M. Spangenberg[178], F. Spanò[94], D. Sperlich[52], T.M. Spieker[61a], G. Spigo[36], M. Spina[156], D.P. Spiteri[57], M. Spousta[142], A. Stabile[69a,69b], B.L. Stamas[121], R. Stamen[61a], M. Stamenkovic[120], A. Stampekis[21], E. Stanecka[85], B. Stanislaus[134], M.M. Stanitzki[46], M. Stankaityte[134], B. Stapf[120], E.A. Starchenko[123], G.H. Stark[145], J. Stark[58], P. Staroba[140], P. Starovoitov[61a], S. Stärz[104], R. Staszewski[85], G. Stavropoulos[44], M. Stegler[46], P. Steinberg[29], A.L. Steinhebel[131], B. Stelzer[152,168a], H.J. Stelzer[138], O. Stelzer-Chilton[168a], H. Stenzel[56], T.J. Stevenson[156], G.A. Stewart[36], M.C. Stockton[36], G. Stoicea[27b], M. Stolarski[139a], S. Stonjek[115], A. Straessner[48], J. Strandberg[154], S. Strandberg[45a,45b], M. Strauss[128], T. Strebler[102], P. Strizenec[28b], R. Ströhmer[177], D.M. Strom[131], R. Stroynowski[42], A. Strubig[45a,45b], S.A. Stucci[29], B. Stugu[17], J. Stupak[128], N.A. Styles[46], D. Su[153], W. Su[60d,148,60c], X. Su[60a], N.B. Suarez[138], V.V. Sulin[111], M.J. Sullivan[91], D.M.S. Sultan[54], S. Sultansoy[4c], T. Sumida[86], S. Sun[106], X. Sun[101], C.J.E. Suster[157], M.R. Sutton[156], S. Suzuki[82], M. Svatos[140], M. Swiatlowski[168a], S.P. Swift[2], T. Swirski[177], A. Sydorenko[100], I. Sykora[28a], M. Sykora[142], T. Sykora[142], D. Ta[100], K. Tackmann[46,x], J. Taenzer[161], A. Taffard[171], R. Tafirout[168a], E. Tagiev[123], R.H.M. Taibah[135], R. Takashima[87], K. Takeda[83], T. Takeshita[150], E.P. Takeva[50], Y. Takubo[82], M. Talby[102], A.A. Talyshev[122b,122a], K.C. Tam[63b], N.M. Tamir[161], J. Tanaka[163], R. Tanaka[65], S. Tapia Araya[173], S. Tapprogge[100], A. Tarek Abouelfadl Mohamed[107], S. Tarem[160], K. Tariq[60b], G. Tarna[27b,e], G.F. Tartarelli[69a], P. Tas[142], M. Tasevsky[140], E. Tassi[41b,41a], G. Tateno[163], A. Tavares Delgado[139a], Y. Tayalati[35f], A.J. Taylor[50], G.N. Taylor[105], W. Taylor[168b], H. Teagle[91], A.S. Tee[90], R. Teixeira De Lima[153], P. Teixeira-Dias[94], H. Ten Kate[36], J.J. Teoh[120], K. Terashi[163], J. Terron[99], S. Terzo[14], M. Testa[51], R.J. Teuscher[167,aa], N. Themistokleous[50], T. Theveneaux-Pelzer[19], D.W. Thomas[94], J.P. Thomas[21], E.A. Thompson[46], P.D. Thompson[21], E. Thomson[136], E.J. Thorpe[93], V.O. Tikhomirov[111,ag], Yu.A. Tikhonov[122b,122a], S. Timoshenko[112], P. Tipton[183], S. Tisserant[102], K. Todome[23b,23a], S. Todorova-Nova[142], S. Todt[48], J. Tojo[88], S. Tokár[28a], K. Tokushuku[82], E. Tolley[127], R. Tombs[32], K.G. Tomiwa[33f], M. Tomoto[82,117], L. Tompkins[153], P. Tornambe[103], E. Torrence[131], H. Torres[48], E. Torró Pastor[174], M. Toscani[30], C. Tosciri[134], J. Toth[102,z], D.R. Tovey[149], A. Traeet[17], C.J. Treado[125], T. Trefzger[177], F. Tresoldi[156], A. Tricoli[29], I.M. Trigger[168a], S. Trincaz-Duvoid[135], D.A. Trischuk[175], W. Trischuk[167], B. Trocmé[58], A. Trofymov[65], C. Troncon[69a], F. Trovato[156], L. Truong[33c], M. Trzebinski[85], A. Trzupek[85], F. Tsai[46], P.V. Tsiareshka[108,ae], A. Tsirigotis[162,v], V. Tsiskaridze[155], E.G. Tskhadadze[159a], M. Tsopoulou[162], I.I. Tsukerman[124], V. Tsulaia[18], S. Tsuno[82], D. Tsybychev[155], Y. Tu[63b], A. Tudorache[27b], V. Tudorache[27b], A.N. Tuna[36], S. Turchikhin[80], D. Turgeman[180], I. Turk Cakir[4b,t], R.J. Turner[21], R. Turra[69a], P.M. Tuts[39], S. Tzamarias[162], E. Tzovara[100], K. Uchida[163], F. Ukegawa[169], G. Unal[36],

M. Unal[11], A. Undrus[29], G. Unel[171], F.C. Ungaro[105], Y. Unno[82], K. Uno[163], J. Urban[28b], P. Urquijo[105], G. Usai[8], Z. Uysal[12d], V. Vacek[141], B. Vachon[104], K.O.H. Vadla[133], T. Vafeiadis[36], A. Vaidya[95], C. Valderanis[114], E. Valdes Santurio[45a,45b], M. Valente[168a], S. Valentinetti[23b,23a], A. Valero[174], L. Valéry[46], R.A. Vallance[21], A. Vallier[36], J.A. Valls Ferrer[174], T.R. Van Daalen[14], P. Van Gemmeren[6], S. Van Stroud[95], I. Van Vulpen[120], M. Vanadia[74a,74b], W. Vandelli[36], M. Vandenbroucke[144], E.R. Vandewall[129], D. Vannicola[73a,73b], R. Vari[73a], E.W. Varnes[7], C. Varni[55b,55a], T. Varol[158], D. Varouchas[65], K.E. Varvell[157], M.E. Vasile[27b], G.A. Vasquez[176], F. Vazeille[38], D. Vazquez Furelos[14], T. Vazquez Schroeder[36], J. Veatch[53], V. Vecchio[101], M.J. Veen[120], L.M. Veloce[167], F. Veloso[139a,139c], S. Veneziano[73a], A. Ventura[68a,68b], A. Verbytskyi[115], V. Vercesi[71a], M. Verducci[72a,72b], C.M. Vergel Infante[79], C. Vergis[24], W. Verkerke[120], A.T. Vermeulen[120], J.C. Vermeulen[120], C. Vernieri[153], P.J. Verschuuren[94], M.C. Vetterli[152,ak], N. Viaux Maira[146d], T. Vickey[149], O.E. Vickey Boeriu[149], G.H.A. Viehhauser[134], L. Vigani[61b], M. Villa[23b,23a], M. Villaplana Perez[174], E.M. Villhauer[50], E. Vilucchi[51], M.G. Vincter[34], G.S. Virdee[21], A. Vishwakarma[50], C. Vittori[23b,23a], I. Vivarelli[156], M. Vogel[182], P. Vokac[141], J. Von Ahnen[46], S.E. von Buddenbrock[33f], E. Von Toerne[24], V. Vorobel[142], K. Vorobev[112], M. Vos[174], J.H. Vossebeld[91], M. Vozak[101], N. Vranjes[16], M. Vranjes Milosavljevic[16], V. Vrba[141,*], M. Vreeswijk[120], N.K. Vu[102], R. Vuillermet[36], I. Vukotic[37], S. Wada[169], P. Wagner[24], W. Wagner[182], J. Wagner-Kuhr[114], S. Wahdan[182], H. Wahlberg[89], R. Wakasa[169], V.M. Walbrecht[115], J. Walder[143], R. Walker[114], S.D. Walker[94], W. Walkowiak[151], V. Wallangen[45a,45b], A.M. Wang[59], A.Z. Wang[181], C. Wang[60a], C. Wang[60c], H. Wang[18], H. Wang[3], J. Wang[63a], P. Wang[42], Q. Wang[128], R.-J. Wang[100], R. Wang[60a], R. Wang[6], S.M. Wang[158], W.T. Wang[60a], W. Wang[15c], W.X. Wang[60a], Y. Wang[60a], Z. Wang[106], C. Wanotayaroj[46], A. Warburton[104], C.P. Ward[32], R.J. Ward[21], N. Warrack[57], A.T. Watson[21], M.F. Watson[21], G. Watts[148], B.M. Waugh[95], A.F. Webb[11], C. Weber[29], M.S. Weber[20], S.A. Weber[34], S.M. Weber[61a], Y. Wei[134], A.R. Weidberg[134], J. Weingarten[47], M. Weirich[100], C. Weiser[52], P.S. Wells[36], T. Wenaus[29], B. Wendland[47], T. Wengler[36], S. Wenig[36], N. Wermes[24], M. Wessels[61a], T.D. Weston[20], K. Whalen[131], A.M. Wharton[90], A.S. White[106], A. White[8], M.J. White[1], D. Whiteson[171], B.W. Whitmore[90], W. Wiedenmann[181], C. Wiel[48], M. Wielers[143], N. Wieseotte[100], C. Wiglesworth[40], L.A.M. Wiik-Fuchs[52], H.G. Wilkens[36], L.J. Wilkins[94], D.M. Williams[39], H.H. Williams[136], S. Williams[32], S. Willocq[103], P.J. Windischhofer[134], I. Wingerter-Seez[5], E. Winkels[156], F. Winklmeier[131], B.T. Winter[52], M. Wittgen[153], M. Wobisch[96], A. Wolf[100], R. Wölker[134], J. Wollrath[52], M.W. Wolter[85], H. Wolters[139a,139c], V.W.S. Wong[175], A.F. Wongel[46], N.L. Woods[145], S.D. Worm[46], B.K. Wosiek[85], K.W. Woźniak[85], K. Wraight[57], S.L. Wu[181], X. Wu[54], Y. Wu[60a], J. Wuerzinger[134], T.R. Wyatt[101], B.M. Wynne[50], S. Xella[40], J. Xiang[63c], X. Xiao[106], X. Xie[60a], I. Xiotidis[156], D. Xu[15a], H. Xu[60a], H. Xu[60a], L. Xu[29], R. Xu[136], T. Xu[144], W. Xu[106], Y. Xu[15b], Z. Xu[60b], Z. Xu[153], B. Yabsley[157], S. Yacoob[33a], D.P. Yallup[95], N. Yamaguchi[88], Y. Yamaguchi[165], A. Yamamoto[82], M. Yamatani[163], T. Yamazaki[163], Y. Yamazaki[83], J. Yan[60c], Z. Yan[25], H.J. Yang[60c,60d], H.T. Yang[18], S. Yang[60a], T. Yang[63c], X. Yang[60a], X. Yang[60b,58], Y. Yang[163], Z. Yang[106,60a], W-M. Yao[18], Y.C. Yap[46], H. Ye[15c], J. Ye[42], S. Ye[29], I. Yeletskikh[80], M.R. Yexley[90], E. Yigitbasi[25], P. Yin[39], K. Yorita[179], K. Yoshihara[79], C.J.S. Young[36], C. Young[153], J. Yu[79], R. Yuan[60b,i], X. Yue[61a], M. Zaazoua[35f], B. Zabinski[85], G. Zacharis[10], E. Zaffaroni[54], J. Zahreddine[135], A.M. Zaitsev[123,af], T. Zakareishvili[159b], N. Zakharchuk[34], S. Zambito[36], D. Zanzi[36], S.V. Zeißner[47], C. Zeitnitz[182], G. Zemaityte[134], J.C. Zeng[173], O. Zenin[123], T. Ženiš[28a], D. Zerwas[65], M. Zgubič[134], B. Zhang[15c], D.F. Zhang[15b], G. Zhang[15b], J. Zhang[6], K. Zhang[15a], L. Zhang[15c], L. Zhang[60a], M. Zhang[173], R. Zhang[181], S. Zhang[106], X. Zhang[60c], X. Zhang[60b], Y. Zhang[15a,15d], Z. Zhang[63a], Z. Zhang[65], P. Zhao[49], Y. Zhao[145], Z. Zhao[60a], A. Zhemchugov[80], Z. Zheng[106], D. Zhong[173], B. Zhou[106], C. Zhou[181], H. Zhou[7], M. Zhou[155], N. Zhou[60c], Y. Zhou[7], C.G. Zhu[60b], C. Zhu[15a,15d], H.L. Zhu[60a], H. Zhu[15a], J. Zhu[106], Y. Zhu[60a], X. Zhuang[15a], K. Zhukov[111], V. Zhulanov[122b,122a], D. Zieminska[66], N.I. Zimine[80], S. Zimmermann[52,*], Z. Zinonos[115], M. Ziolkowski[151], L. Živković[16], G. Zobernig[181], A. Zoccoli[23b,23a], K. Zoch[53], T.G. Zorbas[149], R. Zou[37], L. Zwalinski[36].

[1]Department of Physics, University of Adelaide, Adelaide; Australia.
[2]Physics Department, SUNY Albany, Albany NY; United States of America.
[3]Department of Physics, University of Alberta, Edmonton AB; Canada.
[4(a)]Department of Physics, Ankara University, Ankara;[(b)]Istanbul Aydin University, Application and Research Center for Advanced Studies, Istanbul;[(c)]Division of Physics, TOBB University of Economics and Technology, Ankara; Turkey.
[5]LAPP, Univ. Savoie Mont Blanc, CNRS/IN2P3, Annecy ; France.
[6]High Energy Physics Division, Argonne National Laboratory, Argonne IL; United States of America.
[7]Department of Physics, University of Arizona, Tucson AZ; United States of America.
[8]Department of Physics, University of Texas at Arlington, Arlington TX; United States of America.
[9]Physics Department, National and Kapodistrian University of Athens, Athens; Greece.
[10]Physics Department, National Technical University of Athens, Zografou; Greece.
[11]Department of Physics, University of Texas at Austin, Austin TX; United States of America.
[12(a)]Bahcesehir University, Faculty of Engineering and Natural Sciences, Istanbul;[(b)]Istanbul Bilgi University, Faculty of Engineering and Natural Sciences, Istanbul;[(c)]Department of Physics, Bogazici University, Istanbul;[(d)]Department of Physics Engineering, Gaziantep University, Gaziantep; Turkey.
[13]Institute of Physics, Azerbaijan Academy of Sciences, Baku; Azerbaijan.
[14]Institut de Física d'Altes Energies (IFAE), Barcelona Institute of Science and Technology, Barcelona; Spain.
[15(a)]Institute of High Energy Physics, Chinese Academy of Sciences, Beijing;[(b)]Physics Department, Tsinghua University, Beijing;[(c)]Department of Physics, Nanjing University, Nanjing;[(d)]University of Chinese Academy of Science (UCAS), Beijing; China.
[16]Institute of Physics, University of Belgrade, Belgrade; Serbia.
[17]Department for Physics and Technology, University of Bergen, Bergen; Norway.
[18]Physics Division, Lawrence Berkeley National Laboratory and University of California, Berkeley CA; United States of America.
[19]Institut für Physik, Humboldt Universität zu Berlin, Berlin; Germany.
[20]Albert Einstein Center for Fundamental Physics and Laboratory for High Energy Physics, University of Bern, Bern; Switzerland.
[21]School of Physics and Astronomy, University of Birmingham, Birmingham; United Kingdom.
[22(a)]Facultad de Ciencias y Centro de Investigaciónes, Universidad Antonio Nariño, Bogotá;[(b)]Departamento de Física, Universidad Nacional de Colombia, Bogotá, Colombia; Colombia.
[23(a)]INFN Bologna and Universita' di Bologna, Dipartimento di Fisica;[(b)]INFN Sezione di Bologna; Italy.
[24]Physikalisches Institut, Universität Bonn, Bonn; Germany.
[25]Department of Physics, Boston University, Boston MA; United States of America.
[26]Department of Physics, Brandeis University, Waltham MA; United States of America.
[27(a)]Transilvania University of Brasov, Brasov;[(b)]Horia Hulubei National Institute of Physics and Nuclear Engineering, Bucharest;[(c)]Department of Physics, Alexandru Ioan Cuza University of Iasi, Iasi;[(d)]National Institute for Research and Development of Isotopic and Molecular Technologies, Physics Department, Cluj-Napoca;[(e)]University Politehnica Bucharest, Bucharest;[(f)]West University in Timisoara, Timisoara; Romania.
[28(a)]Faculty of Mathematics, Physics and Informatics, Comenius University, Bratislava;[(b)]Department of Subnuclear Physics, Institute of Experimental Physics of the Slovak Academy of Sciences, Kosice; Slovak Republic.
[29]Physics Department, Brookhaven National Laboratory, Upton NY; United States of America.
[30]Departamento de Física, Universidad de Buenos Aires, Buenos Aires; Argentina.
[31]California State University, CA; United States of America.

[32]Cavendish Laboratory, University of Cambridge, Cambridge; United Kingdom.
[33(a)]Department of Physics, University of Cape Town, Cape Town;[(b)]iThemba Labs, Western Cape;[(c)]Department of Mechanical Engineering Science, University of Johannesburg, Johannesburg;[(d)]National Institute of Physics, University of the Philippines Diliman;[(e)]University of South Africa, Department of Physics, Pretoria;[(f)]School of Physics, University of the Witwatersrand, Johannesburg; South Africa.
[34]Department of Physics, Carleton University, Ottawa ON; Canada.
[35(a)]Faculté des Sciences Ain Chock, Réseau Universitaire de Physique des Hautes Energies - Université Hassan II, Casablanca;[(b)]Faculté des Sciences, Université Ibn-Tofail, Kénitra;[(c)]Faculté des Sciences Semlalia, Université Cadi Ayyad, LPHEA-Marrakech;[(d)]Moroccan Foundation for Advanced Science Innovation and Research (MAScIR), Rabat;[(e)]LPMR, Faculté des Sciences, Université Mohamed Premier, Oujda;[(f)]Faculté des sciences, Université Mohammed V, Rabat; Morocco.
[36]CERN, Geneva; Switzerland.
[37]Enrico Fermi Institute, University of Chicago, Chicago IL; United States of America.
[38]LPC, Université Clermont Auvergne, CNRS/IN2P3, Clermont-Ferrand; France.
[39]Nevis Laboratory, Columbia University, Irvington NY; United States of America.
[40]Niels Bohr Institute, University of Copenhagen, Copenhagen; Denmark.
[41(a)]Dipartimento di Fisica, Università della Calabria, Rende;[(b)]INFN Gruppo Collegato di Cosenza, Laboratori Nazionali di Frascati; Italy.
[42]Physics Department, Southern Methodist University, Dallas TX; United States of America.
[43]Physics Department, University of Texas at Dallas, Richardson TX; United States of America.
[44]National Centre for Scientific Research "Demokritos", Agia Paraskevi; Greece.
[45(a)]Department of Physics, Stockholm University;[(b)]Oskar Klein Centre, Stockholm; Sweden.
[46]Deutsches Elektronen-Synchrotron DESY, Hamburg and Zeuthen; Germany.
[47]Lehrstuhl für Experimentelle Physik IV, Technische Universität Dortmund, Dortmund; Germany.
[48]Institut für Kern- und Teilchenphysik, Technische Universität Dresden, Dresden; Germany.
[49]Department of Physics, Duke University, Durham NC; United States of America.
[50]SUPA - School of Physics and Astronomy, University of Edinburgh, Edinburgh; United Kingdom.
[51]INFN e Laboratori Nazionali di Frascati, Frascati; Italy.
[52]Physikalisches Institut, Albert-Ludwigs-Universität Freiburg, Freiburg; Germany.
[53]II. Physikalisches Institut, Georg-August-Universität Göttingen, Göttingen; Germany.
[54]Département de Physique Nucléaire et Corpusculaire, Université de Genève, Genève; Switzerland.
[55(a)]Dipartimento di Fisica, Università di Genova, Genova;[(b)]INFN Sezione di Genova; Italy.
[56]II. Physikalisches Institut, Justus-Liebig-Universität Giessen, Giessen; Germany.
[57]SUPA - School of Physics and Astronomy, University of Glasgow, Glasgow; United Kingdom.
[58]LPSC, Université Grenoble Alpes, CNRS/IN2P3, Grenoble INP, Grenoble; France.
[59]Laboratory for Particle Physics and Cosmology, Harvard University, Cambridge MA; United States of America.
[60(a)]Department of Modern Physics and State Key Laboratory of Particle Detection and Electronics, University of Science and Technology of China, Hefei;[(b)]Institute of Frontier and Interdisciplinary Science and Key Laboratory of Particle Physics and Particle Irradiation (MOE), Shandong University, Qingdao;[(c)]School of Physics and Astronomy, Shanghai Jiao Tong University, Key Laboratory for Particle Astrophysics and Cosmology (MOE), SKLPPC, Shanghai;[(d)]Tsung-Dao Lee Institute, Shanghai; China.
[61(a)]Kirchhoff-Institut für Physik, Ruprecht-Karls-Universität Heidelberg, Heidelberg;[(b)]Physikalisches Institut, Ruprecht-Karls-Universität Heidelberg, Heidelberg; Germany.
[62]Faculty of Applied Information Science, Hiroshima Institute of Technology, Hiroshima; Japan.
[63(a)]Department of Physics, Chinese University of Hong Kong, Shatin, N.T., Hong Kong;[(b)]Department

of Physics, University of Hong Kong, Hong Kong;[(c)]Department of Physics and Institute for Advanced Study, Hong Kong University of Science and Technology, Clear Water Bay, Kowloon, Hong Kong; China.
[64]Department of Physics, National Tsing Hua University, Hsinchu; Taiwan.
[65]IJCLab, Université Paris-Saclay, CNRS/IN2P3, 91405, Orsay; France.
[66]Department of Physics, Indiana University, Bloomington IN; United States of America.
[67(a)]INFN Gruppo Collegato di Udine, Sezione di Trieste, Udine;[(b)]ICTP, Trieste;[(c)]Dipartimento Politecnico di Ingegneria e Architettura, Università di Udine, Udine; Italy.
[68(a)]INFN Sezione di Lecce;[(b)]Dipartimento di Matematica e Fisica, Università del Salento, Lecce; Italy.
[69(a)]INFN Sezione di Milano;[(b)]Dipartimento di Fisica, Università di Milano, Milano; Italy.
[70(a)]INFN Sezione di Napoli;[(b)]Dipartimento di Fisica, Università di Napoli, Napoli; Italy.
[71(a)]INFN Sezione di Pavia;[(b)]Dipartimento di Fisica, Università di Pavia, Pavia; Italy.
[72(a)]INFN Sezione di Pisa;[(b)]Dipartimento di Fisica E. Fermi, Università di Pisa, Pisa; Italy.
[73(a)]INFN Sezione di Roma;[(b)]Dipartimento di Fisica, Sapienza Università di Roma, Roma; Italy.
[74(a)]INFN Sezione di Roma Tor Vergata;[(b)]Dipartimento di Fisica, Università di Roma Tor Vergata, Roma; Italy.
[75(a)]INFN Sezione di Roma Tre;[(b)]Dipartimento di Matematica e Fisica, Università Roma Tre, Roma; Italy.
[76(a)]INFN-TIFPA;[(b)]Università degli Studi di Trento, Trento; Italy.
[77]Institut für Astro- und Teilchenphysik, Leopold-Franzens-Universität, Innsbruck; Austria.
[78]University of Iowa, Iowa City IA; United States of America.
[79]Department of Physics and Astronomy, Iowa State University, Ames IA; United States of America.
[80]Joint Institute for Nuclear Research, Dubna; Russia.
[81(a)]Departamento de Engenharia Elétrica, Universidade Federal de Juiz de Fora (UFJF), Juiz de Fora;[(b)]Universidade Federal do Rio De Janeiro COPPE/EE/IF, Rio de Janeiro;[(c)]Instituto de Física, Universidade de São Paulo, São Paulo; Brazil.
[82]KEK, High Energy Accelerator Research Organization, Tsukuba; Japan.
[83]Graduate School of Science, Kobe University, Kobe; Japan.
[84(a)]AGH University of Science and Technology, Faculty of Physics and Applied Computer Science, Krakow;[(b)]Marian Smoluchowski Institute of Physics, Jagiellonian University, Krakow; Poland.
[85]Institute of Nuclear Physics Polish Academy of Sciences, Krakow; Poland.
[86]Faculty of Science, Kyoto University, Kyoto; Japan.
[87]Kyoto University of Education, Kyoto; Japan.
[88]Research Center for Advanced Particle Physics and Department of Physics, Kyushu University, Fukuoka ; Japan.
[89]Instituto de Física La Plata, Universidad Nacional de La Plata and CONICET, La Plata; Argentina.
[90]Physics Department, Lancaster University, Lancaster; United Kingdom.
[91]Oliver Lodge Laboratory, University of Liverpool, Liverpool; United Kingdom.
[92]Department of Experimental Particle Physics, Jožef Stefan Institute and Department of Physics, University of Ljubljana, Ljubljana; Slovenia.
[93]School of Physics and Astronomy, Queen Mary University of London, London; United Kingdom.
[94]Department of Physics, Royal Holloway University of London, Egham; United Kingdom.
[95]Department of Physics and Astronomy, University College London, London; United Kingdom.
[96]Louisiana Tech University, Ruston LA; United States of America.
[97]Fysiska institutionen, Lunds universitet, Lund; Sweden.
[98]Centre de Calcul de l'Institut National de Physique Nucléaire et de Physique des Particules (IN2P3), Villeurbanne; France.
[99]Departamento de Física Teorica C-15 and CIAFF, Universidad Autónoma de Madrid, Madrid; Spain.

[100]Institut für Physik, Universität Mainz, Mainz; Germany.
[101]School of Physics and Astronomy, University of Manchester, Manchester; United Kingdom.
[102]CPPM, Aix-Marseille Université, CNRS/IN2P3, Marseille; France.
[103]Department of Physics, University of Massachusetts, Amherst MA; United States of America.
[104]Department of Physics, McGill University, Montreal QC; Canada.
[105]School of Physics, University of Melbourne, Victoria; Australia.
[106]Department of Physics, University of Michigan, Ann Arbor MI; United States of America.
[107]Department of Physics and Astronomy, Michigan State University, East Lansing MI; United States of America.
[108]B.I. Stepanov Institute of Physics, National Academy of Sciences of Belarus, Minsk; Belarus.
[109]Research Institute for Nuclear Problems of Byelorussian State University, Minsk; Belarus.
[110]Group of Particle Physics, University of Montreal, Montreal QC; Canada.
[111]P.N. Lebedev Physical Institute of the Russian Academy of Sciences, Moscow; Russia.
[112]National Research Nuclear University MEPhI, Moscow; Russia.
[113]D.V. Skobeltsyn Institute of Nuclear Physics, M.V. Lomonosov Moscow State University, Moscow; Russia.
[114]Fakultät für Physik, Ludwig-Maximilians-Universität München, München; Germany.
[115]Max-Planck-Institut für Physik (Werner-Heisenberg-Institut), München; Germany.
[116]Nagasaki Institute of Applied Science, Nagasaki; Japan.
[117]Graduate School of Science and Kobayashi-Maskawa Institute, Nagoya University, Nagoya; Japan.
[118]Department of Physics and Astronomy, University of New Mexico, Albuquerque NM; United States of America.
[119]Institute for Mathematics, Astrophysics and Particle Physics, Radboud University/Nikhef, Nijmegen; Netherlands.
[120]Nikhef National Institute for Subatomic Physics and University of Amsterdam, Amsterdam; Netherlands.
[121]Department of Physics, Northern Illinois University, DeKalb IL; United States of America.
[122](a)Budker Institute of Nuclear Physics and NSU, SB RAS, Novosibirsk;(b)Novosibirsk State University Novosibirsk; Russia.
[123]Institute for High Energy Physics of the National Research Centre Kurchatov Institute, Protvino; Russia.
[124]Institute for Theoretical and Experimental Physics named by A.I. Alikhanov of National Research Centre "Kurchatov Institute", Moscow; Russia.
[125]Department of Physics, New York University, New York NY; United States of America.
[126]Ochanomizu University, Otsuka, Bunkyo-ku, Tokyo; Japan.
[127]Ohio State University, Columbus OH; United States of America.
[128]Homer L. Dodge Department of Physics and Astronomy, University of Oklahoma, Norman OK; United States of America.
[129]Department of Physics, Oklahoma State University, Stillwater OK; United States of America.
[130]Palacký University, RCPTM, Joint Laboratory of Optics, Olomouc; Czech Republic.
[131]Institute for Fundamental Science, University of Oregon, Eugene, OR; United States of America.
[132]Graduate School of Science, Osaka University, Osaka; Japan.
[133]Department of Physics, University of Oslo, Oslo; Norway.
[134]Department of Physics, Oxford University, Oxford; United Kingdom.
[135]LPNHE, Sorbonne Université, Université de Paris, CNRS/IN2P3, Paris; France.
[136]Department of Physics, University of Pennsylvania, Philadelphia PA; United States of America.
[137]Konstantinov Nuclear Physics Institute of National Research Centre "Kurchatov Institute", PNPI, St. Petersburg; Russia.

[138]Department of Physics and Astronomy, University of Pittsburgh, Pittsburgh PA; United States of America.
[139(a)]Laboratório de Instrumentação e Física Experimental de Partículas - LIP, Lisboa;[(b)]Departamento de Física, Faculdade de Ciências, Universidade de Lisboa, Lisboa;[(c)]Departamento de Física, Universidade de Coimbra, Coimbra;[(d)]Centro de Física Nuclear da Universidade de Lisboa, Lisboa;[(e)]Departamento de Física, Universidade do Minho, Braga;[(f)]Departamento de Física Teórica y del Cosmos, Universidad de Granada, Granada (Spain);[(g)]Dep Física and CEFITEC of Faculdade de Ciências e Tecnologia, Universidade Nova de Lisboa, Caparica;[(h)]Instituto Superior Técnico, Universidade de Lisboa, Lisboa; Portugal.
[140]Institute of Physics of the Czech Academy of Sciences, Prague; Czech Republic.
[141]Czech Technical University in Prague, Prague; Czech Republic.
[142]Charles University, Faculty of Mathematics and Physics, Prague; Czech Republic.
[143]Particle Physics Department, Rutherford Appleton Laboratory, Didcot; United Kingdom.
[144]IRFU, CEA, Université Paris-Saclay, Gif-sur-Yvette; France.
[145]Santa Cruz Institute for Particle Physics, University of California Santa Cruz, Santa Cruz CA; United States of America.
[146(a)]Departamento de Física, Pontificia Universidad Católica de Chile, Santiago;[(b)]Universidad Andres Bello, Department of Physics, Santiago;[(c)]Instituto de Alta Investigación, Universidad de Tarapacá;[(d)]Departamento de Física, Universidad Técnica Federico Santa María, Valparaíso; Chile.
[147]Universidade Federal de São João del Rei (UFSJ), São João del Rei; Brazil.
[148]Department of Physics, University of Washington, Seattle WA; United States of America.
[149]Department of Physics and Astronomy, University of Sheffield, Sheffield; United Kingdom.
[150]Department of Physics, Shinshu University, Nagano; Japan.
[151]Department Physik, Universität Siegen, Siegen; Germany.
[152]Department of Physics, Simon Fraser University, Burnaby BC; Canada.
[153]SLAC National Accelerator Laboratory, Stanford CA; United States of America.
[154]Physics Department, Royal Institute of Technology, Stockholm; Sweden.
[155]Departments of Physics and Astronomy, Stony Brook University, Stony Brook NY; United States of America.
[156]Department of Physics and Astronomy, University of Sussex, Brighton; United Kingdom.
[157]School of Physics, University of Sydney, Sydney; Australia.
[158]Institute of Physics, Academia Sinica, Taipei; Taiwan.
[159(a)]E. Andronikashvili Institute of Physics, Iv. Javakhishvili Tbilisi State University, Tbilisi;[(b)]High Energy Physics Institute, Tbilisi State University, Tbilisi; Georgia.
[160]Department of Physics, Technion, Israel Institute of Technology, Haifa; Israel.
[161]Raymond and Beverly Sackler School of Physics and Astronomy, Tel Aviv University, Tel Aviv; Israel.
[162]Department of Physics, Aristotle University of Thessaloniki, Thessaloniki; Greece.
[163]International Center for Elementary Particle Physics and Department of Physics, University of Tokyo, Tokyo; Japan.
[164]Graduate School of Science and Technology, Tokyo Metropolitan University, Tokyo; Japan.
[165]Department of Physics, Tokyo Institute of Technology, Tokyo; Japan.
[166]Tomsk State University, Tomsk; Russia.
[167]Department of Physics, University of Toronto, Toronto ON; Canada.
[168(a)]TRIUMF, Vancouver BC;[(b)]Department of Physics and Astronomy, York University, Toronto ON; Canada.
[169]Division of Physics and Tomonaga Center for the History of the Universe, Faculty of Pure and Applied Sciences, University of Tsukuba, Tsukuba; Japan.

[170]Department of Physics and Astronomy, Tufts University, Medford MA; United States of America.
[171]Department of Physics and Astronomy, University of California Irvine, Irvine CA; United States of America.
[172]Department of Physics and Astronomy, University of Uppsala, Uppsala; Sweden.
[173]Department of Physics, University of Illinois, Urbana IL; United States of America.
[174]Instituto de Física Corpuscular (IFIC), Centro Mixto Universidad de Valencia - CSIC, Valencia; Spain.
[175]Department of Physics, University of British Columbia, Vancouver BC; Canada.
[176]Department of Physics and Astronomy, University of Victoria, Victoria BC; Canada.
[177]Fakultät für Physik und Astronomie, Julius-Maximilians-Universität Würzburg, Würzburg; Germany.
[178]Department of Physics, University of Warwick, Coventry; United Kingdom.
[179]Waseda University, Tokyo; Japan.
[180]Department of Particle Physics and Astrophysics, Weizmann Institute of Science, Rehovot; Israel.
[181]Department of Physics, University of Wisconsin, Madison WI; United States of America.
[182]Fakultät für Mathematik und Naturwissenschaften, Fachgruppe Physik, Bergische Universität Wuppertal, Wuppertal; Germany.
[183]Department of Physics, Yale University, New Haven CT; United States of America.
[a] Also at Borough of Manhattan Community College, City University of New York, New York NY; United States of America.
[b] Also at Center for High Energy Physics, Peking University; China.
[c] Also at Centro Studi e Ricerche Enrico Fermi; Italy.
[d] Also at CERN, Geneva; Switzerland.
[e] Also at CPPM, Aix-Marseille Université, CNRS/IN2P3, Marseille; France.
[f] Also at Département de Physique Nucléaire et Corpusculaire, Université de Genève, Genève; Switzerland.
[g] Also at Departament de Fisica de la Universitat Autonoma de Barcelona, Barcelona; Spain.
[h] Also at Department of Financial and Management Engineering, University of the Aegean, Chios; Greece.
[i] Also at Department of Physics and Astronomy, Michigan State University, East Lansing MI; United States of America.
[j] Also at Department of Physics and Astronomy, University of Louisville, Louisville, KY; United States of America.
[k] Also at Department of Physics, Ben Gurion University of the Negev, Beer Sheva; Israel.
[l] Also at Department of Physics, California State University, East Bay; United States of America.
[m] Also at Department of Physics, California State University, Fresno; United States of America.
[n] Also at Department of Physics, California State University, Sacramento; United States of America.
[o] Also at Department of Physics, King's College London, London; United Kingdom.
[p] Also at Department of Physics, St. Petersburg State Polytechnical University, St. Petersburg; Russia.
[q] Also at Department of Physics, University of Fribourg, Fribourg; Switzerland.
[r] Also at Dipartimento di Matematica, Informatica e Fisica, Università di Udine, Udine; Italy.
[s] Also at Faculty of Physics, M.V. Lomonosov Moscow State University, Moscow; Russia.
[t] Also at Giresun University, Faculty of Engineering, Giresun; Turkey.
[u] Also at Graduate School of Science, Osaka University, Osaka; Japan.
[v] Also at Hellenic Open University, Patras; Greece.
[w] Also at Institucio Catalana de Recerca i Estudis Avancats, ICREA, Barcelona; Spain.
[x] Also at Institut für Experimentalphysik, Universität Hamburg, Hamburg; Germany.
[y] Also at Institute for Nuclear Research and Nuclear Energy (INRNE) of the Bulgarian Academy of Sciences, Sofia; Bulgaria.
[z] Also at Institute for Particle and Nuclear Physics, Wigner Research Centre for Physics, Budapest;

Hungary.
[aa] Also at Institute of Particle Physics (IPP); Canada.
[ab] Also at Institute of Physics, Azerbaijan Academy of Sciences, Baku; Azerbaijan.
[ac] Also at Instituto de Fisica Teorica, IFT-UAM/CSIC, Madrid; Spain.
[ad] Also at Istanbul University, Dept. of Physics, Istanbul; Turkey.
[ae] Also at Joint Institute for Nuclear Research, Dubna; Russia.
[af] Also at Moscow Institute of Physics and Technology State University, Dolgoprudny; Russia.
[ag] Also at National Research Nuclear University MEPhI, Moscow; Russia.
[ah] Also at Physics Department, An-Najah National University, Nablus; Palestine.
[ai] Also at Physikalisches Institut, Albert-Ludwigs-Universität Freiburg, Freiburg; Germany.
[aj] Also at The City College of New York, New York NY; United States of America.
[ak] Also at TRIUMF, Vancouver BC; Canada.
[al] Also at Universita di Napoli Parthenope, Napoli; Italy.
[am] Also at University of Chinese Academy of Sciences (UCAS), Beijing; China.
[*] Deceased